TAL TECH

DOCTORAL THESIS

Optimization of Aqueous Media Treatment with Pulsed Corona Discharge: Hydrodynamics and Kinetics Conformed with the Discharge Parameters and Energy Efficiency

Priit Tikker

TALLINNA TEHNIKAÜLIKOOL
TALLINN UNIVERSITY OF TECHNOLOGY
TALLINN 2022

TALLINN UNIVERSITY OF TECHNOLOGY
DOCTORAL THESIS
42/2022

Optimization of Aqueous Media Treatment with Pulsed Corona Discharge: Hydrodynamics and Kinetics Conformed with the Discharge Parameters and Energy Efficiency

PRIIT TIKKER

TAL TECH PRESS

TALLINN UNIVERSITY OF TECHNOLOGY
School of Engineering
Department of Materials and Environmental Technology
This dissertation was accepted for the defence of the degree 26/05/2022

Supervisor: Professor Sergei Preis
School of Engineering
Tallinn University of Technology
Tallinn, Estonia

Opponents: Dr. Petr Lukeš, Senior Researcher
Plasma Chemistry and Materials
Institute of Plasma Physics of the Czech Academy of Sciences
Prague, Czech Republic

Dr. Anton Yu. Nikiforov
Department of Applied Physics
Ghent University
Ghent, Belgium

Defence of the thesis: 18/08/2022, Tallinn

Declaration:
Hereby I declare that this doctoral thesis, my original investigation and achievement, submitted for the doctoral degree at Tallinn University of Technology has not been submitted for doctoral or equivalent academic degree.

Priit Tikker

---
signature

European Union
European Regional
Development Fund

Investing
in your future

Copyright: Priit Tikker, 2022
ISSN 2585-6898 (publication)
ISBN 978-9949-83-871-4 (publication)
ISSN 2585-6901 (PDF)
ISBN 978-9949-83-872-1 (PDF)
Printed by Koopia Niini & Rauam

TALLINNA TEHNIKAÜLIKOOL
DOKTORITÖÖ
42/2022

Impulss koroona elektrilahenduse optimeerimine vesikeskkonna töötlemiseks: hüdrodünaamika ja kineetika lähtuvalt elektrilahenduse parameetritest ning energia efektiivsusest

PRIIT TIKKER

TAL TECH
KIRJASTUS

Contents

List of publications 7
Author's contribution to the publications 8
Introduction 9
Abbreviations 11
1 Literature overview 12
1.1 Conventional tap and wastewater treatment processes 12
1.2 Overview of advanced oxidation processes 12
1.3 Established AOPs 14
1.3.1 Ozonation 14
1.3.2 Enhanced ozonation 15
1.3.3 Fenton and photo-Fenton processes 16
1.3.4 Photocatalytic oxidation 17
1.4 Persulfate AOPs 17
1.5 Electric discharge AOPs 19
1.5.1 Electric discharges: types, characteristics and applications 19
1.5.2 Dielectric barrier discharge 24
1.5.3 Corona discharge 25
1.6 Target compounds under consideration 29
1.7 Objectives of the study 31
2 Materials and methods 32
2.1 Chemicals and materials 32
2.2 Gas-phase pulsed corona discharge 34
2.3 Experimental procedure 35
2.4 Analytical methods 37
3 Results and discussion 39
3.1 Gas-liquid contact surface 39
3.2 Contact-surface and pulse repetition frequency impact on non-assisted PCD treatment 39
3.2.1 OXA and phenol oxidation by non-assisted PCD 39
3.2.2 Oxidation of BPA and BPS by PCD 42
3.3 Contact-surface and pulse repetition frequency impact on assisted PCD treatment . 44
3.3.1 Impact of surfactant on BPA and BPS oxidation 44
3.3.2 Impact of extrinsic oxidants on OXA oxidation 46
Conclusions 51
References 52

Acknowledgements 61
Abstract 62
Lühikokkuvõte 64
Appendix 1 67
Appendix 2 75
Appendix 3 87
Curriculum vitae 105
Elulookirjeldus 107

List of publications

The list of author's publications, on the basis of which the thesis has been prepared:

I **Tikker, P.**, Kornev, I., Preis, S., 2020. Oxidation energy efficiency in water treatment with gas-phase pulsed corona discharge as a function of spray density. J. Electrostat. 106, 103466. https://doi.org/10.1016/j.elstat.2020.103466

II **Tikker, P.**, Dulova, N., Kornev, I., Preis, S., 2021. Effects of persulfate and hydrogen peroxide on oxidation of oxalate by pulsed corona discharge. Chem. Eng. J. 411, 128586. https://doi.org/10.1016/j.cej.2021.128586

III **Tikker, P.**, Nikitin, D., Preis, S., 2022. Oxidation of aqueous bisphenols A and S by pulsed corona discharge: impacts of process control parameters and oxidation products identification. Chem. Eng. J. 438, 135602. https://doi.org/10.1016/j.cej.2022.135602

Author's contribution to the publications

Contribution to the papers in this thesis are:

I The author carried out the experiments and respective analyses, interpreted the obtained data and participated in writing of the paper with the help of co-authors.

II The author fulfilled the majority of experiments, interpreted the obtained data, and wrote the paper with the help of co-authors.

III The author carried out the major part of experimental work, interpreted the results, and wrote the paper with the help of co-authors.

Introduction

The significant growth in human population has caused an increased demand for drinking water, which, in turn, has led to a worldwide problem of declining water supplies. Production, consumption, and utilization of new non-biodegradable pharmaceuticals, plastics, fire retardants etc. have expanded considerably to meet the growing needs of humankind. This has led to the emergence and presence of new anthropogenic pollutants in wastewater. Since traditional wastewater treatment processes are not designed to decompose refractory compounds in effluent streams, only partial, often too small removal can occur, and pollutants are released into the environment accumulating in soil and waterbodies. In nature, these may adversely affect ecosystems, causing, for example, acute or chronic toxicity, as well as the development of antibiotic-resistant pathogens, reducing the effectiveness of existing antibiotics. Besides, the increased organic content in water treated at conventional drinking water plants may result in production of carcinogenic disinfection by-products, when chlorination is used as disinfectant. Furthermore, conventional treatment is ineffective to meet regulations if newer stricter limits to water quality are applied. Therefore, new cost-effective treatment methods are needed.

An alternative to conventional methods has been the use of ozonation. While ozone (O_3) is generated *in situ* without the need for additional chemicals, the O_3-containing gas needs to be transported to the treated water. However, O_3 is only partly utilized in water treatment due to its poor solubility in solutions, having the residual O_3 destruction needed. Besides, in ozone generators, part of energy is wasted in generation of short-living radicals that cannot be transported to solution. Together with the need for generator cooling, and either use of dry ambient air or pure oxygen, ozonation becomes costly both in capital investment and in energy expense. This makes ozonation mainly a privilege of cities, narrowing its overall use and not solving the water treatment problems.

Promising water treatment methods are advanced oxidation processes (AOPs), where *in situ* hydroxyl or sulfate radicals are generated and utilized. The most promising AOP has shown to be pulsed corona discharge (PCD), where plasma is generated by ultra-short high voltage pulses, and the treated aqueous solutions are directly sprayed into the plasma zone. By impacts of high-energy electrons, both short living radicals (e.g., $HO^{\bullet}$) and long living O_3 are generated in the reactor. Differently to ozonation, reactive species are directly generated in the reactor from treatable solution and surrounding air. While O_3 can react being dissolved in the bulk solution or directly at the gas-liquid interface, the surface-borne radicals may react only at the interface due to short lifetimes. Hence, the utilization of surface-borne radicals in reactions at the gas-liquid interface comprises the principal feature of this approach resulting in more useful energy utilization. Besides, the discharge workability in humid gas and the generation of O_3 directly in reactor makes the preparation and transport of gas unnecessary, resulting in higher energy efficiency.

This thesis provides an overview of AOPs, including well-established ones, and electric discharges with the emphasis on PCD as cost-effective applications for degradation of numerous pollutants.

The study provides essential theoretical knowledge for PCD process parameter optimization in the part of the energy efficiency dependent on the gas-liquid contact surface for pollutants with various oxidation kinetics. The dependence was studied with

slowly reacting oxalate and rapidly reacting phenol and bisphenols. The effect of surfactant scavenger on the surface-borne reactions at various gas–liquid contact surfaces was evaluated with bisphenols A and S. Additionally, potential synergistic effect of persulfate (PS) and hydrogen peroxide (H_2O_2) with PCD in degradation of oxalate (OXA) was studied at OXA/extrinsic oxidant dose variations and at different gas-liquid interface areas. The impacts of pulse repetition frequency and pH, except for bisphenols, were assessed for both non-assisted and assisted PCD treatment.

The knowledge obtained from this doctoral research provide necessary theoretical data for upscaling and implementation of PCD in real-life applications as an alternative to conventional water treatment processes.

Abbreviations

A	Gas-liquid contact surface
AOP	Advanced oxidation process
BPA	Bisphenol A
BPS	Bisphenol S
CD	Corona discharge
DBD	Dielectric barrier discharge
E	Energy efficiency
E^0	Oxidation potential
e_{aq}^-	Aqueous electron
$H^\bullet$	Hydrogen radical
H_2O_2	Hydrogen peroxide
HO^-	Hydroxide ion
$HO^\bullet$	Hydroxyl radical
HO_2^-	Hydroperoxide ion
$HO_2^\bullet$	Perhydroxyl radical
$HO_3^\bullet$	Hydrogen trioxy radical
HPLC	High-performance liquid chromatography
HPLC-MS	High-performance liquid chromatography combined with a mass spectrometry
$N^\bullet$	Atomic nitrogen radical
$NO^\bullet$	Nitric oxide radical
$NO_2^\bullet$	Nitrogen oxide radical
$O^\bullet$	Atomic oxygen
$O_2^{\bullet-}$	Superoxide anion radical
O_3	Ozone
$O_3^{\bullet-}$	Ozonide anion radical
OXA	Oxalate; sodium oxalate; oxalic acid
PCD	Pulsed corona discharge
PMS	Peroxymonosulfate
pps	Pulse repetition frequency
PS	Persulfate
q	Spray density
ROS	Reactive oxygen species
SDS	Sodium dodecyl sulfate
$SO_4^{\bullet-}$	Sulfate radical
SR-AOP	Sulfate radical based processes
TIC	Total inorganic carbon
TOC	Total organic carbon

1 Literature overview

1.1 Conventional tap and wastewater treatment processes

Nowadays, there is a growing problem of accumulated emerging contaminants in the environment. Applied in wastewater treatment, coagulation-assisted sedimentation, filtration and aerobic activated sludge processes are often insufficient in degradation of pollutants at trace concentration, i.e. micropollutants. Likewise, the development and production of new non-biodegradable pharmaceuticals and consumer products, such as plastics, resulted in the occurrence of new type of anthropogenic pollutants that are difficult to degrade in conventional wastewater treatment processes. Hence, contaminants can end up in surface water, which is used to produce drinking water (Luo et al., 2014; Mieno, 2016; Gil et al., 2019). Another problem is possible formation of carcinogenic disinfection by-products, such as trihalomethanes and nitroso compounds, if chlorination is used as disinfection method (Mieno, 2016; Gil et al., 2019). These circumstances bring to front the need in alternative cost-effective methods of water and wastewater treatment.

1.2 Overview of advanced oxidation processes

A promising group of methods for micro-pollutants and recalcitrant compounds removal from polluted waters is comprised of advanced oxidation processes (AOPs) (Ribeiro et al., 2015; Sharma et al., 2018; Wardenier et al., 2019). The AOP term was first defined by Glaze et al. describing water treatment processes, which involve *in situ* generation of hydroxyl radical ($HO^{\bullet}$) in amounts sufficient to affect water purification at ambient pressure and temperature (Glaze et al., 1987). Hydroxyl radicals are highly reactive and less selective than other oxidants such as chlorine and molecular ozone (O_3). Due to the oxidation standard potential (E^0 = 2.8 V) higher than of the other conventional oxidants, $HO^{\bullet}$ has a possibility to efficiently degrade a variety of organic pollutants. Comparison of oxidation potentials of the oxidants is shown in Table 1 (Legrini et al., 1993; Bahnemann, 2004; Matzek and Carter, 2016). It can be seen that only positively charged holes and fluorine have a higher oxidation potential than $HO^{\bullet}$. However, since fluorine remains out of scope in water treatment, and positively charged holes are formed only on the surface of photocatalysts, $HO^{\bullet}$ is considered as the strongest oxidant applied in aqueous environment (Legrini et al., 1993; Parvulescu et al., 2012).

Table 1. Oxidation potential of oxidants (Legrini et al., 1993; Bahnemann, 2004; Matzek and Carter, 2016)

Oxidant	Oxidation potential, V
Positively charged holes, h^+ (TiO_2)	3.50
Fluorine, F_2	3.03
Hydroxyl radical, $HO^\bullet$	2.80
Persulfate radical, $SO_4^{\bullet-}$	2.60
Atomic oxygen, $O^\bullet$	2.42
Ozone, O_3	2.07
Hydrogen peroxide, H_2O_2	1.78
Perhydroxyl radical, $HO_2^\bullet$	1.70
Potassium permanganate, $KMnO_4$	1.68
Hypobromous acid, HBrO	1.59
Chlorine dioxide, ClO_2	1.57
Hypochlorous acid, HClO	1.49
Chlorine, Cl_2	1.36
Bromide Br_2	1.09
Iodine I_2	0.54

Organic pollutant (R) degradation by $HO^\bullet$ proceeds mainly by three possible reaction pathways (Legrini et al., 1993; Parvulescu et al., 2012; Kaur and Dulova, 2020):

- Hydrogen abstraction – most common mechanism with reaction of alcohols and saturated aliphatic compounds; produces water and organic radical ($R^\bullet$)

$$HO^\bullet + R\text{-}H \rightarrow R^\bullet + H_2O \quad (1)$$

- Electrophilic addition – common for unsaturated compounds, such as aromatic and aliphatic hydrocarbons having the double carbon (C=C) bond

$$HO^\bullet + R \rightarrow ROH \quad (2)$$

- Electron transfer – common for substances, where other two pathways are not possible due to steric effects or several halogen replacements; $HO^\bullet$ is reduced into hydroxide ion (HO^-) and organic substance into positively charged radical

$$HO^\bullet + R\text{-}X \rightarrow R\text{-}X^{\bullet+} + HO^- \quad (3)$$

The aim of AOPs application to water treatment is degradation of aqueous organic compounds into less toxic and better biodegradable compounds with possible, although often unnecessary, total mineralization into CO_2 and H_2O (Ribeiro et al., 2015). To achieve this objective, AOPs categorized into two groups (Table 2), non-photochemical and photochemical technologies (Sharma et al., 2018), were extensively studied (Legrini et al., 1993; Ribeiro et al., 2015; Sharma et al., 2018). A short overview of processes is given below.

Table 2. Most commonly used AOPs

Non-photochemical methods	Photochemical methods
Ozonation at elevated pH 8.5<	O_3/UV
$O_3 + H_2O_2$	H_2O_2/UV
O_3 + catalyst	O_3/H_2O_2/UV
Fenton	Photo-Fenton
	Photocatalytic oxidation (UV/TiO_2)

1.3 Established AOPs

1.3.1 Ozonation

Molecular ozone is a powerful oxidant and disinfectant that has been used in water treatment for over a century (Glaze et al., 1987). Ozone is generated *ex situ* in an ozone generator and transported to the treated solution with the gas stream. Since either dry ambient air or pure oxygen is used for ozone synthesis in an electric discharge, ozonation can be regarded as a chemical free process. Depending on solution pH, O_3 can oxidize pollutants in two possible pathways: direct and indirect radical oxidation. While direct reactions are dominant in acidic conditions, these are significantly slower than mainly $HO^{\bullet}$-driven indirect reactions preferring electron-rich organic moieties, such as aromatic rings. In indirect reactions, $HO^{\bullet}$ are formed through complex decomposition O_3, which is enhanced with the pH rise (Parvulescu et al., 2012; Sharma et al., 2018; Wardenier et al., 2019). At pH 8.5<, indirect reactions become predominant, having the ozonation process classified as an AOP (Parvulescu et al., 2012; de Luis and Lombraña, 2018). The decomposition of molecular O_3 in water producing $HO^{\bullet}$ is illustrated with the equations Eq. 4–10 (Andreozzi et al., 1999; Homem and Santos, 2011; Parvulescu et al., 2012):

- Hydroxide ion (HO^-) initiate the chain reactions of molecular O_3 decomposition, creating intermediate hydroperoxide ion (HO_2^-), which also reacts with O_3

$$HO^- + O_3 \rightarrow O_2 + HO_2^- \quad (4)$$
$$HO_2^- + O_3 \rightarrow HO_2^{\bullet} + O_3^{\bullet -} \quad (5)$$

- Unstable intermediates (superoxide anion radical $O_2^{\bullet -}$), ozonide anion radical ($O_3^{\bullet -}$) and hydrogen trioxy radical ($HO_3^{\bullet}$) are formed and used in reactions

$$HO_2^{\bullet} \leftrightarrow H^+ + O_2^{\bullet -} \quad (6)$$
$$O_2^{\bullet -} + O_3 \rightarrow O_2 + O_3^{\bullet -} \quad (7)$$
$$O_3^{\bullet -} + H^+ \rightarrow HO_3^{\bullet} \quad (8)$$
$$HO_3^{\bullet} \rightarrow HO^{\bullet} + O_2 \quad (9)$$

- If solution has low alkalinity and dissolved organic carbon, a fast side reaction starts to lessen the oxidation potential of the system

$$HO^{\bullet} + O_3 \rightarrow HO_2^{\bullet} + O_2 \quad (10)$$

Since ozonation efficiency is highly depended on the character of target substance and pH, ozonation has been combined with other processes to enhance the O_3 decomposition to $HO^{\bullet}$ (de Luis and Lombraña, 2018).

1.3.2 Enhanced ozonation

There are many different processes found to enhance indirect ozonation (Gligorovski et al., 2015). Ozone decomposition is accelerated in presence of homogenous or heterogeneous transition metal catalysts, such as Fe^{2+}, Fe^{3+}, Mn^{2+}, MnO_2 and Fe_2O_3 (Munter, 2001; Sharma et al., 2018). Heterogeneous catalysts cause O_3 breakdown by electron transfer from metal to O_3, generating $O_3^{\bullet-}$, which eventually leads to production of $HO^{\bullet}$ (Eq. 8-9). In presence of a homogeneous catalyst, $O_2^{\bullet-}$ is first formed from O_3, followed by an electron transfer from $O_2^{\bullet-}$ to another O_3 molecule (Eq. 7), creating $O_3^{\bullet-}$ and subsequently $HO^{\bullet}$ (Eq. 8–9) (Homem and Santos, 2011; Sharma et al., 2018).

Besides catalysis, O_3 may be combined with other oxidants. A combination of H_2O_2 with O_3 called peroxone has been found to enhance organic pollutants degradation. Although H_2O_2 could directly react with O_3 (Eq. 11), this reaction is rather slow. Ozone decomposition is rapidly initiated by conjugate base of H_2O_2 (HO_2^-) as described in Eq. 12–15 (Legrini et al., 1993; Hernandez et al., 2002; Parvulescu et al., 2012):

- Hydrogen peroxide direct reaction with molecular O_3

$$O_3 + H_2O_2 + \rightarrow O_2 + HO^{\bullet} + HO_2^{\bullet} \text{ (very slow)} \quad (11)$$

- Formation of hydroperoxide ion

$$H_2O_2 + H_2O \leftrightarrow H_3O^+ + HO_2^- \quad (12)$$

- Generation of $HO^{\bullet}$

$$O_3 + HO_2^- + \rightarrow HO^{\bullet} + O_2^{\bullet-} + O_2 \quad (13)$$
$$O_3 + O_2^{\bullet-} + \rightarrow O_3^{\bullet-} + O_2 \quad (14)$$
$$O_3^{\bullet-} + H_2O + \rightarrow HO^{\bullet} + HO^- + O_2 \quad (15)$$

Ozone decomposition with $HO^{\bullet}$ formation may also be accelerated with UV of proper wavelength. Due to O_3 having a high molar extinction coefficient of $\varepsilon = 3300\ M^{-1}\ cm^{-1}$, it readily absorbs UV light at 254 nm to create H_2O_2 as an intermediate. Under UV light, H_2O_2 decomposes into $HO^{\bullet}$ by homolytic cleavage of peroxide bond. Previously mentioned processes can be illustrated by the equations Eq. 16–18 (Andreozzi et al., 1999; Munter, 2001; Sharma et al., 2018):

- Photolysis of O_3 produces excited oxygen ($O^1(D)$), followed by formation of H_2O_2

$$O_3 + hv \rightarrow O^1(D) + O_2 \quad (16)$$
$$O^1(D) + H_2O \rightarrow H_2O_2 \quad (17)$$

- Homolytic cleavage of peroxide bond by UV light

$$H_2O_2 + hv \rightarrow 2HO^{\bullet} \quad (18)$$

Similarly, UV irradiation can also be used to decompose externally added H_2O_2 in solution. Furthermore, combination of both H_2O_2 and UV with O_3 can also improve formation of $HO^{\bullet}$ (Liu et al., 2018). However, the desired combinations have constraints. Since H_2O_2 has a low molar extinction coefficient of ε = 19,6 M^{-1} cm^{-1} at 254 nm, which is smaller than for some organic pollutants, it presents a limitation to the amount of generated $HO^{\bullet}$ and the overall process efficiency. Besides, the degradation efficiency can be inhibited by impurities in solutions and absorption of UV light by pollutants (Andreozzi et al., 1999; Munter, 2001; Sharma et al., 2018). While the cost of H_2O_2 is rather low, the energy consumed in generation O_3 makes the overall process costly, thus restricting the application in water treatment processes (Krichevskaya et al., 2011). The costs of AOPs application are discussed more in details in the chapter 1.5 Electric discharge AOPs.

1.3.3 Fenton and photo-Fenton processes

Classical Fenton reagent was first developed by Henry John Horstman Fenton in the 1890s. Traditional Fenton consist of H_2O_2 and catalyst ferrous ions (Fe^{2+}) in acidic medium at pH 3, where the solution has strong oxidizing properties. Hydroxyl radicals are generated through a series of reactions, where ferrous Fe^{2+} (Eq. 19) and ferric ion Fe^{3+} (Eq. 20) catalyze the H_2O_2 decomposition. During reactions, Fe^{2+} is utilized and regenerated in reactions Eq. 21–23. Fenton oxidation is illustrated with equations Eq. 19–23 (Homem and Santos, 2011):

- Hydrogen peroxide decomposition catalyzed by iron ions

$$Fe^{2+} + H_2O_2 \rightarrow Fe^{3+} + OH^- + HO^{\bullet} \quad (19)$$
$$Fe^{3+} + H_2O_2 \leftrightarrow H^+ + Fe(HO_2)^{2+} \quad (20)$$

- Regeneration of ferrous ion

$$Fe(HO_2)^{2+} \rightarrow Fe^{2+} + HO_2\cdot \quad (21)$$
$$FeOH^{2+} + H_2O_2 \rightarrow Fe(OH)(HO_2)^+ + H^+ \quad (22)$$
$$Fe(OH)(HO_2)^+ \rightarrow Fe^{2+} + HO_2^{\bullet} + OH^- \quad (23)$$

Similar to ozonation, the combination of Fenton with UV radiation (photo-Fenton) increases the process efficiency. The enhancement is mainly caused by photolysis of ferric iron complex, which produces Fe^{2+} and additional $HO^{\bullet}$ (Eq. 24) (Homem and Santos, 2011). A slower benefit consist of the direct photolysis of H_2O_2 (Eq. 18) (Sharma et al., 2018):

$$FeOH^{2+} + hv \rightarrow Fe^{2+} + HO^{\bullet} \quad (24)$$

Although Fenton process is highly capable of degradation of organic substances, its efficiency is dependent on pH. Since H_2O_2 becomes more stable at the pH lower than 3.0, Fe^{2+} reaction with H_2O_2 (Eq. 20) is inhibited in strongly acidic media (Homem and Santos, 2011). From the other side, at elevated pH (pH>4), ferric ion is precipitated as $Fe(OH)_3$

making the reduction of ferrous ion obstructed (Arslan-Alaton and Gurses, 2004; Homem and Santos, 2011). This makes the $Fe^{2+}/Fe^{3+}/H_2O_2$ system exhibit its maximum efficiency in a narrow pH diapason between 2.8 and 3.0, limiting its practical use (Arslan-Alaton and Gurses, 2004).

1.3.4 Photocatalytic oxidation

Photocatalytic oxidation is an AOP, in which a semiconductor, such as most commonly used titanium dioxide (TiO_2) is irradiated with UV light creating electron/hole pairs. After a photon with the energy equal to or higher than the energy bandgap of the semiconductor is absorbed, an electron is excited from the valence band into the conduction band generating a positive hole inside the valence band with oxidation potential of 3.5 V (Table 1) (Eq. 25) (Bahnemann, 2004; Sharma et al., 2018). In presence of oxygen and water, the electron/hole pair may produce highly reactive species on semiconductor surface, $HO^{\bullet}$ and $O_2^{\bullet-}$ (Eq. 26 – 28) (Homem and Santos, 2011; Sharma et al., 2018).

$$TiO_2 + hv \rightarrow h^+ + e^- \quad (25)$$

$$h^+ + H_2O \rightarrow HO^{\bullet} + H^+ \quad (26)$$

$$h^+ + HO^- \rightarrow HO^{\bullet} \quad (27)$$

$$e^- + O_2 \rightarrow O_2^{\bullet-} \quad (28)$$

While photocatalysis has the benefit being activated with the UV fraction of the direct or diffused sunlight, the industrial scale application suffers several limitations: the screening effect of impurities blocking the UV light from activation of the catalyst, and the difficulties associated with separation of the catalyst slurries. Fixed layer catalysts usually have a big deal of the lost contact surface thus showing seriously reduced efficiencies (Homem and Santos, 2011).

1.4 Persulfate AOPs

An interest towards oxidation of recalcitrant and micro-pollutants in reactions with sulfate radicals (SR-AOP) has recently arisen. The SR-AOP process uses sulfate radicals ($SO_4^{\bullet-}$), which are highly reactive (E^0 = 2.60 V) and non-selective oxidants (He et al., 2014; Zhang et al., 2015; Matzek and Carter, 2016). Although $SO_4^{\bullet-}$ may react with organic pollutants through hydrogen abstraction and electrophilic addition, these pathways are unlikely, having pollutants mainly degraded via electron transfer (Matzek and Carter, 2016; Y. Liu et al., 2016). Sulfate radicals are generated by activation of either persulfate ($S_2O_8^{2-}$; PS) or peroxymonosulfate (HSO_5^-; PMS) (Zhang et al., 2015). Compared to PMS, PS is used more often for the lower energy of bond dissociation, i.e., having theoretically lower energy needed for the radicals formation. Besides, PMS has the standard oxidation-reduction potential of 1.4 V lower than the one of PS, 2.01 V. Although PMS and PM can react directly with pollutants, these reactions are usually slow, the reactants need to be activated to generate $SO_4^{\bullet-}$ (Wacławek et al., 2017). Eq. 29 shows the general activation mechanism (Matzek and Carter, 2016):

$$S_2O_8^{2-} + \text{activator} \rightarrow SO_4^{\bullet-} + (SO_4^{\bullet-} \text{ or } SO_4^{2-}) \quad (29)$$

The activation may be provided in two ways: the energy- and the catalysis-based activations. In energy-based activation, the peroxide bond (O - O) is fissured to produce $SO_4^{\bullet-}$ (Eq. 30–31) (Zhang et al., 2015):

$$HSO_5^- + \text{energy} \rightarrow SO_4^{\bullet-} + HO^{\bullet} \quad (30)$$

$$S_2O_8^{2-} + \text{energy} \rightarrow 2SO_4^{\bullet-} \quad (31)$$

The energy may be delivered either by heat, UV, radiolysis or ultrasound (Zhang et al., 2015). For example, ionizing radiation may act concurrently activating persulfate and purifying the water. The ionizing radiation in water generates oxidative species $HO^{\bullet}$, $HO_2^{\bullet}$, and H_2O_2, and reductive ones - aqueous electrons e_{aq}^- and hydrogen radicals $H^{\bullet}$. Although the main two reactive species are $HO^{\bullet}$ and e_{aq}^-, electrons are mostly scavenged by dissolved oxygen forming less reactive $O_2^{\bullet-}$. The addition of persulfate, however, provides an effective use of e_{aq}^- activating $S_2O_8^{2-}$ for $SO_4^{\bullet-}$ formation illustrated in Eq. 32–34 (Criquet and Karpel Vel Leitner, 2011):

- Radiolysis of water

$$H_2O \rightarrow 0.27e_{aq}^- + 0.06H^{\bullet} + 0.27HO^{\bullet} + 0.27H^+ + 0.045H_2 + 0.07H_2O_2 \quad (32)$$

- Aqueous electron scavenging by dissolved oxygen

$$e_{aq}^- + O_2 \rightarrow O_2^{\bullet-} \quad (33)$$

- Persulfate activation by e_{aq}^-

$$S_2O_8^{2-} + e_{aq}^- \rightarrow SO_4^{\bullet-} + SO_4^{2-} \quad (34)$$

The other activation method is catalysis (Zhang et al., 2015). Catalysts include transition metals, non-metal activators, e.g., activated carbon, and alkalis. Oxidants may also be activated electrochemically (Liang et al., 2009; Furman et al., 2010; Chen et al., 2014; Matzek and Carter, 2016). For example, PS is activated by one electron transfer using iron, silver, zinc, cobalt, manganese or copper catalysts (Matzek and Carter, 2016). Activation using transition metal catalysts may be illustrated with Eq. 35–36 (Zhang et al., 2015):

$$HSO_5^- + M^{n+} \rightarrow M^{(n+1)} + SO_4^{\bullet-} + OH^- \quad (35)$$

$$S_2O_8^{2-} + M^{n+} \rightarrow M^{(n+1)} + SO_4^{\bullet-} + SO_4^{2-} \quad (36)$$

Iron is the most widely studied transition metal in catalysis being an effective, low-cost and environmentally friendly activator. Persulfate may be activated by zero-valent iron or ferrous ions Fe^{2+}. It was found out, that the activation efficiency in the $S_2O_8^{2-}/Fe^{2+}$ combination is dependent on ferrous ions concentration, making the oxidant/catalyst pair sensitive to the dosing of Fe^{2+}: the shortage of activator makes persulfate activation ineffective, whereas an excess of it scavenges a part of $SO_4^{\bullet-}$ radicals. The activation and scavenging of in persulfate reactions are shown in Eq. 37–39 (Matzek and Carter, 2016):

- Zero-valent iron-based activation

$Fe^0 + S_2O_8^{2-} \rightarrow Fe^{2+} + 2SO_4^{2-}$ (37)

- Ferrous ion-based activation

$S_2O_8^{2-} + Fe^{2+} \rightarrow Fe^{3+} + SO_4^{2-} + SO_4^{\bullet-}$ (38)

- Sulfate radical scavenging by Fe^{2+}

$SO_4^{\bullet-} + Fe^{2+} \rightarrow Fe^{3+} + SO_4^{2-}$ (39)

Regardless of activation methods, PS has been used to remove micropollutants from soil, water, groundwater and wastewater (Matzek and Carter, 2016; Wang and Wang, 2018; Kaur et al., 2019; Kaur and Dulova, 2020).

1.5 Electric discharge AOPs

1.5.1 Electric discharges: types, characteristics and applications

There is a growing interest in application of plasma-based water treatment technologies due to the progress in power electronics solutions accompanied with design and production of high capability electronic devices at their growing availability. Progressive application of electric discharges towards aqueous media treatment resulted in formation of a new branch of AOPs, plasma-based processes. These processes involve *in situ* generation of highly reactive oxygen species (ROS), including O_3 and $HO^{\bullet}$, applied to water treatment (Becker et al., 2005; Parvulescu et al., 2012; Yang et al., 2012; Chu and Lu, 2013; Jiang et al., 2014; Ajo et al., 2015; Bruggeman et al., 2016). Commonly, however, the electric discharge applications are often associated with the O_3 generation in ozonation cells by using dielectric barrier discharge (DBD) (Figure 1.) (Schiavon et al., 2012). Conventional ozonation, however, has certain drawbacks shortly discussed here. Since O_3 gas has a relatively long lifetime, 10 to 60 min in air, O_3 is produced remotely before being delivered into the treated aqueous media solution with the gas stream. While other short-living oxidants are also formed in the discharge, such as, e.g., $O^{\bullet}$, these cannot be transported to the solution due to significantly shorter lifetimes. This makes a part of energy wasted in useless production of short-living oxidants having no chance to be utilized in the target reactions. One should keep in mind that the electric discharge, being a highly non-equilibrium medium, creates conditions for not only dissociation of oxygen with subsequent ozone synthesis, but also dissociation of ozone thus making the ozone synthesis a reversible process and ozone – an equilibrium, i.e., residual product of the reverse overall reaction (Eq. 40):

$3O_2 \rightarrow 2O_3$ (40)

A part of energy in DBD of the ozone generation cell is spent for the maintenance of the equilibrium between oxygen and ozone. Besides, O_3 is only partially consumed in degradation reactions due to its poor solubility in water. The residual ozone must be destroyed thermally or thermo-catalytically thus wasting the energy even more. The ozone generation cells are cooled contributing to overall costs together with the necessity to waste the bulk amounts of dry air or oxygen used as ozone transportation media. These circumstances brings to front the idea of using the electric discharge

plasma technologies directly in water treatment for full utilization of ROS, increasing overall efficiency (Becker et al., 2005; Parvulescu et al., 2012; Yang et al., 2012; Chu and Lu, 2013; Ajo et al., 2015; Bruggeman et al., 2016).

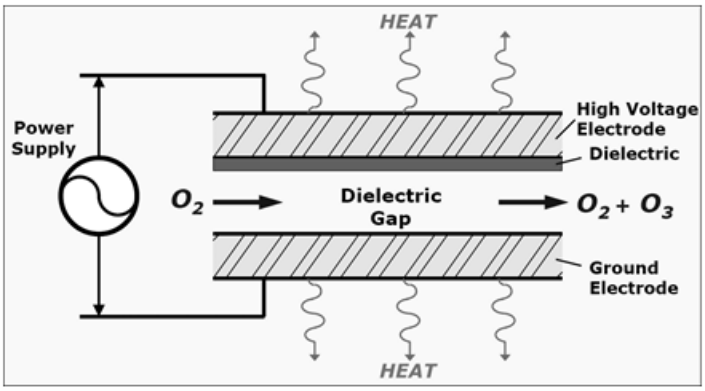

Figure 1. Dielectric barrier discharge ozone generator cell schematic outline (Schiavon et al., 2012)

The term 'plasma' refers to a fourth state of matter, in which a fraction of gas is ionized (Yang et al., 2012). If a solid referring to as the first state of matter is provided with enough heat, the particles loosen their structure and start to melt forming the second state of matter, a liquid. Further energy delivery results in the liquid vaporizing to the third state of matter, a gas. If gas is provided with sufficient energy in the form of electric discharge, the electrons escape from atoms and molecules forming gas-phase ions. These not only move freely, but also generate additional ions and electrons through collisions with electrons accelerated by the electric field, thermal energy, radiation and beams (UV photons, lasers). Ultimately, large amounts of ions and electrons are generated alternating the gas properties, consequently becoming a plasma or ionized gas (Chu and Lu, 2013; Meichsner et al., 2013). The transitions of states of mater caused by heat can be illustrated with Figure 2 (Chu and Lu, 2013).

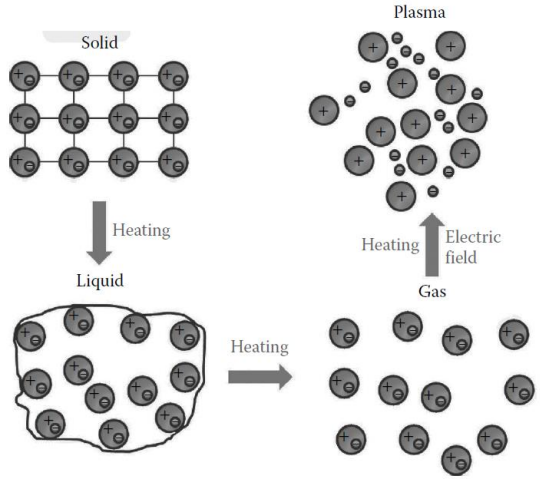

Figure 2. Transition of states of matter caused by heat (Chu and Lu, 2013)

Based on thermal equilibrium, plasmas are divided into two main categories: thermal and non-thermal plasmas. In case of thermal equilibrium, electrons, ions and heavy neutral particles are in thermal balance, i.e. at equal temperature (Chu and Lu, 2013). These are usually operated in power range of kW to MW and at high temperatures of 10,000 K and higher. Although thermal plasmas could also be used in water treatment providing full mineralization of organic compounds, they are too destructive, leaving behind no treated water itself. Besides, huge amount of energy is needed for thermal plasma formation, putting treated media and reactor walls under severe thermal stress (Meichsner et al., 2013). In water treatment, non-equilibrium non-thermal plasmas are used, where only electrons are heated to high temperatures (~10,000 K), while heavy neutral molecules and ions remain at an ambient temperature. Compared to thermal plasmas, cold plasma energy consumption is relatively low since heating of the medium is unnecessary, having only high-energy electrons for generation of reactive species. Heating of electrons is achieved through implementation of external electric field, where electrons gain sufficient energy by acceleration (Chu and Lu, 2013). High energy (1–10 eV) electrons collide with background gas molecules and atoms breaking chemical bonds and produce new variety of electrons, free radicals and ions. Since the electron collide with a heavy particle, only a 10^{-4} energy fraction is transferred to the latter due to a large mass difference, making the heavy particles staying at significantly lower temperature than the electron temperature (Parvulescu et al., 2012; Chu and Lu, 2013).

As previously mentioned, O_3 is one of the main active reactive species produced in gas-phase non-thermal plasma if oxygen-containing gas is used (Parvulescu et al., 2012). It is proposed that generation of O_3 is composed of two stages, excitement and dissociation of oxygen molecules by high-energy electron impacts (Eq. 41–43) followed by three-body reaction of O_3 formation (Eq. 44–46) (Chu and Lu, 2013). The third body is needed for energy and momentum conservation, i.e., for absorbing the excess energy. In air, high-energy electrons dissociate stable nitrogen molecules N_2 to atomic nitrogen radicals $N^{\bullet}$ (Eq. 44). Those may also initiate the first step of ozone generation (Eq. 45) (Magureanu et al., 2018). Ozone three-body reaction with O_2 and N_2 can be illustrated with following equations (Eq. 41–47) (Parvulescu et al., 2012; Chu and Lu, 2013; Magureanu et al., 2018):

- Oxygen molecule dissociation into $O^{\bullet}$

$$O_2 + e^- \rightarrow O^+ + O^{\bullet} + 2e^- \quad (41)$$
$$O_2 + e^- \rightarrow 2O^{\bullet} + e^- \quad (42)$$
$$O_2 + e^- \rightarrow O^- + O^{\bullet} \quad (43)$$

- Atomic oxygen generation from nitrogen species, $N^{\bullet}$ and nitric oxide radical $NO^{\bullet}$

$$N_2 + e^- \rightarrow 2N^{\bullet} + e^- \quad (44)$$
$$N^{\bullet} + O_2 \rightarrow NO^{\bullet} + O^{\bullet} \quad (45)$$
$$N^{\bullet} + NO^{\bullet} \rightarrow N_2 + O^{\bullet} \quad (46)$$

- Ozone formation through the three-body reaction

$$O^{\bullet} + O_2 + M \rightarrow O_3 + M \qquad M = O_2, O_3, O^{\bullet} \text{ or } N_2 \quad (47)$$

Participation of nitrogen species in ozone generation, however, makes the generation of O_3 in air slower (~ 100 µs) than in pure oxygen (~10 µs) due to production of nitrogen oxide species, $NO^{\bullet}$ and NO_2 (Chu and Lu, 2013). While nitrogen compounds contribute to the ozone generation (Eq. 44 – 46), the contribution may result in a negative effect if the concentration of nitrogen and nitrogen oxide is high. These might start to quench oxygen atoms and destroy O_3 (Eq. 48 – 51) (Lukes et al., 2005).

$$O^{\bullet} + NO^{\bullet} + N_2 \rightarrow NO_2 + N_2 \quad (48)$$
$$O^{\bullet} + NO_2 \rightarrow NO^{\bullet} + O_2 \quad (49)$$
$$N^{\bullet} + O_3 \rightarrow NO^{\bullet} + O_2 \quad (50)$$
$$NO^{\bullet} + O_3 \rightarrow NO_2^{\bullet} + O_2 \quad (51)$$

Besides O_3 formation, other undesired side reactions are taking place limiting the amount of generated O_3. If $O^{\bullet}$ concentration becomes high, recombination into oxygen molecule starts to dominate (Eq. 52–53). Higher temperatures also accelerate decomposition of unstable ozone (Eq. 54) (Ono and Oda, 2003; Chu and Lu, 2013).

$$O^{\bullet} + O^{\bullet} + M \rightarrow O_2 + M \qquad M = O_2, O_3, O^{\bullet} \text{ or } N_2 \quad (52)$$
$$O^{\bullet} + O_3 + M \rightarrow 2O_2 + M \qquad M = O_2, O_3, O^{\bullet} \text{ or } N_2 \quad (53)$$
$$O_3 + O_2 \rightarrow O^{\bullet} + O_2 + O_2 \quad (54)$$

In presence of water vapor, O_3 generation is less efficient than in dry gas: the addition of 2.4% wt. of water reduced the amount of produced O_3 by the factor of six. This is likely related to the shorter lifetime of $O^{\bullet}$ in humid air, reducing the amount of generated O_3 (Eq. 47) (Ono and Oda, 2003). However, the water-electron collision can generate other reactive species, such as H_2O_2 and $HO^{\bullet}$ (Eq. 55–59). Dependent on the plasma type, surrounding environment, applied electrical parameters (character and value of voltage and current) and temperature, a variety of reactions are expected. For example, over a 500 probable reactions have been proposed in He plasma for water-electron collisions (Parvulescu et al., 2012). Nevertheless, a broad view may still be derived: $HO^{\bullet}$ mostly formed from water dissociation by high energy electrons (Eq. 55) may recombine into hydrogen peroxide (Eq. 57) (Lukes et al., 2005; Parvulescu et al., 2012; Magureanu et al., 2018). Besides, in humid air, nitrogen oxide species may form resulting in the decreased pH related to $NO^{\bullet}$ and nitrogen dioxide radical $NO_2^{\bullet}$ species dissolved in water forming nitrous and nitric acids (Eq. 58–60) (Parvulescu et al., 2012; Kornev et al., 2013).

- Hydroxyl and hydrogen radical formation from water

$$H_2O + e^- \rightarrow H^{\bullet} + HO^{\bullet} + e^- \quad (55)$$
$$H_2O + e^- \rightarrow 2H^{\bullet} + O^{\bullet} + e^- \quad (56)$$

- Formation of hydrogen peroxide

$$HO^{\bullet} + HO^{\bullet} \rightarrow H_2O_2 \quad (57)$$

- Formation of nitrogen oxide species

$$NO^{\bullet} + HO^{\bullet} \rightarrow HNO_2 \quad (58)$$

$HNO_2 + HO^\bullet \rightarrow NO_2^\bullet + H_2O$ (59)
$NO_2^\bullet + HO^\bullet \rightarrow HNO_3$ (60)

Besides reactive species, plasmas provide UV emissions dependent in their intensity on the variety of conditions, i.e., type of plasma and the gas composition. The generated UV light emission might be used to dissociate H_2O_2 (Eq. 18), oxygen (Eq. 61) and water (Eq. 62), together with reaction of nitrogen oxide dissociation (Eq. 63), producing $O^\bullet$ and O_3 (Eq. 46 - 47) (Parvulescu et al., 2012).

$O_2 + hv \rightarrow O^\bullet + O^\bullet$ (61)
$H_2O + hv \rightarrow H^\bullet + HO^\bullet$ (62)
$NO_2^\bullet + hv \rightarrow NO^\bullet + O^\bullet$ (63)

In addition to operation in a gas phase with or without water vapor, electric discharges can also be operated in gas-liquid mixtures, as well as in liquid (Parvulescu et al., 2012; Mieno, 2016; Wardenier et al., 2019). Possible ways of electrons interaction with water is present in Figure 3 (Parvulescu et al., 2012). Formed in continuous liquid media, plasmas either form a plasma channel between electrodes or produce bubbles as a result of liquid evaporation by local heating at the tip of an electrode (Yang et al., 2012). Eventually, the bubble implosion may also have a shocking effect on the liquid and the discharge. The liquid discharges, however, are more complex than the gas-phase ones, because of the electrodes' erosion in high-temperature discharge channels and the liquid evaporation destabilizing the discharge. In addition, plasma generation in liquids needs higher energies due to higher density of fluids, i.e. requiring more energy for electrical breakdown (Bruggeman and Leys, 2009). For the gas-liquid configuration, in which water is a discrete phase, plasma interacts with water molecules as the air humidity, or water is sprayed in the gas phase in the form of aerosols, droplets, jets and films, electric discharge formation is easier and more stable. Plasma may be positioned over the still surface of treated water, where it may impinge the solution. Even in presence of liquid, the gas-phase plasma chemistry is similar to the one of gas-liquid mixtures, having the description of reactions given above applicable (Parvulescu et al., 2012).

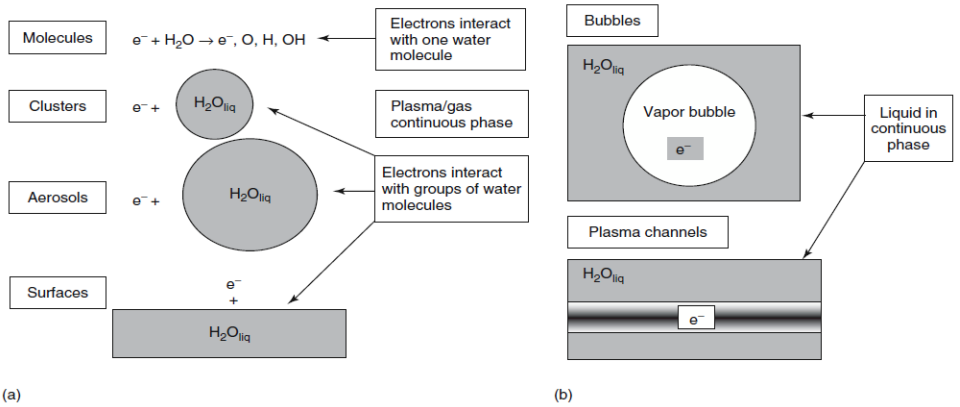

Figure 3. Plasma possible contact with gas (a) and liquid (b) phase (Parvulescu et al., 2012)

For gas-phase plasmas, the contact surface between liquid and plasma is usually improved by making the treated solution flowing as a thin film (Grabowski et al., 2007), spraying solution into plasma zone as droplets and jets (Preis et al., 2013; Sugai et al., 2015) or even using atomizing nozzles producing aerosols (Pokryvailo et al., 2006; Jiang et al., 2014). Regardless of configuration, the plasma-liquid contact surface was reported to be an important parameter providing enhancement of oxidation efficiency with its enlargement mainly by increasing beneficial utilization of radicals (Pokryvailo et al., 2006; Malik, 2010; Preis et al., 2013; Jiang et al., 2014; Ajo et al., 2015; Sugai et al., 2015; Mieno, 2016). Similarly, the input power and the generator-reactor electric capacity matching are important parameters directly affecting the pollutant degradation and mineralization efficiency (Jiang et al., 2014; Kornev et al., 2017).

1.5.2 Dielectric barrier discharge

Dielectric barrier discharge was used by Siemens in 1857 for the first time to generate O_3 (Kogelschatz, 2003). Since DBD is operable at atmospheric conditions, it has been nowadays one of the most popular plasma types for the research in air and water treatment. As was mentioned earlier, DBD is applied mostly in the form of ozone generators (Kogelschatz, 2003; Schiavon et al., 2012; Chang et al., 2022). Dielectric barrier discharge consist of two metal electrodes, the high voltage and the grounded electrode with the discharge gap ranging from less than 0.1 mm up to a few centimeters (Kogelschatz, 2003). At atmospheric pressure, the gap is usually not exceeding 1.0 cm, the electrodes are energized by high voltage from 1 to 20 kV, and the amplifying current frequencies of 50 Hz to 500 kHz are used. In order to avoid formation of thermal plasmas, sparks or arcs, one or both electrodes are covered with a dielectric material having a breakdown field strength exceeding air many times in configurations shown in Figure 4 (Becker et al., 2005; Chu and Lu, 2013; Meichsner et al., 2013; Lukes et al., 2014). After applying sufficiently high voltage to the electrodes, electrical current flows through the gaseous medium between those. This causes electrical charges accumulating on the surface of dielectric, thus creating an electrical potential counteracting the applied high voltage (Becker et al., 2005). The former inhibits the current and suppress formation of arcs and sparks. However, since the electrical charges may stay on the dielectric surfaces for a few seconds exceeding the time of the applied voltage amplifying period (milliseconds), the second pulse with the same polarity cannot generate a discharge due to the described counteraction of the surface charge. Therefore, DBD cannot be operated with the direct current, but only with voltage variation, such as pulsed and alternating voltage with sine waves providing the displacement current (Parvulescu et al., 2012). In addition, the dielectric barrier helps even spreading of the micro-discharges, which are formed during the charge accumulation. Due to the interaction of deposited surface charges, the electric field created by the applied voltage collapses, until the external voltage is varied again to produce new micro-discharges distributed evenly over the whole dielectric surface. In DBD, microdischarges can be considered as tiny non-thermal plasma chemical reactors (Becker et al., 2005; Chu and Lu, 2013).

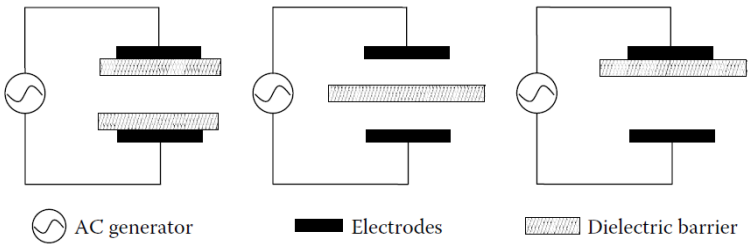

Figure 4. Configurations of dielectric barrier discharge (Chu and Lu, 2013)

1.5.3 Corona discharge

Similarly to DBD, corona discharge (CD) may be operated at atmospheric pressure and has been widely used for treatment of water and air in the form of ozone generation (Chu and Lu, 2013). Corona discharge occurs in the inter-electrode areas of electric field concentration near the curved surfaces, needles or thin wires (Meichsner et al., 2013). These discharges expand into outer space of the curved surface, where the electric field decreases until the discharge is not further supported (Parvulescu et al., 2012). Therefore, ionization and emission in CD is happening only around the needle or the wire. Corona discharge is also known as a partial discharge, since the discharge does not reach the opposite counter-electrode (Chu and Lu, 2013).

Corona discharge cell consists of power supply generator, high voltage electrode and grounded electrode (Ajo et al., 2015). Dependent on the electrode placement, there is a variety in the cell geometries (Parvulescu et al., 2012; Chu and Lu, 2013). In Figure 5, the principle configurations of corona discharge electrodes are shown (Parvulescu et al., 2012). The needle-to-plate configuration has been mostly used in laboratory studies, although industrial applications use wire-to-plane and wire-to-cylinder geometries ensuring more homogeneous distribution of the discharge. Dependent on the type of power supply, CDs are distinguished as continuous and pulsed discharges. Continuous CDs are generated by direct or low-frequency alternating voltages. Since the continuous CD at high currents may transform into stationary glow or spark discharge, it is generated only if the current is restricted (Parvulescu et al., 2012). The spark formation is avoided in pulsed corona discharge (PCD), where ultra-short voltage pulses of nanosecond duration scale are applied to electrodes providing application of higher voltages and currents (Parvulescu et al., 2012; Chu and Lu, 2013; Kornev et al., 2017). Higher voltage strengthens the electric field accelerating electrons, thus raising the rate of gas molecules' ionization and dissociation, having the gas temperature kept low: ultra-short pulses significantly accelerate only electrons. These PCD properties make it preferred in environmental applications (Parvulescu et al., 2012; Chu and Lu, 2013).

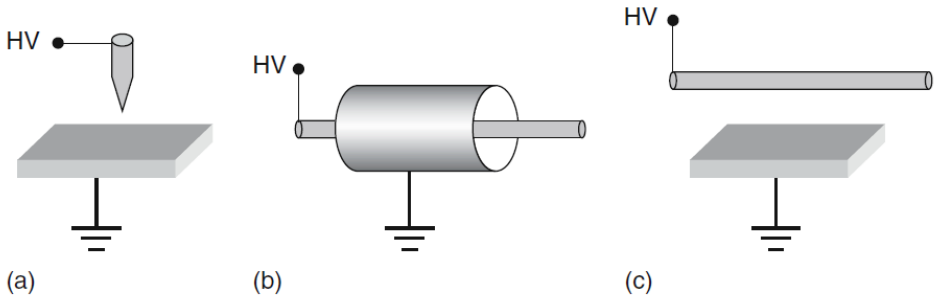

Figure 5. Configuration of corona discharges: a) needle-to-plate; b) wire-to-cylinder and c) wire-to-plane; HV – high voltage (Parvulescu et al., 2012)

Corona discharges have been successfully formed in the gas phase, gas-liquid mixtures and directly in liquid (Pokryvailo et al., 2006; Bruggeman and Leys, 2009; Malik, 2010; Panorel et al., 2011). However, direct discharges in liquid have been reported to be more energy consuming and less efficient than coronas above water. The submerged corona discharge is likely related to the gas bubbles and channels inside water requiring heating and vaporization (Hoeben et al., 1999; Pokryvailo et al., 2006). For example, phenol was reported having two orders of magnitude higher degradation efficiency in corona above water than in the in-bulk discharge (Hoeben et al., 1999). Pulsed corona discharge applied to the gas-liquid mixtures with the continuous gas phase was reported having the highest efficiency among non-thermal plasmas, where the treated water is sprayed directly into the plasma zone in the form of jets and droplets of 1–3 mm (Malik, 2010; Kornev et al., 2017). The efficiency of 50% degradation of indigo carmine reached 622 g kW^{-1} h^{-1} in PCD treatment of water sprayed in air, 294 g kW^{-1} h^{-1} in air PCD over a thin film of water, and only 1.38 g kW^{-1} h^{-1} in the in-bulk PCD with O_2 bubbling (Malik, 2010).

Previous studies clarified, that in the presence of water in the discharge zone short-living ROS are formed at the gas side of the gas-liquid interface (Ajo et al., 2017). Since the reactive species except O_3 have the life time too short for any transportation, e.g., $HO^{\bullet}$ has the maximum lifetime of about 200 µs in gas and about 20 µs in aqueous media, these may only react with pollutants at the gas-liquid interface or in close vicinity to it (Malik, 2010; Parvulescu et al., 2012; Guerra-Rodríguez et al., 2018). Differently to $HO^{\bullet}$, long-living O_3 may participate in reactions at the gas-liquid interface and being dissolved in the bulk solution (Preis et al., 2013). Under these circumstances, the plasma-liquid contact surface becomes utterly important for effective utilization of short-living ROS. Water spraying directly to the plasma zone with even distribution of the droplets becomes an important control factor of water treatment with PCD (Malik, 2010). The benefits of enlarged gas-liquid contact surface by increased spray flowrate in the PCD reactor were observed in respect to the degradation of rapidly reacting phenol (Preis et al., 2013), slowly oxidized oxalate (Ajo et al., 2015), and indigo carmine (Sugai et al., 2015), thus confirming the efficient utilization of ROS dependent on the treated surface.

The usage of PCD reactors has been restricted by a lack of reliable pulse generator. Although water sprayed into the discharge zone has the benefit of the developed surface, plasma research groups rarely use them. In the wire-to-plate configuration, where the high-voltage electrodes are placed horizontally between two vertical

grounded plates, water droplets alter the electric field pattern in the inter-electrode gap changing the discharge propagation with the risk of high-temperature spark formation damaging the electrodes. The sparking is related to the residual voltage remaining at the electrodes up to the value of 13 – 15 kV at applied voltage of 20 kV, after the discharge current goes to zero as shown on Figure 6 (Kornev et al., 2017). The problem was solved with the application of saturating inductor resulting in the pulse duration reduced to about 100 ns and the pulse shape changed to the bipolar one (Preis et al., 2016). This modification eliminated sparks observed in the treatment of relatively low conductivity solutions, up to 3.0 mS cm^{-1}, and significantly reduced the number of sparks formed in the treatment of conductive electrolyte solutions. Although some sparks are still formed in the treatment of solutions with conductivity above 10 mS cm^{-1}, these do not affect the current and voltage waveforms of PCD and leave no erosion marks on electrodes even after several years of treatment of up to 120 mS cm^{-1} conductivity solutions. One may conclude that a reliable PCD method was developed for water and wastewater treatment (Kornev et al., 2017).

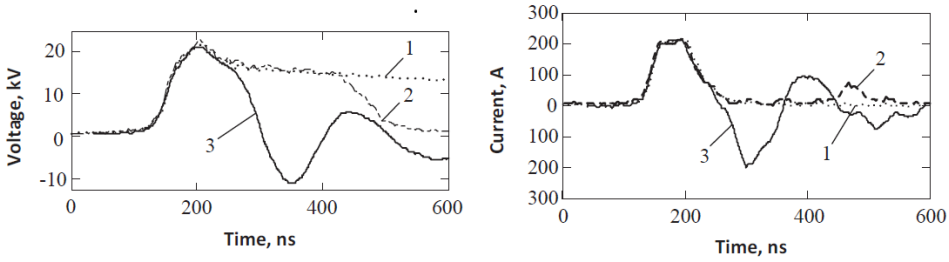

Figure 6. Waveform of voltage and current in diverse plasma discharge modes; 1 – long pulse; 2 – a partial breakdown after 300 ns in long pulse; 3 – pulse with saturable inductor applied (Kornev et al., 2017)

The PCD treatment, in which the treated aqueous medium is sprayed directly to the plasma zone, has been studied in oxidation of a variety of substances. The data obtained from the available literature for non-assisted PCD treatment in ambient conditions is presented in Table 3, where oxidation efficiency (g kW^{-1} h^{-1}) is given as ratio of pollutant amount removed per unit of pulsed energy delivered to the reactor. Besides substances shown in Table 3, PCD has been used to treat hospital wastewaters, containing pharmaceuticals. For example, with the energy dose of 1.0 kWh m^{-3} delivered to the PCD reactor, the pharmaceuticals in the hospital raw wastewater containing 29 quantified compounds in concentration range from 0.21 to 580 µg L^{-1} were removed for at least 89%. Only hydrocortisone (c_0 = 0.45 µg L^{-1}), metronidazole (c_0 = 0.37 µg L^{-1}) and caffeine (c_0 = 470 µg L^{-1}) showed stronger resistance to oxidation, being removed for only 22%, 18% and 19%, respectively. Similarly, biologically treated effluent of a healthcare institute containing 17 quantified pharmaceuticals in concentration range of 0.007–3.1 µg L^{-1} was treated by PCD. The pulsed energy dose of 0.1 kWh m^{-3} was sufficient to decrease the total content of drugs (6.286 µg L^{-1}) by 90.7%, leaving few residuals, such as, e.g., metronidazole (c_0 = 0.059 µg L^{-1} → $c_{residual}$ = 0.025 µg L^{-1}). Complete removal of drugs was achieved with the PCD energy dose of 0.5 kWh m^{-3}. These results showed that PCD has a potential in pre-treatment of the hospital wastewater with higher concentrations of target micro-pollutants in smaller volumes of

the wastewater, thus having higher energy efficiencies. Alternatively, PCD could provide an effective tertiary treatment (Ajo et al., 2018).

Although non-assisted PCD has shown promising results in both simulated and real-life applications, the efficiencies were obtained mainly at a fixed gas-liquid contact surface. Even though a few studies examined the effect of contact surface on the pollutant degradation, the values of interface area were varied within narrow range (Panorel et al., 2011; Preis et al., 2013; Kornev et al., 2014; Ajo et al., 2015). Likewise, wastewaters may contain surfactants, such as sodium dodecyl sulfate (SDS), affecting surface PCD reactions: dependent on the target pollutant structure, addition of SDS either inhibits or enhances PCD oxidation efficiency, although the observation was made only at a fixed gas-liquid interface area (Wang et al., 2019; Onga et al., 2020, 2021, 2022). Variation of the contact surface in PCD treatment, however, is of extreme importance determining the energy efficiency in optimization of the treatment parameters, and thus deserves attention.

As with other AOPs, PCD combination with extrinsic oxidants may exceed the energy efficiency of the non-assisted PCD (Jiang et al., 2014). Previously, a synergy combination of PCD with H_2O_2 was found for 4-chlorphenol, although in-liquid PCD was applied (Wen et al., 2005). At the same time, the addition of H_2O_2 to the N-nitrosodiethylamine solution showed only neutral effect in the gas-phase PCD (Kask et al., 2021a). Therefore, combinations of PCD with extrinsic oxidants may have an effect and should be studied in respect of other pollutants. For example, PS was studied as the extrinsic oxidant, although under conditions of discharges incomparable with the present research (Parvulescu et al., 2012; Jiang et al., 2014; Tang et al., 2018). The author failed to find published articles regarding PS combination with PCD, although the potential generation of $SO_4^{\bullet-}$ could led to higher degradation rates, i.e., energy efficiencies.

Table 3. Degradation of different compounds with PCD at ambient conditions

Substance	Initial concentration, mg L^{-1}	Energy efficiency, g kW^{-1} h^{-1}	References
Indomethacin	100.0	150.0	(Panorel et al., 2013)
Ibuprofen		41.0	
Paracetamol		52.0	
β-Oestradiol	3.0	3.8	
Aqueous dissolved oil fractions	~2 – 7.0	12.5	(Kornev et al., 2014)
Aqueous benzene	15.0	28.0	(Kornev and Preis, 2016)
	94.0	59.0	
Carbamazepine	99.0	125.0	(Ajo et al., 2016)
	127.0	189.0	
	0.00083	0.008	
	0.00221	0.017	
Phenol	100.0	47.0	(Wang et al., 2019)
Oxalic acid		30.0	
Humic substances	10.0	5.5	
Reactive Blue 4	40.0	132.8	(Onga et al., 2020)
Reactive Blue 19		132.0	
Alachlor	2.0	8.1	(Bolobajev et al., 2021)
	20.0	21.2	
Ibuprofen	10.0	20.0	(Derevshchikov et al., 2021)
Diclofenac		53.0	
Metformin		15.0	
Tramadol		89.0	
N-nitrosodiethylamine	1.02	1.42	(Kask et al., 2021a)
Aqueous toluene	1.0	6.4	(Kask et al., 2021b)
	3.7	7.5	
	6.3	8.6	
Paracetamol	48.0	39.0	(Onga et al., 2021)
Indomethacin	42.0	129.0	
Acid Orange 7	10.0	66.0	
Indigotetrasulfonate	35.0	676.0	
Dexamethasone	10.0	8.9	(Onga et al., 2022)

1.6 Target compounds under consideration

For the current thesis, **oxalate (OXA)** was chosen as a model pollutant due to having refractory properties towards conventional chemical oxidation, i.e. OXA can be regarded as slowly reacting compound (Beltrán et al., 2002; Vecitis et al., 2010). Naturally occurring compound in plants and even synthesized inside human body (Castellaro et al., 2015),

OXA is regularly formed as intermediate or end product in oxidation of organic pollutants (Beltrán et al., 2002). While OXA is regularly obtained from plant consumption by humans, it is not metabolized in the human body, being either excreted or accumulated. At high concentrations, OXA may cause harmful health effects, such as kidney damage, lithiasis and even breast cancer (Castellaro et al., 2015; Patel et al., 2018). In household and industrial application, OXA has wide array of usage, such as bleaching and rust removal. Therefore, OXA is discharged to the aqueous environment being present in wastewaters (Martínez-Huitle et al., 2008; Vecitis et al., 2010).

In scientific research, **phenol** is often used as a model pollutant for the data availability from a significant number of research reports (Pokryvailo et al., 2006; Mohd, 2020). In the present thesis, phenol was used as a fast reacting pollutant, serving as a reference substance contrary to the slowly degrading OXA (Preis et al., 2013). Phenol is an aromatic compound formed naturally in decomposition of some organic substances, such as, e.g., lignin (Cotrim da Cunha et al., 2001). Industrially, phenol is mainly synthesized with cumene process (Michałowicz and Duda, 2007) and used in plentiful applications, e.g., as a raw material in plastic synthesis, such as bisphenol A (Prokop et al., 2004). Beside plastics, phenol is used in petroleum refineries, pharmaceuticals, and pulp and paper industries (Eryılmaz and Genç, 2021). Phenol concentration in industrial wastewaters have been found in the range from 1 to 7,000 mg L^{-1} (Mohd, 2020). In natural surface waters, phenol was detected between 2.6 and 5.6 µg L^{-1} (Michałowicz and Duda, 2007).

Bisphenol A (BPA) is a chemical used widely as monomer for polycarbonate plastics of excellent chemical and physical properties, e.g., thermal stability and strength. Polycarbonates made of BPA are used in production of plastic bottles, toys, sportswear, CDs etc. Also, BPA is used as a bulk chemical for epoxy resins, stabilizer and antioxidant for plastics (Yamamoto et al., 2001; Ma et al., 2019). Its mass production and widespread use made BPA present in wastewaters, natural waters, and landfill leachate. For example, BPA was detected in wastewater treatment plant effluents at concentrations of up to 370 µg L^{-1}, and in surface waters – up to 56 µg L^{-1} (Corrales et al., 2015). In landfill leachate, up to 17.2 mg L^{-1} has been detected (Yamamoto et al., 2001). Besides, BPA exhibits an endocrine disruptor's properties causing a damage to reproductive and nervous systems. Thus, the EU banned the BPA usage in baby feeding bottles with its Directive 2011/8/EU (The European Parliament and the Council of the European Union, 2011; Grignard et al., 2012) and with the EU Directive 2020/2184 a maximum limit of 2.5 µg L^{-1} of BPA in drinking water must be guaranteed by 2026 (The European Parliament and the Council of the European Union, 2020). While traditional water treatment methods are often insufficient in BPA removal, AOPs are considered as promising methods (Umar et al., 2013; Mehrabani-Zeinabad et al., 2016; Wanda et al., 2017).

Bisphenol S (BPS), similarly to BPA, is used in production of plastics and epoxy resins. Since limitations have been set for BPA, BPS is used as substitution, increasing in production (Liao et al., 2012; Cao et al., 2013). Although BPS was considerably less studied than BPA, it was found as a potential endocrine disruptor as well (Grignard et al., 2012; Ahsan et al., 2018), being already detected in surface water in concentrations of up to 7.2 µg L^{-1} (Liao et al., 2012; Yamazaki et al., 2015). Since the production of BPS is gradually increasing, the emission of it into the environment will also grow. Likewise with BPA, AOPs may also be a possible response of the BPS pollution problem (Mehrabani-Zeinabad et al., 2016).

1.7 Objectives of the study

Although PCD has been studied in degradation of a variety of pollutants, the data available for the energy efficiency dependent on the gas-liquid contact surface for the substances of various oxidation kinetics is still limited. Similarly, the role of a surfactant radical scavenger in variations of the target pollutant kinetics and the contact surface development received little attention. Besides, the potential of PCD in activation of extrinsic oxidants, persulfate and hydrogen peroxide, in degradation of recalcitrant compounds requires clarification.

The objectives of the study include provisions of experimentally obtained knowledge necessary for optimization of operational parameters as a prerequisite for upscaling the PCD technology.

The tasks in this study include:

- establishing the dependence of oxidation efficiency on the gas-liquid contact surface for organic substances of various oxidation kinetics at the pulse repetition rate variations;
- establishing the regularities in PCD-oxidation of endocrine disrupting bisphenols A (BPA) and S (BPS) with special attention towards the effects of gas-liquid contact surface and surfactant radical scavenger on the energy efficiency;
- evaluating the potential of PCD in activation of extrinsic oxidants persulfate (PS) and hydrogen peroxide (H_2O_2) in oxidation of slowly oxidized oxalate.

2 Materials and methods

2.1 Chemicals and materials

All used reagents were of analytical grade and used without further purification. All stock solutions were prepared in bi-distilled water. Treated solutions were prepared using distilled water. The chemical structure and physicochemical properties of organic compounds under consideration, i.e., oxalic acid, sodium oxalate, phenol, bisphenols A and S are presented in Table 4.

Table 4. The properties of target compounds

Properties	Oxalate		Phenol	Bisphenol A	Bisphenol S
	Oxalic acid	Sodium oxalate			
Molecular structure	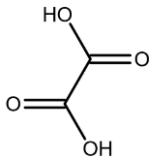	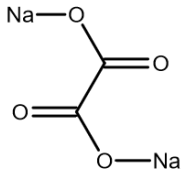	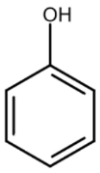	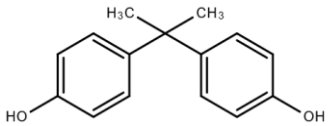	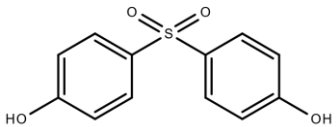
Characterization	Naturally occurring organic compound Intermediate or end-product of oxidation		Bulk chemical	Endocrine disruptor	Potential endocrine disruptor
CAS nr	144-62-7 (anhydrous) 6153-56-6 (dihydrate)	62-76-0	108-95-2	80-05-7	80-09-1
Elementary formula	$C_2H_2O_4$	$Na_2C_2O_4$	C_6H_5OH	$C_{15}H_{16}O_2$	$C_{12}H_{10}O_4S$
Molecular mass, g mol^{-1}	90.04	134.00	94.11	228.29	250.27
Solubility in water, g L^{-1}	86.0 (20°C) (Yalkowsky et al., 2010)	37.2 (25°C) (Hefter et al., 2018)	82.0 (20°C) (Yalkowsky et al., 2010)	0.35 (20°C) (Yalkowsky et al., 2010)	1.1 (20°C) (Wu et al., 2018)
pKa	1.3 and 4.3 (Getoff et al., 1971)		9.9 (Tay et al., 2012)	9.6 and 10.2 (Tay et al., 2012)	7.4 and 8.0 (Gao et al., 2018)

2.2 Gas-phase pulsed corona discharge

The experimental setup consists of PCD reactor (Flowrox Oy, Finland) with a 40-L storage tank made of stainless steel as schematically illustrated in Figure 7. The device includes plasma reactor, high voltage pulse generator, and a water circulation pump (Iwaki Co. Ltd., Japan) controlled with a frequency regulator (Yaskawa, Japan). Inside the plasma reactor case, an electrode system with 24 high voltage wire electrodes of 0.5 mm in diameter and total length of 20 m positioned horizontally between two grounded vertical parallel plate electrodes is placed. The high voltage electrodes are 18 mm apart from each grounded plate electrode. The vertical plate electrodes are 500 mm in width and 722 mm in length. The plasma reactor interior volume comprised 110 L with the plasma zone volume of 13 L. The treatable solutions can be subjected to the treatment with varying pulse frequencies ranging from 50 to 880 pulses per second (pps) corresponding to the power of 9.0 to 123.2 W. The solution is showered to the plasma zone through a perforated plate of 30 mm in width and 500 mm in length with 51 perforations of 1 mm diameter in a single row above the high voltage electrodes. After passing through the reactor, treated water falls to storage tank, from where it is circulated to the top of the reactor thus executing a batch mode of operation.

The water circulation rate is varied by means of frequency regulator, which is used to control the rotation rate of the pump's electric motor. The water flowrate is controlled from 2.0 to 29.5 L min^{-1}, making the spray densities from 0.002 to 0.26 m s^{-1}. The spray densities were calculated by using Eq. 64:

$$q = \frac{v}{S} \tag{64}$$

where v – volumetric flowrate of solution, $m^3\ s^{-1}$;
S – horizontal cross section area of the plasma zone, m^2.

The horizontal cross section of plasma zone S was found by multiplying the distance between two grounded electrodes (36 mm) by the width of a grounded electrode (500 mm), giving a value of 0.018 m^2.

The pulse peak voltage and current, and duration were 18 kV, 380 A and 100 ns, respectively. The pulse characteristics were quantified with a Rigol DS1102E Mixed Signal Oscilloscope, a Tektronix P6015 high voltage probe (Tektronix Inc., USA) and a current monitor PT-7802 (PinTek, China).

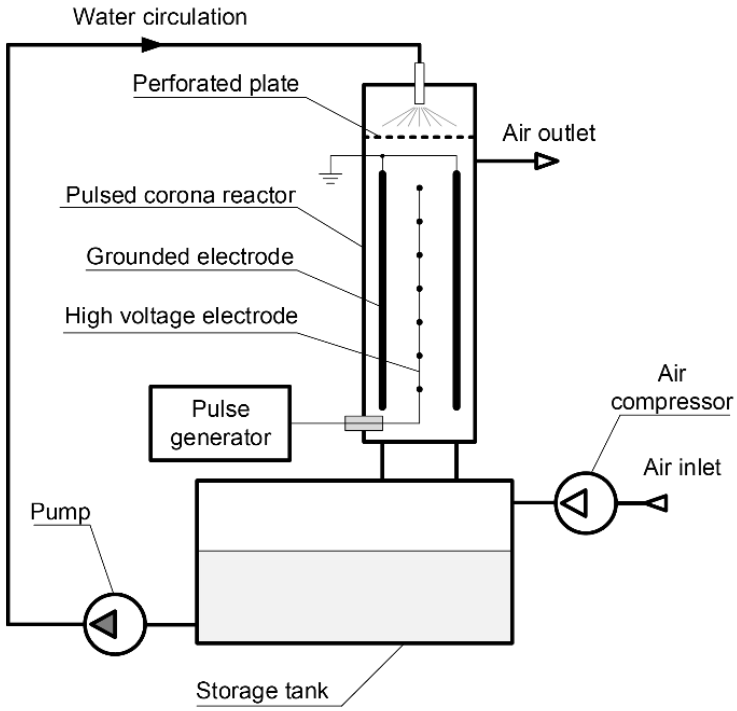

Figure 7. Schematic illustration of the PCD reactor

2.3 Experimental procedure

The PCD oxidation experiments were conducted with solutions of oxalic acid (OXA) (Paper I–II), sodium oxalate (OXA) (Paper I–II), phenol (Paper I), BPA and BPS (Paper III) at ambient temperature 20 ±2 °C. Solutions were prepared in 1-L volumetric flask with bi-distilled water with subsequent dilution of its content to a total volume of 20-L (Paper I–II) or 10-L (Paper III) using the distilled water in the reactor tank making the initial concentrations of 100 mg L^{-1} (Paper I), 1.11 mM (Paper II) and 50 mg L^{-1} (Paper III) in the PCD-treated samples. For accelerated dissolution, BPA was dissolved in 1-L flask with bi-distilled water containing 10 mL of 1-M NaOH using the ultrasonic bath for 20–30 min at 50 °C. The solution was cooled to a room temperature and diluted by distilled water to the total volume of 10 L in the reactor tank. The BPS solution was prepared similarly to BPA except sonication for higher BPS solubility (Paper III). In PCD/PS and PCD/H_2O_2 combinations, pre-selected amounts of H_2O_2 and PS were dissolved in 200 mL volumetric flasks and added to the tank before the start of treatment (Paper II). The OXA/oxidant molar ratios were ranged in the row of 1:0.1, 1:0.25, 1:0.5 and 1:1, corresponding to the oxidant concentrations of 0.111, 0.278, 0.555 and 1.11 mM, respectively (Paper II). In the experiments with a surfactant scavenger, 1.0 g of sodium dodecyl sulfate (SDS) was dissolved in 1-L measuring flask with bi-distilled water and added together with BPA solution to the reactor tank and diluted to a total volume of 10 L making the resultant concentration 100 mg L^{-1} of SDS (Paper III).

Oxidation experiments were conducted in acidic (Paper I–II), neutral (Paper II) and alkaline media (Paper I–III). At experimental conditions, oxalic acid dissolved in distilled water set the initial pH 3.0 (Paper I–II). The pH of sodium oxalate solutions was adjusted

to 7.4 (Paper II), 10.3 ±0.2 (Paper I) and 10.4±0.2 (Paper II). Phenol aqueous solutions were treated at pH values of 3.0 and 11.5 (Paper I). Due to the BPA and BPS poor solubility in acidic and neutral media, experiments were carried out at pH 9.5 ±0.5 (Paper III). The pH adjustment was done with H_2SO_4 and NaOH 5.0-M solutions.

Experiments were performed at two generator power output values of 32 W and 123.2 W, corresponding to frequencies of 200 and 880 pps (Paper I–III). Plasma treatment time comprised up to 60 min at 200 pps and 15 min at 880 pps with similar energy doses of 1.60 and 1.54 kWh m^{-3}, respectively, delivered to the reactor (Paper I–II). In paper III, BPA and BPS solutions were treated for 20 min at 200 pps and 320 s at 880 pps to provide similar energy doses of 1.07 and 1.10 kWh m^{-3}, respectively. The extended plasma treatment experiments were lasting for 95 min at 200 pps (energy dose 5.06 kWh m^{-3}) and 24 min and 40 s at 880 pps (5.07 kWh m^{-3}) (Paper III). The delivered energy doses were calculated using Eq. 65:

$$Delivered\ energy\ dose = \frac{P*t}{V} \quad (65)$$

where P – pulse generator output power, kW,
t – treatment time, h,
V – volume of treated solution sample, m^3.

Before the treatment, solutions were mixed for 5-10 minutes at 0.015 m s^{-1} spray density (flow rate of about 16 L min^{-1}) for concentration uniformity. The flow rate was measured using water meter and the stopwatch. The experimental run started when the pulse generator was turned on. Samples were collected from the storage tank at the pre-set treatment time intervals in correspondence with the planned delivered energy doses. Before sampling, the pulse generator was turned off and the treated solution was mixed by circulating of at least six volumes of solution at the set flow rate to obtain uniformity in concentration. The energy efficiency of oxidation for oxalate (Paper I–II) and phenol (Paper I) at the end of treatment and for bisphenols at 90% of removal were calculated using Eq. 66:

$$E = \frac{\Delta C*V}{W} \quad (66)$$

where E – energy efficiency, g kW^{-1} h^{-1},
ΔC – the decrease in pollutant's concentration, g m^{-3},
V – volume of treated solution sample, m^3,
W – energy consumption as a product of power delivered to the reactor and the time of treatment, kWh.

In Paper II, non-plasma reference experiments with OXA/PS and OXA/H_2O_2 at the OXA/oxidant molar ratio of 1:1 were conducted in a 1-L glass beakers containing 800 mL of treated solution. These experiments were conducted at the pH values identical to the ones used in PCD treatment (Paper II). In all oxidation experiments containing H_2O_2 or PS, oxidation reactions were quenched by adding sodium sulfite crystals to vials at the Na_2SO_3/oxidant molar ratio of 10:1 (Paper II).

All experiments (plasma and non-plasma) were at least duplicated with the results deviations fitting into the 5-% confidential interval (Paper I–III).

2.4 Analytical methods

Since OXA has no stable organic oxidation intermediates, pollutant content was determined by measuring total organic carbon (TOC) using Multi N/C 3100 analyzer (Analytic Jena, Germany) (Paper I–II). Besides, the analyzer was used to measure TOC in untreated and treated samples containing BPA and BPS solutions (Paper III). TOC removal percentage (%) was calculated using Eq. 67 (Paper II, III):

$$TOC\ removal\ = \left(1 - \frac{TOC_t}{TOC_0}\right) * 100\% \quad (67)$$

where TOC_0 and TOC_t are the TOC values at treatment times 0 and t, mg C L^{-1}

Aqueous phenol (Paper I) and bisphenols (Paper III) concentrations were measured by the YL 9300 HPLC (YL Instrument Co., Korea) equipped with XBridge BEH C18 Column (130Å, 3.5 µm, 3 mm x 150 mm). The sample injection volume was 20 µL at the eluent flow rate of 0.2 mL min^{-1} (Paper I, III).

Phenol (Paper I) and BPS (Paper III) analyses were performed using an isocratic method with a mobile phase comprised of a mixture of 60% water (acidified with 0.1% acetic acid) and 40% acetonitrile. Samples containing BPA were analysed analogously using the water-acetonitrile ratio of 40:60. The pollutants were analysed at the detection wavelength of 270, 275 or 258 nm for phenol (Paper I), BPA (Paper III) and BPS (Paper III), respectively. Calibrations of BPA and BPS contents were derived in the range from 0.5 to 100 mg L^{-1} with and without SDS additions. The presence of SDS had no effect on calibration results. However, pH affects the area of peaks in chromatograms requiring its thorough adjustment in samples to the range of 10.9–11.0 prior to analysis (Paper III). The analysis of oxidation by-products was carried out by HPLC equipped with Phenomenex Gemini NX-C18 column (110Å, 5 µm, 2 mm x 150 mm) combined with mass spectrometer (HPLC-MS, LC-MS 2020, Shimadzu) using diode array detector (HPLC-PDA, SPD-M20A, Shimadzu). Samples containing BPA were analysed using an isocratic method with a mobile phase mixture composed of 55% of aqueous solution of 0.3-% formic acid and 45% of acetonitrile also containing 0.3% of formic acid. Solutions of BPS were analysed analogously using the water-acetonitrile ratio of 70:30. Mass-spectra were acquired by quadrupole mass separation in full-scan mode (scanning range 50–500 m/z). The nebulizing and drying gas flow rates were set to 1.5 and 10.0 L min^{-1}, respectively. The temperatures of the heat block and the desolvation line were both set to 250 °C, and the interface voltage comprised 4.5 kV. The device was operated in positive ESI mode and the results obtained with MS detector were handled using Shimadzu Lab Solutions software (Paper III).

The pH was measured using a digital pH/Ion meter (Mettler Toledo S220, USA) (Paper I–III). Conductivity measurements were carried out using Multi-parameter meter HQ430d (Hach Company, USA) (Paper III). Residual H_2O_2 was measured using spectrophotometer (Genesys 10S, Thermo Scientific) at 410 nm by adding samples to the Ti^{4+} solution to form pertitanic acid (Eisenberg, 1943) (Paper II). Concentrations of anions in samples were measured using the 761 Compact IC ion chromatograph with chemical suppression of eluent conductivity (Metrohm Ltd) (Paper III). The device was equipped with METROSEP A Supp 5 column (150 mm x 4.0 mm). The sample injection volume was 20 µL. Separation of ions was attained using an eluent mixture of 3.2 mM Na_2CO_3 + 1.0 mM $NaHCO_3$ with flowrate of 0.7 mL min^{-1}. The gas-liquid contact surface

A, m^{-1} (m^2 m^{-3}), at various spray densities was measured by classical method of sulfite oxidation by air oxygen in the presence of cobalt sulfate catalyst (Danckwerts, 1970). Oxidation rate of 0.1-M Na_2SO_3 into Na_2SO_4 was determined iodometrically using sodium thiosulfate as titrant. The contact surface was calculated as described previously (Ajo et al., 2015).

3 Results and discussion

3.1 Gas-liquid contact surface

The gas-liquid contact surface *A*, was found to have a linear dependence on spray density (Figure 8). As the latter increased from 0 to 0.0243 m s^{-1}, the contact surface reached from 17.6 to 138 m^{-1}, respectively, as described in Eq. 68 with correlation factor R^2 averaging 0.9974 (Paper I):

$$A = 4954q + 17.6 \quad (68)$$

where q is the spray density, m s^{-1}.

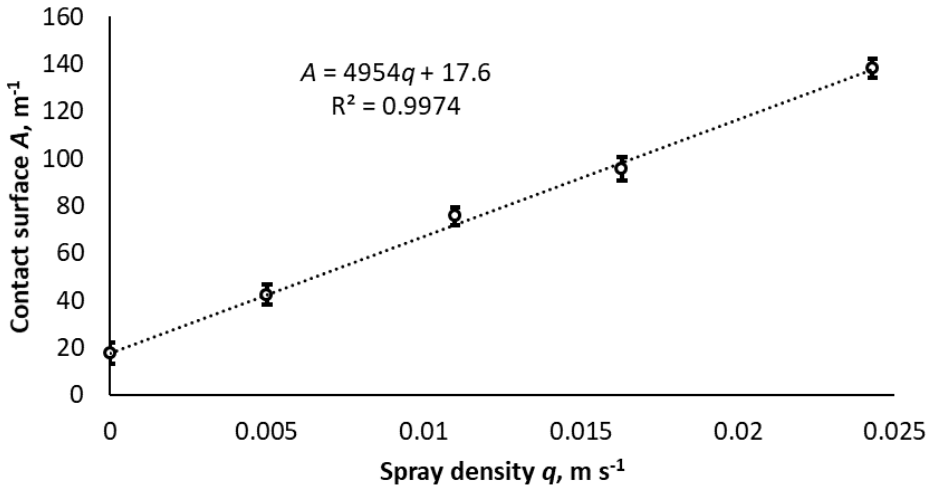

Figure 8. Dependence of contact surface area A on spray density q in PCD device

3.2 Contact-surface and pulse repetition frequency impact on non-assisted PCD treatment

3.2.1 OXA and phenol oxidation by non-assisted PCD

The impact of gas-liquid contact surface on PCD efficiency was studied with the refractory OXA and rapidly reacting phenol. The obtained energy efficiency results at treatment time of 60 min at 200 pps and 15 min at 880 pps, are presented in Figure 9 and 10 for oxalate and phenol, respectively. In experiments, the energy dose delivered to the reactors comprised 1.60 and 1.54 kWh m^{-3} at the end of treatment at 200 and 880 pps, respectively (Paper I).

During OXA oxidation experiments, pH of acidic solutions remained practically constant, whereas pH of alkaline solutions decreased from 10.3 ±0.2 to 8.5 ±0.2. The pH descent in alkaline solutions is likely related to formation of nitric acid in PCD, having little effect in acidic medium (Preis et al., 2014). Regardless of pH, energy efficiency of OXA oxidation within the range of experimental conditions was found to have a linear dependence on the gas-liquid contact surface (Figure 9), which is consistent with the

surface character of the reaction proved earlier (Ajo et al., 2017; Wang et al., 2019). Since OXA is mostly oxidized with $HO^{\bullet}$, its oxidation rate is proportional to the surface treated with the discharge (Paper 1).

One can see higher average energy efficiencies in acidic medium: oxalic acid average energy efficiency reached up to 30.0 g kW^{-1} h^{-1} at 200 pps and about 22.0 g kW^{-1} h^{-1} at 880 pps, when the gas-liquid contact surface was increased up to 138 m^{-1}. In alkaline conditions, only 12.7 g kW^{-1} h^{-1} at 200 pps and 9.7 g kW^{-1} h^{-1} at 880 pps were achieved at the maximum contact surface (Paper I). The reduced oxidation efficiency with increasing pH is likely explained by $HO^{\bullet}$ oxidation potential, which decreases from 2.8 V to 1.9 V as the pH is changed from acidic to the neutral one (Wardman, 1989). Supposedly, at lower oxidation potential, reaction rate of $HO^{\bullet}$ formed at the gas-liquid interface with OXA is lower than recombination and other side-reactions resulting in a lesser efficiency as pH rises. Besides, $HO^{\bullet}$ reactivity depends on OXA form in solution. At pH 3 OXA exists as $C_2O_4H^-$, which has higher reaction rate constant with $HO^{\bullet}$ ($3.2 \cdot 10^7$ M^{-1} s^{-1}) than $C_2O_4^{2-}$ ($5.3 \cdot 10^6$ M^{-1} s^{-1}), which is, starting from pH 6, only present in the aqueous solution (Paper II, Eq. 17 and 18) (Getoff et al., 1971). Additionally, the reduced OXA degradation rate at higher pH may be related to $HO^{\bullet}$ scavenged with O_3, forming less reactive $HO_2^{\bullet}$ (E^0 = 1.65 V) (Paper II, Eq. 26) or scavenged by bicarbonates/carbonates (Paper II, Eq. 27–28), accumulated from the contact of treated OXA solution with atmospheric CO_2 (Crittenden et al., 1999; Von Gunten, 2003; Chiang et al., 2006; Kattel et al., 2017). For instance, the concentration of total inorganic carbon (TIC) was about 10.2 mg C L^{-1}, i.e., about 51 mg L^{-1} of bicarbonate/carbonate in 1 h of treatment in alkaline media, while the TIC content in acidic medium did not exceed 1.9 mg C L^{-1} (Paper II).

At the initial pH 3.0, a tendency similar to OXA was observed for phenol, where maximum average energy efficiency of 27.7 and 22.0 g kWh^{-1} was achieved at 200 and 880 pps at maximum contact surface of 140 m^{-1}, respectively (Figure 10). Unlike with OXA, where the gas-liquid contact surface increased for about 4.5 times enhanced energy efficiency for about 13 times, phenol efficiency grew for only about 1.3 times with the increased contact surface. The weaker dependency on the contact surface may be explained by rapid reaction of phenol not only with $HO^{\bullet}$, but also with O_3 making the oxidants consumed entirely even at low contact surfaces. In alkaline media, phenol was almost invariant towards contact surface rise, showing positive effect only at narrow range at low contact surface values. Thus, the oxidation efficiency observed at 200 pps was in the range from 37 to 41 g kWh^{-1} and at 880 pps – from 32 to 38 g kWh^{-1}. Since the amount of ROS is determined by the power of pulses delivered to the reactor, phenol consumption of ROS seems to be close to maximum under alkaline conditions. These results suggest that for a relatively rapid reaction of phenol oxidation, a gas-liquid interface sufficient for oxidants consumption was developed already at low spray densities, and energy efficiency appeared to depend on the amount of generated ROS. The difference between oxidation rates at various pH is related to the phenol dissociation into phenolates reported to be more reactive towards O_3 than molecular phenol (Poznyak et al., 2006; Marotta et al., 2012). A similar degradation characteristics was observed previously (Preis et al., 2013) (Paper I).

Regarding the application of different pulse repetition frequencies, this is used to determine the utilization of short- and long-living oxidative species in reactions. As was mentioned earlier, the amount of generated ROS is determined by the pulsed energy delivered to the reactor. The same energy dose may be delivered to the reactor at

different pulse repetition frequencies within times reciprocally proportional to the frequency. For both OXA and phenol, the higher pulse repetition frequency resulted in smaller oxidation energy efficiency, likely explained by the role of O_3 (Preis et al., 2013; Ajo et al., 2015; Wang et al., 2019). For long-living O_3, there is a better chance for more useful utilization in reactions with pollutants, if longer time between pulses is provided: next energy-delivering discharge pulse destroys residual gas-phase long-living ROS along with the synthesis of new ones. This means that pollutants reacting fast enough to have long-living ROS utilized between pulses at high frequency will benefit from higher powers applied for fast oxidation, no effect will be seen with lower pulse repetition frequency. Similarly, low repetition frequency will bring no benefits in oxidation of pollutants oxidized solely with more powerful short-living ROS and refractory towards long-living oxidants (Preis et al., 2013). The effect of pulse repetition frequency was observed with both studied pollutants: oxalic acid and sodium oxalate demonstrated about 25% difference in oxidation efficiency between two frequencies, 200 and 880 pps, while phenol showed 20% and 5% difference in acidic and alkaline media, respectively. One should keep in mind, however, that the increased pulse repetition frequency at somewhat reduced oxidation efficiency results in approximately four times shorter treatment time, in which a comparable treatment result is achieved. Thus, for real-life application, where the treatment time is crucial, a higher pulse repletion rate may be preferred. The concentration of O_3 in PCD reactors was found earlier reaching the equilibrium concentration of 5.0 mg L^{-1} in air regardless the pulse repetition frequency (Paper I).

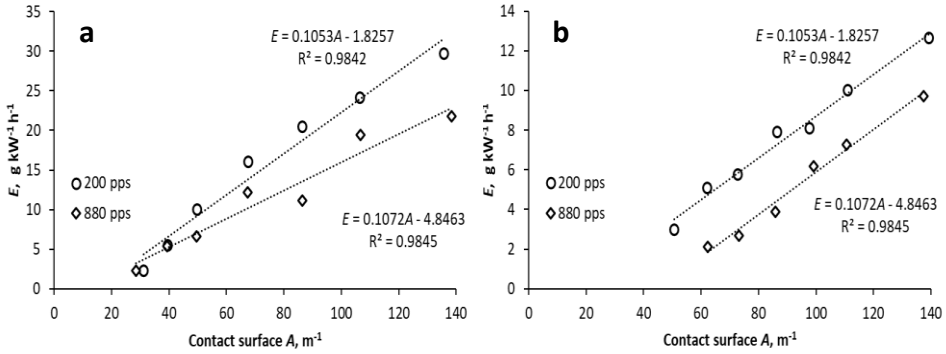

Figure 9. Impact of contact surface on oxalic acid (a) and sodium oxalate (b) oxidation energy efficiency: oxalate starting concentration 100 mg L^{-1}, delivered energy dose 1.54–1.60 kWh m^{-3}

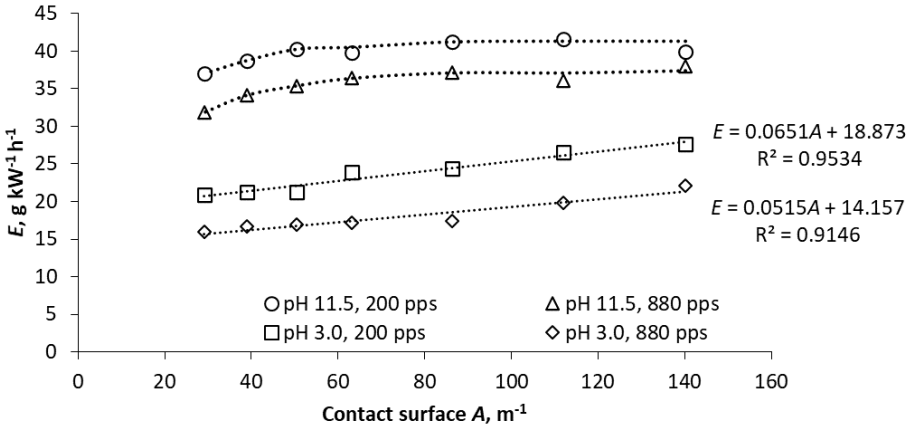

Figure 10. Impact of contact surface on phenol at acidic and alkaline media oxidation energy efficiency: phenol starting concentration 100 mg L^{-1}, delivered energy dose 1.54–1.60 kWh m^{-3}

3.2.2 Oxidation of BPA and BPS by PCD

Pulsed corona discharge was observed to completely degrade BPA and BPS from their starting concentrations of 50 mg L^{-1} at the pulsed energy of 1.07-1.10 kWh m^{-3} delivered within 20 min and 5 min 20 s at 200 and 880 pps, respectively (Paper III, Figure 1). The energy efficiency at 200 pps slightly exceeds the one at 880 pps, showing about 25% and 12% difference between the discharge powers at the contact surface of 115 m^{-1} (Figure 11). The similarity of oxidation results at different pulse repetition frequencies could be explained by rapid consumption of O_3 by bisphenols. The rapid ROS consumption is supported by the similarity of bisphenols' oxidation efficiencies dependent on the gas-liquid contact surface as for phenol: the gas-liquid contact surface increased for 3.5 times enhanced the BPA degradation for about 17%, whereas BPS appeared to be almost invariant towards contact surface at 200 pps (Figure 11). Thus, for BPA, the gas-liquid contact surface increased from 40 to 140 m^{-1} caused the energy efficiency increased from 54.5 to 63.9 g kW^{-1} h^{-1} calculated for 90% of removal, while for BPS, the energy efficiency oscillated within the range of 49.5 to 53.0 g kW^{-1} h^{-1}. Similar dependencies on the gas-liquid contact surface rise were observed for 880 pps (Figure 11). However, it must be noted that even at sufficiently developed contact surface, the difference in oxidation rates between frequencies indicate certain, although moderate contribution of O_3 to BPA and BPS oxidation at longer treatment times (Paper III).

Similarly to phenol (Paper I), the bisphenols oxidation indicate the discharge power as a determining factor for oxidation efficiency. The difference between dependence characters of BPA and BPS is consistent with their hydrophobicity (Derevshchikov et al., 2021): less water-soluble BPA demonstrated noticeable growth of oxidation efficiency with the increased interface area, whereas better soluble BPS behaved similarly to phenol in alkaline conditions (Figure 10; Paper I). Certain increase in oxidation rate of BPA may also be explained by its faster oxidation with O_3 when compared with BPS, which is confirmed by the impact of pulse repetition frequency (Figure 11) and the data of other studies (Paper III, Table 1). The indifference of BPS PCD-oxidation towards the interface area indicates, besides lower hydrophobicity, the pollutant's superior susceptibility to $HO^{\bullet}$ oxidation. Besides, it must be noted that the energy efficiencies

obtained for BPA and BPS exceed ozonation and other AOPs, such as O_3/UVA and DBD (Paper III, Table 1). During oxidation, pH descended from 9.5±0.5 to about 7.0 explained by accumulation of nitric acid and formation of carboxylic acids as oxidation products (Paper III, Table 2) (Kornev et al., 2013; Preis et al., 2014).

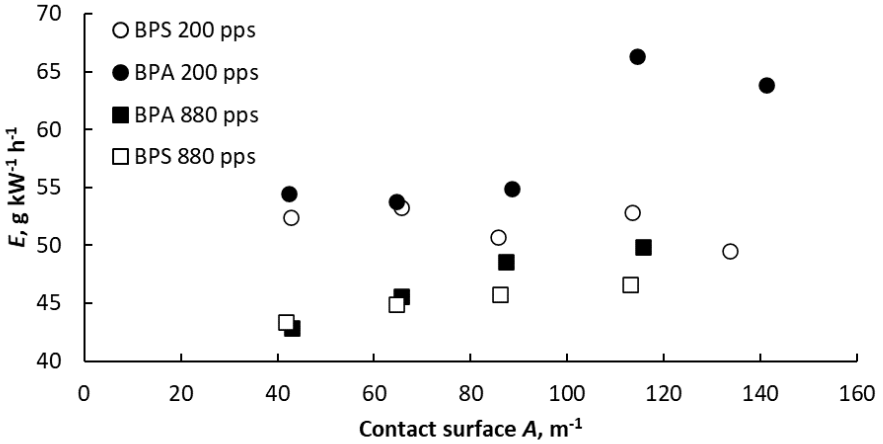

Figure 11. Bisphenols' oxidation efficiency dependent on the contact surface: pH_0 9.5 ±0.5, BPA and BPS starting concentrations 50 mg L^{-1}, bisphenols' removal 90%, delivered energy dose 5.06–5.07 kWh m^{-3}

Although the contact surface variation had only a moderate impact on bisphenols' degradation, its effect was stronger in TOC removal. Until parent compound was degraded at delivered energy dose of about 1.1 kWh m^{-3} (Paper III, Figure 1), TOC removal achieved maximum values of 9–11% for BPA and 9–14% for BPS regardless of pulse repetition frequency and gas-liquid interface. In further treatment up to delivered energy dose of about 5.0 kWh m^{-3}, TOC removal benefitted from both well-developed contact surface and lower pulse repetition frequency (Figure 12). For example, TOC removal increased from 52.7% to 69.4% for BPS as contact surface was increased from 42 to 115 m^{-1}. The beneficial effect of contact surface is related to formation of carboxylic acids probably produced with benzene ring opening of proposed potential bisphenols intermediate products formed through hydroxylation and oxidation (Paper III, Table 3 and 4) or from other intermediates not detected with HPLC-MS. These carboxylic acids include acetate, formate, and oxalate, which are formed in oxidation of aromatic compounds (Panorel et al., 2013) and were detected with ion chromatography analysis in degradation of bisphenols (Paper III, Table 2). This observation is in agreement with slow oxidation of ultimate oxidation products with surface-borne ROS dependent on the area of contact surface (Preis et al., 2013). The difference in TOC removal rates at various pulse repetition frequencies is explained by participation of aqueous O_3 decomposing to $HO^{\bullet}$. The pH dropped from 9.5 ±0.5 to 3.5 ±0.3 caused by formation of carboxylic acids and nitrates. It must be noted that with IC analysis quantification, nitrate production in PCD was independent of the bisphenol structure and comprised 14.76 and 12.32 g kW^{-1} h^{-1} at 200 and 880 pps, respectively. The obtained values are similar with previously obtained values in PCD with up to 16 g kW^{-1} h^{-1} (Paper III) (Preis et al., 2014).

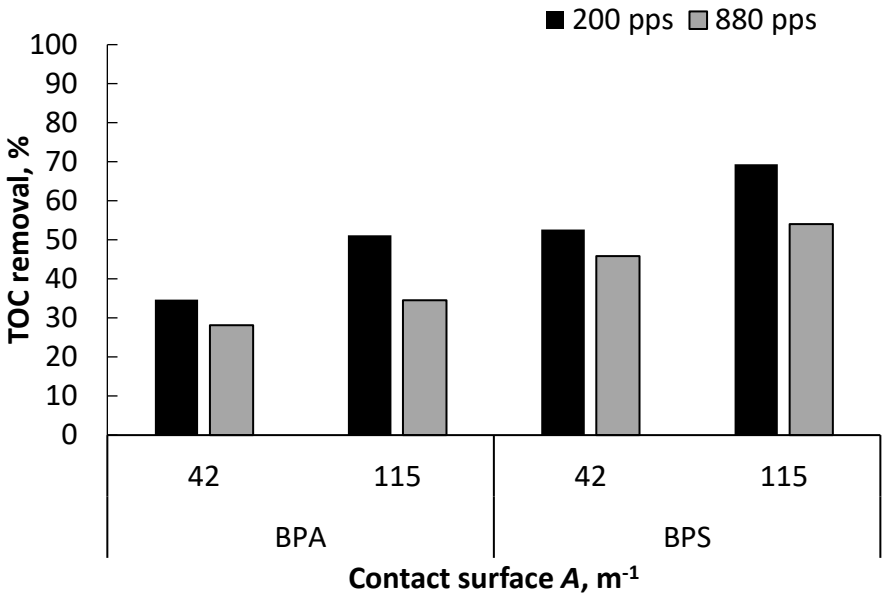

Figure 12. Impact of contact surface on BPA and BPS TOC removal efficiency: initial pH 9.5 ±0.5, BPA and BPS starting concentration 50 mg L^{-1}, delivered energy dose 5.06–5.07 kWh m^{-3}.

3.3 Contact-surface and pulse repetition frequency impact on assisted PCD treatment

3.3.1 Impact of surfactant on BPA and BPS oxidation

Previously, surfactant SDS has been used in PCD studies as a scavenger of surface-borne HO• radical to clarify the importance of surface oxidation of target pollutants (Wang et al., 2019; Onga et al., 2020). The effect of SDS addition, however, appeared to be dependent on the target compound molecular structure: SDS sulfate groups may either interact with the hydrophilic moieties of target pollutants submerging those below the gas-liquid interface thus screening them from the HO• attack, or SDS-radical, once formed under the HO• attack, may raise the radicalized target molecule to the surface for more effective radical oxidation (Onga et al., 2021). Thus, for rapidly reacting bisphenols, addition of SDS, together with the impacts of contact surface area and pulse repetition frequency, helps clarifying the character of their oxidation (Paper III).

The addition of SDS showed a neutral or moderately negative impact on energy efficiency of BPA and BPS oxidation at all studied conditions (Figure 13): for BPS, a minor decrease in energy efficiency was observed with SDS addition, whereas BPA showed a stronger negative effect. The inhibition effect was even greater at larger contact surfaces for BPA: when the contact surface was increased to 115 m^{-1}, the addition of SDS caused efficiency to drop from 66.4 to 45.1 at 200 pps, showing about 32% difference in oxidation. At the contact surface of 42 m^{-1}, the difference was only about 9%. Similar observations were found for 880 pps, where the oxidation differences were about 5% and 23% at contact surface values of 42 and 115 m^{-1}, respectively. It must be noted, that at the contact surface of 140 m^{-1} the SDS foaming with BPA solution was strong enough to reach the inter-electrode gap and cause

theoretically possible partial short-circuit in the discharge. For this, the contact surface in BPA oxidation at the SDS concentration of 100 mg L^{-1} was limited by 115 m^{-1} (Paper III).

Contrary to BPA, considerably less foam was seen during BPS treatment, having no technical limits within the experiments at the highest contact surface available (Paper III, Figure 5). Besides, SDS addition to BPS solutions demonstrated minor sensitivity of oxidation efficiency towards the contact surface: the efficiency decreased for about 7% and 10% at 200 and 880 pps, respectively, with the SDS addition at the contact surface of 115 m^{-1} (Figure 13) (Paper III).

The minor inhibition effect of the surfactant on the bisphenols oxidation efficiency may be related to the screening effect of SDS surfactant attached with its sulfate group to hydrophilic phenolic moieties compensated partly by the affinity between the surfactant radical and a radicalized bisphenol molecule brought closer to the interface, thus making the SDS effect close to neutral. At well-developed contact surface, the balance likely shifted towards the SDS screening effect. The difference between BPA and BPS might be related to the difference in hydrophobic characteristics of bisphenols. Previously, it was found that SDS addition significantly inhibited oxidation of hydrophilic phenol in PCD (Wang et al., 2019). However, since BPA and BPS molecules are bigger having two benzene rings in their molecular structure and less polar, these show higher affinity with the SDS radical formed at the end of hydrophobic tail. Poorer aqueous solubility of bisphenols also points to their less hydrophilic character than phenol thus being faster oxidized in surface-borne reactions as described earlier (Derevshchikov et al., 2021). The role of hydrophobicity in the rate of oxidation is also indirectly supported by the fact of poorer BPA aqueous solubility than the one of BPS. Therefore, SDS interacts differently with more hydrophobic BPA and less hydrophobic BPS. These observations confirm the complex character of surfactant effect to various pollutants deserving attention also for the practical reason – disclosing the surfactant effect, often characteristic to industrial and municipal wastewaters, to PCD oxidation (Paper III).

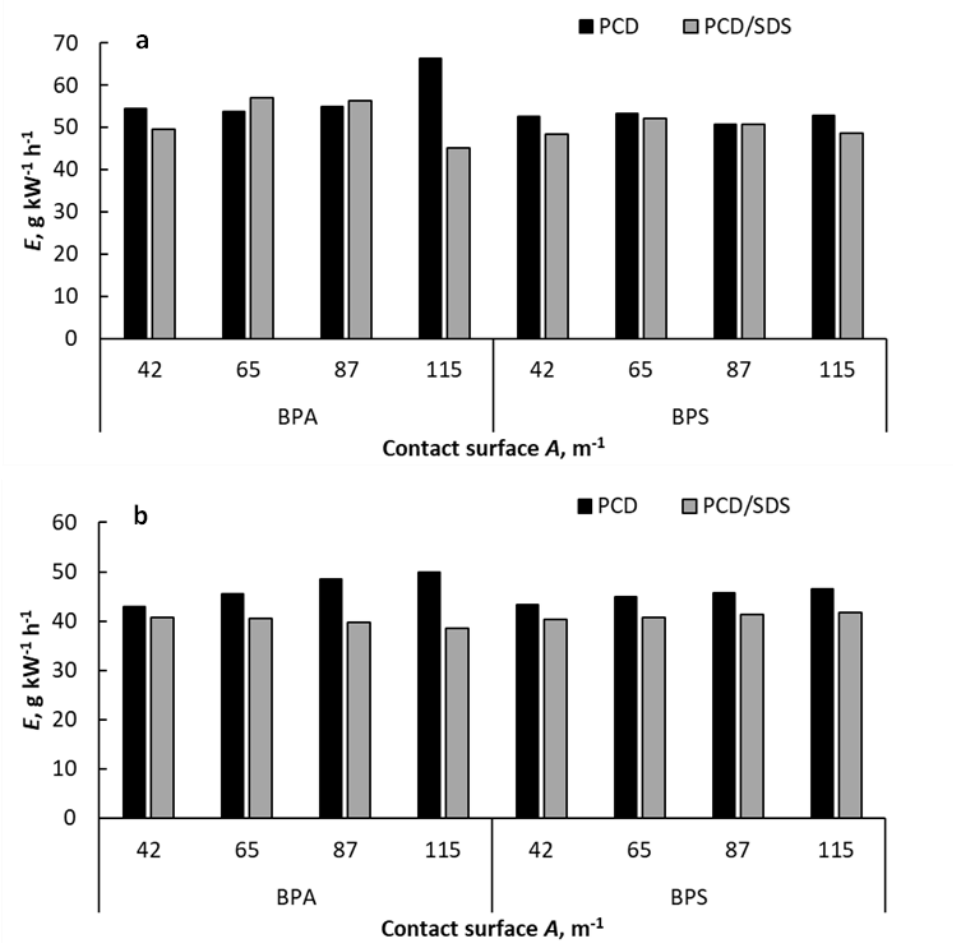

Figure 13. Impact of contact surface on BPA and BPS oxidation efficiency without SDS and with SDS (a) at 200 pps and (b) at 880 pps: initial pH 9.5 ±0.5, BPA and BPS starting concentrations 50 mg L^{-1}, SDS concentration 100 mg L^{-1}, bisphenols' removal 90%.

3.3.2 Impact of extrinsic oxidants on OXA oxidation

Improved AOPs often activate extrinsic oxidants, providing higher removal efficiencies than AOPs without a companion (Wen et al., 2005; Guerra-Rodríguez et al., 2018). Thus, potential activation of PS and H_2O_2 by PCD in oxidation of OXA was evaluated. The obtained oxidation efficiencies and TOC removals at various experimental conditions are presented in Table 5 and Table 6. The delivered energy dose comprised of 1.60 and 1.54 kWh m^{-3}, corresponding to the treatment time of 60 min at 200 pps and 15 min at 880 pps. The pH changed on course of the PCD treatment of OXA solutions similarly in non-assisted and PS- and H_2O_2-assisted treatment: pH remained practically constant in acidic and neutral solutions, although decreased in alkaline medium from 10.4 ±0.2 to 9.3 ±0.3. The incline was likely due to formation of nitric acid in PCD, which had minimal effect in acidic medium (Preis et al., 2014). In neutral solutions, residuals of sodium oxalate and bicarbonate preserved pH at a constant level (Paper II).

Table 5. Energy efficiencies and TOC removal of OXA in non-plasma treatment and in PCD treatment (OXA starting concentration 1.11 mM, delivered energy dose 1.60 kWh m^{-3})

	Process	Pulse repetition frequency	pH	A, m^{-1}	OXA/oxidant molar ratio	E, g kW^{-1} h^{-1}	TOC removal, %
Non-plasma treatment							
(a)	H_2O_2	-	3.0	-	1:1	-	-
(b)			7.4				
(c)			10.4				
(d)	PS	-	3.0	-	1:1	-	-
(e)			7.4				
(f)			10.4				
PCD treatment							
	Effect of extrinsic oxidant dose						
(g)	PCD	200	3.0	149	-	31.2	51.5
(h)	PCD/PS	200	3.0	149	1:0.1	34.0	55.9
(i)					1:0.25	42.1	67.7
(j)					1:0.5	52.7	86.9
(k)					1:1	56.0	94.6
(l)	PCD/H_2O_2	200	3.0	149	1:0.1	30.5	52.1
(m)					1:0.25	30.7	51.7
(n)					1:0.5	28.6	49.0
(o)					1:1	25.4	43.9
	Effect of pH						
(p)	PCD	200	3.0	149	-	31.2	51.5
(q)			7.4			19.8	33.2
(r)			10.4			8.6	14.2
(s)	PCD/PS	200	3.0	149	1:0.5	52.7	86.9
(t)			7.4			22.3	38.2
(u)			10.4			9.1	15.9
(v)	PCD/ H_2O_2	200	3.0	149	1:0.5	28.6	49.0
(w)			7.4			18.7	33.9
(x)			10.4			7.7	14.6

Table 6. Impact of gas-liquid contact surface and pulse repetition frequency on energy efficiencies and TOC removal in PCD treatment (OXA starting concentration 1.11 mM, delivered energy dose 1.54–1.60 kWh m^{-3})

	Process	Pulse repetition frequency	pH	A, m^{-1}	OXA/oxidant molar ratio	E, g kW^{-1} h^{-1}	TOC removal, %
	Effect of gas-liquid contact surface						
(a)	PCD	200	3.0	42	-	10.8	18.0
(b)				90	-	20.9	35.3
(c)				149	-	31.2	51.5
(d)	PCD/PS	200	3.0	42	1:0.5	32.5	56.8
(e)				90		45.6	77.7
(f)				149		52.7	86.9
(g)	PCD/ H_2O_2	200	3.0	42	1:0.5	8.7	15.0
(h)				90		19.1	34.1
(i)				149		28.6	49.0
	Effect of pulse repetition frequency						
(j)	PCD	200	3.0	149	-	31.2	51.5
(k)		880				22.0	34.6
(l)	PCD/PS	200	3.0	149	1:0.5	52.7	86.9
(m)		880				44.8	72.5
(n)	PCD/ H_2O_2	200	3.0	149	1:0.5	28.6	49.0
(o)		880				19.6	33.2

At OXA/oxidant molar ratio of 1:1, non-plasma treatment showed absent reactivity of PS and H_2O_2 with OXA at experimental conditions (Table 5 (a)-(e), Paper II, Figure 2). Contrary to non-plasma, the addition of PS to PCD showed beneficial effect in OXA treatment in acidic medium. This indicates PCD activating PS producing sulfate radicals with further formation of additional $HO^{\bullet}$ (Paper III, Eq. 7). Persulfate in PCD/PS combination is presumably activated by reactions with species formed in plasma, such as e_{aq}^-, $HO^{\bullet}$, $HO_2^{\bullet}$, $H^{\bullet}$ and $O_2^{\bullet-}$ (Paper II, Eq. 29–32) (Homem and Santos, 2011; Yang et al., 2016; Z. Liu et al., 2016; Shang et al., 2019; Cuerda-Correa et al., 2020). The role of $H^{\bullet}$ radical, however, is reasonably negligible due to its scavenging by abundant oxygen (Ono et al., 2020). Potentially, UV radiation (Paper II, Eq. 33–34) and strong electric field may also activate PS (Bruggeman and Leys, 2009; Tang et al., 2018). The beneficial effect of PCD/PS combination was observed increasing with the PS dose in acidic medium (Table 5 (h)–(k), Paper II, Figure 3a): OXA TOC removal increased from 56% to 95% as PS concentration was increased from 0.111 mM to 1.11 mM. The enhanced impact was likely caused by generation of $SO_4^{\bullet-}$ improving OXA degradation. At highest PS dose, PCD/PS combination surpassed non-assisted PCD in energy efficiency by about 1.8 times. However, it must be that noted that twofold upsurge in PS dosage from 0.555 mM to 1.11 mM achieved only a modest grow in oxidation efficiency. This could be related to a fixed amount of oxidants acting as PS activators produced in PCD at the applied power. Additionally, at high concentrations of PS, $SO_4^{\bullet-}$ may recombine (Paper II, Eq. 36) or become scavenged by excess persulfate anion ($S_2O_8^{2-}$) (Paper II, Eq. 37) (Wang and Zhou, 2016; Yang et al., 2016). Considering

the expense of persulfate, the treatment at the OXA/PS molar ratio of 1:0.5 appears optimum and was chosen for further experimentation as the cost-effective one (Paper II).

Different from PCD/PS, the PCD/H_2O_2 combination at OXA/H_2O_2 molar ratios from 1:0.1 to 1:1 did not promote OXA degradation in acidic medium (Table 5 (l)–(o), Paper II, Figure 3b). Since H_2O_2 is formed in PCD and accumulated during OXA non-assisted PCD treatment, addition of hydrogen peroxide makes little difference in OXA degradation rate even at the lowest doses of added H_2O_2 (Paper II, Table 1). However, while up to H_2O_2 concentration of 0.278 mM no effect was observed, further increase up to 1.11 mM caused an inhibition in OXA oxidation. As the dose of H_2O_2 was increased from 0 mM up to 1.11 mM, OXA TOC removal decreased down from 51.5% to 44% (Table 5 (g), (o)). The effect could be related to the excess amount of H_2O_2 reacting with $HO^{\bullet}$ observed earlier (Paper II, Eq. 35) (Lee et al., 2003; Homem and Santos, 2011; Iervolino et al., 2020). The scavenging effect is supported by residual H_2O_2 at the end of treatment: starting from OXA/oxidant molar ratio 1:0.5, H_2O_2 consumption prevailed over its formation thus supporting explanation of its negative role in OXA oxidation (Paper II, Table 1). For the reason of uniformity in comparison with the PCD/PS process, OXA/H_2O_2 molar ratio of 1:0.5 was chosen for further experiments with PCD/H_2O_2 combination (Paper II).

Consistently with non-assisted PCD (Table 5, (p)-(r)), Figure 9), OXA degradation efficiency dropped with the pH rise in assisted PCD at OXA/oxidant molar ratio of 1:0.5 (Table 5 (s)–(x) (Paper II, Figure 4). In PCD/PS application, the OXA removal declines faster with growing pH than in non-assisted PCD. While at acidic pH, TOC removal in PCD/PS treatment proceeded 1.7 times faster than in PCD, at neutral and alkaline pH the TOC removal in PCD/PS treatment differed from PCD for only 5% and less than 2%, respectively. That small difference is likely related to $SO_4^{\bullet-}$ reactions with H_2O and HO^- (Paper II, Eq. 7–8) forming $HO^{\bullet}$, which has lower oxidation potential at higher pH and shorter lifetime compared to $SO_4^{\bullet-}$ (Wardman, 1989; Matzek and Carter, 2016; Wacławek et al., 2017; Guerra-Rodríguez et al., 2018). In addition, the inhibition of oxidation at higher pH may be caused by the increased bicarbonates and carbonates accumulation during the treatment, which are well-known $SO_4^{\bullet-}$ scavengers, forming less reactive carbonate radicals (Paper II, Eq. 45–46) (Izadifard et al., 2017; Kattel et al., 2017; Wacławek et al., 2017).

In PCD/H_2O_2 treatment at OXA/oxidant molar ratio of 1:0.5, negligible effect of H_2O_2 addition was observed in all pH ranges (Table 5 (v)–(x)). Since H_2O_2 showed its instability at high pH (Paper II, Table 10), it did not promote OXA degradation. Since both PCD and PCD/H_2O_2 treatment approaches showed similar OXA oxidation results in neutral and alkaline media, H_2O_2 was presumably readily and uselessly reacting with O_3 and surface-borne $HO^{\bullet}$ playing little role in OXA oxidation most probably compensating consumed active oxidants with newly produced replacement (Paper II).

As to the OXA treatment by PCD, PCD/PS and PCD/H_2O_2 combinations at OXA/oxidant molar ratio of 1:0.5 benefitted from well-developed contact surface at acidic pH (Table 6 (a)-(fj)), Paper II, Figure 5). While PCD/H_2O_2 system (Table 6 (g)–(j)) caused slight inhibition of OXA oxidation at all contact surfaces, the obtained values with PCD/PS (Table 6 (d)–(f) exceed ones with obtained in OXA degradation by PCD (Table 6 (a)–(c)). However, it must be noted that the effect of PS addition to the PCD-treated OXA solution is somewhat lessened with increased contact surface being relatively smaller at higher solution circulation rate. As contact surface increased from 42 to 149 m^{-1}, the difference between the PCD/PS combination and PCD decreased

from 3.2 to 1.7 times. Thus, the impact of contact surface area is smaller for the PCD/PS combination than for the non-assisted PCD (Paper II).

The effect of pulse repetition frequency was similar for all oxidant combinations: the results obtained with 200 pps exceeded the ones achieved with 880 pps in acidic medium at OXA/oxidant molar ratio of 1:0.5 and maximum gas-liquid contact surface 149±3 m^{-1} (Table 6 (j) – (o), Paper II, Figure 6). The highest TOC removal and energy efficiencies were obtained with PCD/PS, followed by PCD and PCD/H_2O_2. However, neither PS nor H_2O_2 benefited much from extended O_3 lifetime during longer treatment times at lower frequency witnessing predominant radical mechanism of their activation in target or scavenging reactions (Paper II).

The treatment cost comparison showed that in acidic medium at the OXA/PS molar ratio of 1:0.5, gas-liquid contact surface 149±3 m^{-1} and at the pulse repetition frequency of 200 pps, PCD/PS combinations with the energy efficiency of 53 g kW^{-1} h^{-1} exceeds the corresponding number for PCD in air at similar experimental conditions for 1.7 times. At similar conditions in neutral and alkaline medium, PS did not exhibit significant acceleration of oxidation reaction thus making its economic effect negligible. Keeping in mind simpler operation without additional cost for chemicals transportation, storage and dosing, addition of PS to PCD is feasible in OXA treatment in acidic medium, while for neutral and alkaline media, non-assisted PCD remains preferable (Paper II).

Conclusions

Operational parameters affecting the oxidation efficiency in pulsed corona discharge (PCD) treatment of aqueous media were studied with compounds modelling fast and slow oxidation reactions, as well as with rapidly reacting endocrine disrupting pollutants. The dependence of PCD oxidation efficiency on gas-liquid contact surface area within its wide span was studied with refractory oxalate (OXA) and rapidly reacting phenol. The results confirmed the dominant surface character of PCD oxidation of aqueous dissolved organic compounds. Radical-driven slow reactions, such as oxidation of OXA, unambiguously benefit from the developed contact surface. Oxidation rate of rapidly reacting phenolate in alkaline media only moderately benefits from the extended contact surface at its low values, becoming virtually independent of it with increasing flow rates. Similar observations were made for bisphenols A and S confirming the dominant character of rapid surface reaction. These observations indicate complete consumption of oxidants generated in the reactor even at moderately developed contact surface. The well-developed gas-liquid contact surface was beneficial for mineralization of bisphenols' intermediates formed during the oxidation. Regardless of gas-liquid interface area, the presence of surfactant radical scavenger showed insignificantly negative effect on the bisphenols oxidation due to the radical screening effect overpowering the advancement of surface reaction promoted with the SDS tail radical.

The synergetic effect of persulfate (PS) added to the PCD-treated oxalate solution was observed in acidic medium with the optimum performance at the OXA/PS molar ratio of 1:0.5. Compared to the non-assisted PCD treatment, OXA mineralization improved for 1.7 times at a slightly increased combined cost. The OXA/PS combination in acidic medium showed the strongest synergy at the lowest gas-liquid contact surface tested in experiments; increased interface improved PCD performance to a larger extent than the one of PCD/PS combination. In neutral solutions, persulfate addition resulted in substantially smaller acceleration of oxalate oxidation, and in alkaline solutions the effect may be considered as negligible explained by the decreased oxidative potential of surface-borne $HO^{\bullet}$ radicals activating PS. From the energy and chemical expenses, non-assisted PCD treatment of neutral and alkaline aqueous media appears preferable. Regardless of operation conditions, addition of hydrogen peroxide (H_2O_2) exhibited negative or neutral impact in OXA treatment compared to non-assisted PCD.

The higher oxidation efficiencies of target compounds at lower pulse repetition frequency indicate the increased contribution of ozone in oxidation at longer pauses between pulses. However, the shortened treatment time in real life situations may overpower somewhat higher oxidation efficiency at longer treatment times.

The results of the study provide practical knowledge for a proper energy-saving watering regime in PCD reactors with simple perforated plate sprinklers dependently of the oxidation reaction rate. These substantiate theoretical knowledge necessary for upscaling and implementation of PCD in real-life applications.

References

Ahsan, N., Ullah, H., Ullah, W., Jahan, S., 2018. Comparative effects of bisphenol S and bisphenol A on the development of female reproductive system in rats; a neonatal exposure study. Chemosphere 197, 336–343. https://doi.org/10.1016/j.chemosphere.2017.12.118

Ajo, P., Kornev, I., Preis, S., 2017. Pulsed corona discharge induced hydroxyl radical transfer through the gas-liquid interface. Sci. Rep. 7, 1–6. https://doi.org/10.1038/s41598-017-16333-1

Ajo, P., Kornev, I., Preis, S., 2015. Pulsed corona discharge in water treatment: the effect of hydrodynamic conditions on oxidation energy efficiency. Ind. Eng. Chem. Res. 54, 7452–7458. https://doi.org/10.1021/acs.iecr.5b01915

Ajo, P., Krzymyk, E., Preis, S., Kornev, I., Kronberg, L., Louhi-Kultanen, M., 2016. Pulsed corona discharge oxidation of aqueous carbamazepine micropollutant. Environ. Technol. (United Kingdom) 37, 2072–2081. https://doi.org/10.1080/09593330.2016.1141236

Ajo, P., Preis, S., Vornamo, T., Mänttäri, M., Kallioinen, M., Louhi-Kultanen, M., 2018. Hospital wastewater treatment with pilot-scale pulsed corona discharge for removal of pharmaceutical residues. J. Environ. Chem. Eng. 6, 1569–1577. https://doi.org/10.1016/j.jece.2018.02.007

Andreozzi, R., Caprio, V., Insola, A., Marotta, R., 1999. Advanced oxidation processes (AOP) for water purification and recovery. Catal. Today 53, 51–59. https://doi.org/10.1016/S0920-5861(99)00102-9

Arslan-Alaton, I., Gurses, F., 2004. Photo-fenton-like and photo-fenton-like oxidation of Procaine Penicillin G formulation effluent. J. Photochem. Photobiol. A Chem. 165, 165–175. https://doi.org/10.1016/j.jphotochem.2004.03.016

Bahnemann, D., 2004. Photocatalytic water treatment: Solar energy applications. Sol. Energy 77, 445–459. https://doi.org/10.1016/j.solener.2004.03.031

Becker, K.H., Kogelschatz, U., Schoenbach, K.H., Barker, R.J., 2005. Non-equilibrium air plasmas at atmospheric pressure. CRC Press, Boca Raton, pp. 1–700. https://doi.org/10.1201/9781482269123

Beltrán, F.J., Rivas, F.J., Montero-de-Espinosa, R., 2002. Catalytic ozonation of oxalic acid in an aqueous TiO2 slurry reactor. Appl. Catal. B Environ. 39, 221–231. https://doi.org/10.1016/S0926-3373(02)00102-9

Bolobajev, J., Gornov, D., Kornev, I., Preis, S., 2021. Degradation of aqueous alachlor in pulsed corona discharge. J. Electrostat. 109, 103543. https://doi.org/10.1016/j.elstat.2020.103543

Bruggeman, P., Leys, C., 2009. Non-thermal plasmas in and in contact with liquids. J. Phys. D. Appl. Phys. 42, 053001. https://doi.org/10.1088/0022-3727/42/5/053001

Bruggeman, P.J., Kushner, M.J., Locke, B.R., Gardeniers, J.G.E., Graham, W.G., Graves, D.B., Hofman-Caris, R.C.H.M., Maric, D., Reid, J.P., Ceriani, E., Fernandez Rivas, D., Foster, J.E., Garrick, S.C., Gorbanev, Y., Hamaguchi, S., Iza, F., Jablonowski, H., Klimova, E., Kolb, J., Krcma, F., Lukes, P., MacHala, Z., Marinov, I., Mariotti, D., Mededovic Thagard, S., Minakata, D., Neyts, E.C., Pawlat, J., Petrovic, Z.L., Pflieger, R., Reuter, S., Schram, D.C., Schröter, S., Shiraiwa, M., Tarabová, B., Tsai, P.A., Verlet, J.R.R., Von Woedtke, T., Wilson, K.R., Yasui, K., Zvereva, G., 2016. Plasma-liquid interactions: A review and roadmap. Plasma Sources Sci. Technol. 25. https://doi.org/10.1088/0963-0252/25/5/053002

Cao, G., He, R., Cai, Z., Liu, J., 2013. Photolysis of bisphenol S in aqueous solutions and the effects of different surfactants. React. Kinet. Mech. Catal. 109, 259–271. https://doi.org/10.1007/s11144-013-0553-6

Castellaro, A.M., Tonda, A., Cejas, H.H., Ferreyra, H., Caputto, B.L., Pucci, O.A., Gil, G.A., 2015. Oxalate induces breast cancer. BMC Cancer 15, 1. https://doi.org/10.1186/s12885-015-1747-2

Chang, T., Wang, Yaqi, Zhao, Z., Wang, Yu, Ma, C., Gao, R., Huang, Y., Chen, Q., Nikiforov, A., 2022. Nonthermal plasma: An emerging innovative technology for the efficient removal of cooking fumes. J. Environ. Chem. Eng. 10, 107721. https://doi.org/10.1016/j.jece.2022.107721

Chen, W.S., Jhou, Y.C., Huang, C.P., 2014. Mineralization of dinitrotoluenes in industrial wastewater by electro-activated persulfate oxidation. Chem. Eng. J. 252, 166–172. https://doi.org/10.1016/j.cej.2014.05.033

Chiang, Y.P., Liang, Y.Y., Chang, C.N., Chao, A.C., 2006. Differentiating ozone direct and indirect reactions on decomposition of humic substances. Chemosphere 65, 2395–2400. https://doi.org/10.1016/j.chemosphere.2006.04.080

Chu, P.K., Lu, X.P., 2013. Low temperature plasma technology: Methods and applications. CRC Press, Boca Raton, pp. 1–493. https://doi.org/10.1201/b15153

Corrales, J., Kristofco, L.A., Baylor Steele, W., Yates, B.S., Breed, C.S., Spencer Williams, E., Brooks, B.W., 2015. Global assessment of bisphenol a in the environment: Review and analysis of its occurrence and bioaccumulation. Dose-Response 13, 1–29. https://doi.org/10.1177/1559325815598308

Cotrim da Cunha, L., Serve, L., Gadel, F., Blazi, J.L., 2001. Lignin-derived phenolic compounds in the particulate organic matter of a French Mediterranean river: Seasonal and spatial variations. Org. Geochem. 32, 305–320. https://doi.org/10.1016/S0146-6380(00)00173-X

Criquet, J., Karpel Vel Leitner, N., 2011. Radiolysis of acetic acid aqueous solutions-effect of pH and persulfate addition. Chem. Eng. J. 174, 504–509. https://doi.org/10.1016/j.cej.2011.07.079

Crittenden, J.C., Hu, S., Hand, D.W., Green, S.A., 1999. A kinetic model for H2O2/UV process in a completely mixed batch reactor. Water Res. 33, 2315–2328. https://doi.org/10.1016/S0043-1354(98)00448-5

Cuerda-Correa, E.M., Alexandre-Franco, M.F., Fernández-González, C., 2020. Advanced oxidation processes for the removal of antibiotics from water. An overview. Water (Switzerland) 12, 102. https://doi.org/10.3390/w12010102

Danckwerts, P. V, 1970. Gas-liquid reactions. McGraw-Hill Book Co., New York, pp. 1–276.

de Luis, A., Lombraña, J.I., 2018. pH-Based strategies for an efficient addition of H2O2 during ozonation to improve the mineralisation of two contaminants with different degradation resistances. Water. Air. Soil Pollut. 229. https://doi.org/10.1007/s11270-018-4014-8

Derevshchikov, V., Dulova, N., Preis, S., 2021. Oxidation of ubiquitous aqueous pharmaceuticals with pulsed corona discharge. J. Electrostat. 110, 103567. https://doi.org/10.1016/j.elstat.2021.103567

Eisenberg, G.M., 1943. Colorimetric determination of hydrogen peroxide. Ind. Eng. Chem. - Anal. Ed. 15, 327–328. https://doi.org/10.1021/i560117a011

Eryılmaz, C., Genç, A., 2021. Review of treatment technologies for the removal of phenol from wastewaters. J. Water Chem. Technol. https://doi.org/10.3103/s1063455x21020065

Furman, O.S., Teel, A.L., Watts, R.J., 2010. Mechanism of base activation of persulfate. Environ. Sci. Technol. 44, 6423–6428. https://doi.org/10.1021/es1013714

Gao, Y., Jiang, J., Zhou, Y., Pang, S., Ma, J., Jiang, C., 2018. Chlorination of bisphenol S : Kinetics, products, and effect of humic acid. Water Res. 131, 208–217. https://doi.org/10.1016/j.watres.2017.12.049

Getoff, N., Schwörer, F., Markovic, V.M., Sehested, K., Nielsen, S.O., 1971. Pulse radiolysis of oxalic acid and oxalates. J. Phys. Chem. 75, 749–755. https://doi.org/10.1021/j100676a004

Gil, A., Galeano, L.A., Vicente, M.Á., 2019. Applications of advanced oxidation processes (AOPs) in drinking water treatment. Springer Cham, Cham, pp. 1–429. https://doi.org/10.1007/978-3-319-76882-3

Glaze, W.H., Kang, J.W., Chapin, D.H., 1987. The chemistry of water treatment processes involving ozone, hydrogen peroxide and ultraviolet radiation. Ozone Sci. Eng. 9, 335–352. https://doi.org/10.1080/01919518708552148

Gligorovski, S., Strekowski, R., Barbati, S., Vione, D., 2015. Environmental implications of hydroxyl radicals (•OH). Chem. Rev. 115, 13051–13092. https://doi.org/10.1021/cr500310b

Grabowski, L.R., Van Veldhuizen, E.M., Pemen, A.J.M., Rutgers, W.R., 2007. Breakdown of methylene blue and methyl orange by pulsed corona discharge. Plasma Sources Sci. Technol. 16, 226–232. https://doi.org/10.1088/0963-0252/16/2/003

Grignard, E., Lapenna, S., Bremer, S., 2012. Weak estrogenic transcriptional activities of bisphenol A and bisphenol S. Toxicol. Vitr. 26, 727–731. https://doi.org/10.1016/j.tiv.2012.03.013

Guerra-Rodríguez, S., Rodríguez, E., Singh, D.N., Rodríguez-Chueca, J., 2018. Assessment of sulfate radical-based advanced oxidation processes for water and wastewater treatment: A review. Water (Switzerland) 10, 1828. https://doi.org/10.3390/w10121828

He, X., Mezyk, S.P., Michael, I., Fatta-Kassinos, D., Dionysiou, D.D., 2014. Degradation kinetics and mechanism of β-lactam antibiotics by the activation of H2O2and Na2S2O8under UV-254nm irradiation. J. Hazard. Mater. 279, 375–383. https://doi.org/10.1016/j.jhazmat.2014.07.008

Hefter, G., Tromans, A., May, P.M., Königsberger, E., 2018. Solubility of sodium oxalate in concentrated electrolyte solutions. J. Chem. Eng. Data 63, 542–552. https://doi.org/10.1021/acs.jced.7b00690

Hernandez, R., Zappi, M., Colucci, J., Jones, R., 2002. Comparing the performance of various advanced oxidation processes for treatment of acetone contaminated water. J. Hazard. Mater. 92, 33–50. https://doi.org/10.1016/S0304-3894(01)00371-5

Hoeben, W.F.L.M., Van Veldhuizen, E.M., Rutgers, W.R., Kroesen, G.M.W., 1999. Gas phase corona discharges for oxidation of phenol in an aqueous solution. J. Phys. D. Appl. Phys. 32. https://doi.org/10.1088/0022-3727/32/24/103

Homem, V., Santos, L., 2011. Degradation and removal methods of antibiotics from aqueous matrices - A review. J. Environ. Manage. 92, 2304–2347. https://doi.org/10.1016/j.jenvman.2011.05.023

Iervolino, G., Vaiano, V., Palma, V., 2020. Enhanced azo dye removal in aqueous solution by H2O2 assisted non-thermal plasma technology. Environ. Technol. Innov. 19, 100969. https://doi.org/10.1016/j.eti.2020.100969

Izadifard, M., Achari, G., Langford, C.H., 2017. Degradation of sulfolane using activated persulfate with UV and UV-Ozone. Water Res. 125, 325–331. https://doi.org/10.1016/j.watres.2017.07.042

Jiang, B., Zheng, J., Qiu, S., Wu, M., Zhang, Q., Yan, Z., Xue, Q., 2014. Review on electrical discharge plasma technology for wastewater remediation. Chem. Eng. J. 236, 348–368. https://doi.org/10.1016/j.cej.2013.09.090

Kask, M., Krichevskaya, M., Preis, S., Bolobajev, J., 2021a. Oxidation of aqueous N-nitrosodiethylamine: Experimental comparison of pulsed corona discharge with H2O2-assisted ozonation. J. Environ. Chem. Eng. 9, 105102. https://doi.org/10.1016/j.jece.2021.105102

Kask, M., Krichevskaya, M., Preis, S., Bolobajev, J., 2021b. Oxidation of aqueous toluene by gas-phase pulsed corona discharge in air-water mixtures followed by photocatalytic exhaust air cleaning. Catalysts 11. https://doi.org/10.3390/catal11050549

Kattel, E., Trapido, M., Dulova, N., 2017. Oxidative degradation of emerging micropollutant acesulfame in aqueous matrices by UVA-induced H2O2/Fe2+and S2O82−/Fe2+processes. Chemosphere 171, 528–536. https://doi.org/10.1016/j.chemosphere.2016.12.104

Kaur, B., Dulova, N., 2020. UV-assisted chemical oxidation of antihypertensive losartan in water. J. Environ. Manage. 261, 110170. https://doi.org/10.1016/j.jenvman.2020.110170

Kaur, B., Kuntus, L., Tikker, P., Kattel, E., Trapido, M., Dulova, N., 2019. Photo-induced oxidation of ceftriaxone by persulfate in the presence of iron oxides. Sci. Total Environ. 676, 165–175. https://doi.org/10.1016/j.scitotenv.2019.04.277

Kogelschatz, U., 2003. Dielectric-barrier discharges: their history, discharge physics, and industrial applications. Plasma Chem. Plasma Process. 23, 1–46. https://doi.org/10.1023/A:1022470901385

Kornev, I., Osokin, G., Galanov, A., Yavorovskiy, N., Preis, S., 2013. Formation of nitrite- and nitrate-ions in aqueous solutions treated with pulsed electric discharges. Ozone Sci. Eng. 35, 22–30. https://doi.org/10.1080/01919512.2013.720898

Kornev, I., Preis, S., 2016. Aqueous benzene oxidation in low-temperature plasma of pulsed corona discharge. J. Adv. Oxid. Technol. 19, 284–289. https://doi.org/10.1515/jaots-2016-0212

Kornev, I., Preis, S., Gryaznova, E., Saprykin, F., Khryapov, P., Khaskelberg, M., Yavorovskiy, N., 2014. Aqueous dissolved oil fraction removed with pulsed corona discharge. Ind. Eng. Chem. Res. 53, 7263–7267. https://doi.org/10.1021/ie403730q

Kornev, I., Saprykin, F., Preis, S., 2017. Stability and energy efficiency of pulsed corona discharge in treatment of dispersed high-conductivity aqueous solutions. J. Electrostat. 89, 42–50. https://doi.org/10.1016/j.elstat.2017.07.001

Krichevskaya, M., Klauson, D., Portjanskaja, E., Preis, S., 2011. The cost evaluation of advanced oxidation processes in laboratory and pilot-scale experiments. Ozone Sci. Eng. 33, 211–223. https://doi.org/10.1080/01919512.2011.554141

Lee, H.J., Kang, D.W., Chi, J., Lee, D.H., 2003. Degradation kinetics of recalcitrant organic compounds in a decontamination process with UV/H2O2 and UV/H2O2/TiO2 processes. Korean J. Chem. Eng. 20, 503–508. https://doi.org/10.1007/BF02705556

Legrini, O., Oliveros, E., Braun, A.M., 1993. Photochemical processes for water treatment. Chem. Rev. 93, 671–698. https://doi.org/10.1021/cr00018a003

Liang, C., Lin, Y.T., Shih, W.H., 2009. Treatment of trichloroethylene by adsorption and persulfate oxidation in batch studies. Ind. Eng. Chem. Res. 48, 8373–8380. https://doi.org/10.1021/ie900841k

Liao, C., Liu, F., Kannan, K., 2012. Bisphenol S, a new bisphenol analogue, in paper products and currency bills and its association with bisphenol a residues. Environ. Sci. Technol. 46, 6515–6522. https://doi.org/10.1021/es300876n

Liu, Y., He, X., Fu, Y., Dionysiou, D.D., 2016. Kinetics and mechanism investigation on the destruction of oxytetracycline by UV-254 nm activation of persulfate. J. Hazard. Mater. 305, 229–239. https://doi.org/10.1016/j.jhazmat.2015.11.043

Liu, Z., Guo, W., Han, X., Li, X., Zhang, K., Qiao, Z., 2016. In situ remediation of ortho-nitrochlorobenzene in soil by dual oxidants (hydrogen peroxide/persulfate). Environ. Sci. Pollut. Res. 23, 19707–19712. https://doi.org/10.1007/s11356-016-7188-x

Liu, Z., Wardenier, N., Hosseinzadeh, S., Verheust, Y., De Buyck, P.J., Chys, M., Nikiforov, A., Leys, C., Van Hulle, S., 2018. Degradation of bisphenol A by combining ozone with UV and H2O2 in aqueous solutions: mechanism and optimization. Clean Technol. Environ. Policy 20, 2109–2118. https://doi.org/10.1007/s10098-018-1595-2

Lukes, P., Clupek, M., Babicky, V., Janda, V., Sunka, P., 2005. Generation of ozone by pulsed corona discharge over water surface in hybrid gas-liquid electrical discharge reactor. J. Phys. D. Appl. Phys. 38, 409–416. https://doi.org/10.1088/0022-3727/38/3/010

Lukes, P., Dolezalova, E., Sisrova, I., Clupek, M., 2014. Aqueous-phase chemistry and bactericidal effects from an air discharge plasma in contact with water: Evidence for the formation of peroxynitrite through a pseudo-second-order post-discharge reaction of H2O2 and HNO2. Plasma Sources Sci. Technol. 23. https://doi.org/10.1088/0963-0252/23/1/015019

Luo, Y., Guo, W., Ngo, H.H., Nghiem, L.D., Hai, F.I., Zhang, J., Liang, S., Wang, X.C., 2014. A review on the occurrence of micropollutants in the aquatic environment and their fate and removal during wastewater treatment. Sci. Total Environ. 473–474, 619–641. https://doi.org/10.1016/j.scitotenv.2013.12.065

Ma, Y., Liu, H., Wu, J., Yuan, L., Wang, Y., Du, X., Wang, R., Marwa, P.W., Petlulu, P., Chen, X., Zhang, H., 2019. The adverse health effects of bisphenol A and related toxicity mechanisms. Environ. Res. 176. https://doi.org/10.1016/j.envres.2019.108575

Magureanu, M., Bradu, C., Parvulescu, V.I., 2018. Plasma processes for the treatment of water contaminated with harmful organic compounds. J. Phys. D. Appl. Phys. 51. https://doi.org/10.1088/1361-6463/aacd9c

Malik, M.A., 2010. Water purification by plasmas: Which reactors are most energy efficient? Plasma Chem. Plasma Process. 30, 21–31. https://doi.org/10.1007/s11090-009-9202-2

Marotta, E., Ceriani, E., Schiorlin, M., Ceretta, C., Paradisi, C., 2012. Comparison of the rates of phenol advanced oxidation in deionized and tap water within a dielectric barrier discharge reactor. Water Res. 46, 6239–6246. https://doi.org/10.1016/j.watres.2012.08.022

Martínez-Huitle, C.A., Ferro, S., Reyna, S., Cerro-López, M., De Battisti, A., Quiroz, M.A., 2008. Electrochemical oxidation of oxalic acid in the presence of halides at boron doped diamond electrode. J. Braz. Chem. Soc. 19, 150–156. https://doi.org/10.1590/S0103-50532008000100021

Matzek, L.W., Carter, K.E., 2016. Activated persulfate for organic chemical degradation: A review. Chemosphere 151, 178–188. https://doi.org/10.1016/j.chemosphere.2016.02.055

Mehrabani-Zeinabad, M., Langford, C.H., Achari, G., 2016. Advanced oxidative degradation of bisphenol A and bisphenol S. J. Environ. Eng. Sci. 10, 92–102. https://doi.org/10.1680/jenes.15.00015

Meichsner, J., Schmidt, M., Schneider, R., Wagner, H.E., 2013. Nonthermal plasma chemistry and physics. CRC Press, Boca Raton, pp. 1–564. https://doi.org/10.1201/b12956

Michałowicz, J., Duda, W., 2007. Phenols - Sources and toxicity. Polish J. Environ. Stud. 16, 347–362.

Mieno, T., 2016. Plasma science and technology - Progress in physical states and chemical reactions. IntechOpen, London, pp. 1–548. https://doi.org/10.5772/60692

Mohd, A., 2020. Presence of phenol in wastewater effluent and its removal: an overview. Int. J. Environ. Anal. Chem. 102, 1362–1384. https://doi.org/10.1080/03067319.2020.1738412

Munter, R., 2001. Advanced oxidation processes - Current status and prospects. Treatise Water Sci. 4, 377–408. https://doi.org/10.1016/B978-0-444-53199-5.00093-2

Onga, L., Boroznjak, R., Kornev, I., Preis, S., 2021. Oxidation of aqueous organic molecules in gas-phase pulsed corona discharge affected by sodium dodecyl sulphate: Explanation of variability. J. Electrostat. 111, 103581. https://doi.org/10.1016/j.elstat.2021.103581

Onga, L., Kattel-Salusoo, E., Trapido, M., Preis, S., 2022. Oxidation of aqueous dexamethasone solution by gas-phase pulsed corona discharge. Water 14. https://doi.org/10.3390/w14030467

Onga, L., Kornev, I., Preis, S., 2020. Oxidation of reactive azo-dyes with pulsed corona discharge: Surface reaction enhancement. J. Electrostat. 103, 103420. https://doi.org/10.1016/j.elstat.2020.103420

Ono, R., Oda, T., 2003. Dynamics of ozone and OH radicals generated by pulsed corona discharge in humid-air flow reactor measured by laser spectroscopy. J. Appl. Phys. 93, 5876–5882. https://doi.org/10.1063/1.1567796

Ono, R., Zhang, X., Komuro, A., 2020. Effect of oxygen concentration on the postdischarge decay of hydroxyl density in humid nitrogen-oxygen pulsed streamer discharge. J. Phys. D. Appl. Phys. 53, 425201. https://doi.org/10.1088/1361-6463/ab98c3

Panorel, I., Kornev, I., Hatakka, H., Preis, S., 2011. Pulsed corona discharge for degradation of aqueous humic substances. Water Sci. Technol. Water Supply 11, 238–245. https://doi.org/10.2166/ws.2011.045

Panorel, I., Preis, S., Kornev, I., Hatakka, H., Louhi-Kultanen, M., 2013. Oxidation of aqueous pharmaceuticals by pulsed corona discharge. Environ. Technol. 34, 923–930. https://doi.org/10.1080/09593330.2012.722691

Parvulescu, V.I., Magureanu, M., Lukes, P., 2012. Plasma chemistry and catalysis in gases and liquids. Wiley-VCH Verlag & Co. KGaA, Weinheim, pp. 1–422. https://doi.org/10.1002/9783527649525

Patel, M., Yarlagadda, V., Adedoyin, O., Saini, V., Assimos, D.G., Holmes, R.P., Mitchell, T., 2018. Oxalate induces mitochondrial dysfunction and disrupts redox homeostasis in a human monocyte derived cell line. Redox Biol. 15, 207–215. https://doi.org/10.1016/j.redox.2017.12.003

Pokryvailo, A., Wolf, M., Yankelevich, Y., Wald, S., Grabowski, L.R., Veldhuizen, E.M. Van, Rutgers, W.R., Reiser, M., Glocker, B., Eckhardt, T., Kempenaers, P., Welleman, A., 2006. High-power pulsed corona for treatment of pollutants in heterogeneous media 34, 1731–1743.

Poznyak, T., Tapia, R., Vivero, J., Chairez, I., 2006. Effect of pH to the decomposition of aqueous phenols mixture by ozone. J. Mex. Chem. Soc. 50, 28–35.

Preis, S., Kornev, I., Hatakka, H., Kallas, J., Yavorovskiy, N., 2016. Method and device for a liquid purifying and use of device. FI125772B.

Preis, S., Panorel, I., Llauger Coll, S., Kornev, I., 2014. Formation of nitrates in aqueous solutions treated with pulsed corona discharge: the impact of organic pollutants. Ozone Sci. Eng. 36, 94–99. https://doi.org/10.1080/01919512.2013.836955

Preis, S., Panorel, I.C., Kornev, I., Hatakka, H., Kallas, J., 2013. Pulsed corona discharge: the role of ozone and hydroxyl radical in aqueous pollutants oxidation. Water Sci. Technol. 68, 1536–1542. https://doi.org/10.2166/wst.2013.399

Prokop, Z., Hanková, L., Jeřábek, K., 2004. Bisphenol A synthesis - Modeling of industrial reactor and catalyst deactivation. React. Funct. Polym. 60, 77–83. https://doi.org/10.1016/j.reactfunctpolym.2004.02.013

Ribeiro, A.R., Nunes, O.C., Pereira, M.F.R., Silva, A.M.T., 2015. An overview on the advanced oxidation processes applied for the treatment of water pollutants defined in the recently launched Directive 2013/39/EU. Environ. Int. 75, 33–51. https://doi.org/10.1016/j.envint.2014.10.027

Schiavon, G.J., Andrade, C.M.G., Jorge, L.M.M., Paraiso, P.R., 2012. Design and analysis of an ozone generator system operating at high frequency with digital signal controller. Rev. Ciência e Tecnol. 15, 23–35.

Shang, K., Li, W., Wang, X., Lu, N., Jiang, N., Li, J., Wu, Y., 2019. Degradation of p-nitrophenol by DBD plasma/Fe2+/persulfate oxidation process. Sep. Purif. Technol. 218, 106–112. https://doi.org/10.1016/j.seppur.2019.02.046

Sharma, A., Ahmad, J., Flora, S.J.S., 2018. Application of advanced oxidation processes and toxicity assessment of transformation products. Environ. Res. 167, 223–233. https://doi.org/10.1016/j.envres.2018.07.010

Sugai, T., Nguyen, P.T., Tokuchi, A., Jiang, W., Minamitani, Y., 2015. The effect of flow rate and size of water droplets on the water treatment by pulsed discharge in air. IEEE Trans. Plasma Sci. 43, 3493–3499. https://doi.org/10.1109/TPS.2015.2450741

Tang, S., Yuan, D., Rao, Y., Li, N., Qi, J., Cheng, T., Sun, Z., Gu, J., Huang, H., 2018. Persulfate activation in gas phase surface discharge plasma for synergetic removal of antibiotic in water. Chem. Eng. J. 337, 446–454. https://doi.org/10.1016/j.cej.2017.12.117

Tay, K.S., Rahman, N.A., Abas, M.R. Bin, 2012. Degradation of bisphenol A by ozonation: Rate constants, influence of inorganic anions, and by-products. Maejo Int. J. Sci. Technol. 6, 77–94. https://doi.org/10.14456/mijst.2012.7

The European Parliament and the Council of the European Union, 2020. Directive (EU) 2020/2184, EU (revised) Drinking Water Directive. Annex 1. Part B. Off. J. Eur. Communities 2019, 35.

The European Parliament and the Council of the European Union, 2011. Comission Directive 2011/8/EU. Off. J. Eur. Communities 29–32.

Umar, M., Roddick, F., Fan, L., Aziz, H.A., 2013. Application of ozone for the removal of bisphenol A from water and wastewater - A review. Chemosphere 90, 2197–2207. https://doi.org/10.1016/j.chemosphere.2012.09.090

Vecitis, C.D., Lesko, T., Colussi, A.J., Hoffmann, M.R., 2010. Sonolytic decomposition of aqueous bioxalate in the presence of ozone. J. Phys. Chem. A 114, 4968–4980. https://doi.org/10.1021/jp9115386

Von Gunten, U., 2003. Ozonation of drinking water: Part I. Oxidation kinetics and product formation. Water Res. 37, 1443–1467. https://doi.org/10.1016/S0043-1354(02)00457-8

Wacławek, S., Lutze, H. V., Grübel, K., Padil, V.V.T., Černík, M., Dionysiou, D.D., 2017. Chemistry of persulfates in water and wastewater treatment: A review. Chem. Eng. J. 330, 44–62. https://doi.org/10.1016/j.cej.2017.07.132

Wanda, E.M.M., Nyoni, H., Mamba, B.B., Msagati, T.A.M., 2017. Occurrence of emerging micropollutants in water systems in Gauteng, Mpumalanga, and North West provinces, South Africa. Int. J. Environ. Res. Public Health 14, 8–20. https://doi.org/10.3390/ijerph14010079

Wang, J., Wang, S., 2018. Activation of persulfate (PS) and peroxymonosulfate (PMS) and application for the degradation of emerging contaminants. Chem. Eng. J. 334, 1502–1517. https://doi.org/10.1016/j.cej.2017.11.059

Wang, S., Zhou, N., 2016. Removal of carbamazepine from aqueous solution using sono-activated persulfate process. Ultrason. Sonochem. 29, 156–162. https://doi.org/10.1016/j.ultsonch.2015.09.008

Wang, Y.X., Kornev, I., Wei, C.H., Preis, S., 2019. Surfactant and non-surfactant radical scavengers in aqueous reactions induced by pulsed corona discharge treatment. J. Electrostat. 98, 82–86. https://doi.org/10.1016/j.elstat.2019.03.001

Wardenier, N., Liu, Z., Nikiforov, A., Van Hulle, S.W.H., Leys, C., 2019. Micropollutant elimination by O3, UV and plasma-based AOPs: An evaluation of treatment and energy costs. Chemosphere 234, 715–724. https://doi.org/10.1016/j.chemosphere.2019.06.033

Wardman, P., 1989. Reduction potentials of one electron couples involving free radicals in aqueous solution. J. Phys. Chem. Ref. Data 18, 1637–1755. https://doi.org/10.1063/1.555843

Wen, Y.Z., Liu, H.J., Liu, W.P., Jiang, X.Z., 2005. Degradation of organic contaminants in water by pulsed corona discharge. Plasma Chem. Plasma Process. 25, 137–146. https://doi.org/10.1007/s11090-004-8839-0

Wu, L.H., Zhang, X.M., Wang, F., Gao, C.J., Chen, D., Palumbo, J.R., Guo, Y., Zeng, E.Y., 2018. Occurrence of bisphenol S in the environment and implications for human exposure: A short review. Sci. Total Environ. 615, 87–98. https://doi.org/10.1016/j.scitotenv.2017.09.194

Yalkowsky, S.H., He, Y., Jain, P., 2010. Handbook of aqueous solubility data. CRC Press, Boca Raton, pp. 1–1620. https://doi.org/10.1201/EBK1439802458

Yamamoto, T., Yasuhara, A., Shiraishi, H., Nakasugi, O., 2001. Bisphenol A in hazardous waste landfill leachates. Chemosphere 42, 415–418. https://doi.org/10.1016/S0045-6535(00)00079-5

Yamazaki, E., Yamashita, N., Taniyasu, S., Lam, J., Lam, P.K.S., Moon, H.B., Jeong, Y., Kannan, P., Achyuthan, H., Munuswamy, N., Kannan, K., 2015. Bisphenol A and other bisphenol analogues including BPS and BPF in surface water samples from Japan, China, Korea and India. Ecotoxicol. Environ. Saf. 122, 565–572. https://doi.org/10.1016/j.ecoenv.2015.09.029

Yang, Y., Cho, Y.I., Fridman, A., 2012. Plasma discharge in liquid : water treatment and applications. Taylor & Francis Inc, Boca Raton, pp. 1–210. https://doi.org/10.1201/b11650

Yang, Y., Guo, H., Zhang, Y., Deng, Q., Zhang, J., 2016. Degradation of bisphenol A using ozone/persulfate process: kinetics and mechanism. Water. Air. Soil Pollut. 227, 53. https://doi.org/10.1007/s11270-016-2746-x

Zhang, B.T., Zhang, Y., Teng, Y., Fan, M., 2015. Sulfate radical and its application in decontamination technologies. Crit. Rev. Environ. Sci. Technol. 45, 1756–1800. https://doi.org/10.1080/10643389.2014.970681

Acknowledgements

I would like to express my gratitude to my supervisor Prof. Sergei Preis for the possibility of doctoral studies, guidance, assistance, and academic and non-academic discussions through the years. Also, I would like to thank Prof. Marina Trapido for teaching me various subjects related to environmental technology and for giving me a chance to travel abroad. I am sincerely grateful for the continuous support from Dr. Niina Dulova and Dr. Eneliis Kattel-Salusoo, who taught me many things about science as whole. Without their help, doctoral studies would have been much harder. Also, I would like to express my gratitude to Dr. Maarja Kask and Dr. Liina Onga for continuous support, interesting discussions, exciting events we participated together, and for all the times I will remember for the rest of my life, and, of course, for the times yet to come. Additionally, I would like to thank for the assistance and discussion from all colleagues from Laboratory of Environmental Technology and from our neighbors from Chemical Engineering Research and Development Centre through the years. I would also say thank you for all the MSc-students, who I had the possibility to supervise: Ms Mirjam Lätt, Mr Dmitri Nikitin and Mrs Anne Mari Kääp.

I am sincerely grateful for two of my main foundations in my life: my Gooseberries and my friends. With all of you, I would not have made it so far. I appreciate the support, push and knowing that wherever I am, you always will be behind my back.

I would like to acknowledge the financial support from Estonian Ministry of Education and Research (IUT1-7), Estonian Research Council (PRG776), Institutional Development Program of Tallinn University of Technology for 2016-2022, European Regional Development Fund (project 2014-2020.4.01.16-0032 and Dora Pluss program), ASTRA “TUT Institutional Development Programme for 2016-2022” Graduate School of Functional Materials and Technologies (2014-2020.4.01.16-0032), Tallinn University of Technology, City of Tallinn, European Social Fund under the Knowledge Education Development Operational Programme POWR.03.03.00-00-PN13/18, Polish National Agency for Academic Exchange, Cracow University of Technology and MonGOS.

Abstract

Optimization of aqueous media treatment with pulsed corona discharge: hydrodynamics and kinetics conformed with the discharge parameters and energy efficiency

Production and usage of highly potent non-biodegradable pharmaceuticals, personal care products and plastic compounds result in their accumulation in waterbodies. Insufficient performance of traditional wastewater treatment processes and accumulation of recalcitrant pollutants in the environment causes a significant deterioration of aquatic resources. This makes alternative cost-effective treatment methods necessary to solve the problem. A possible solution is the implementation of advanced oxidation processes (AOPs) involving generation of highly reactive hydroxyl radical ($HO^{\bullet}$). Gas-phased pulsed corona discharge (PCD), in which the treated aqueous media are sprayed directly into the plasma zone, is one of the most promising AOPs with unequalled energy efficiency. Unlike widely used ozonation, both long-living (ozone) and short-living (e.g., $HO^{\bullet}$) reactive oxygen species (ROS) generated in PCD participate in pollutant degradation reactions, thus making applied electric energy used more efficiently. However, since PCD studied in this research is a novel water treatment technique, there is limited data available for operational parameters, such as the impact of gas-liquid contact-surface on the energy efficiency, which was studied only in narrow interface diapason. For radical scavenger surfactants, substances often present in wastewaters, the dependence has not yet been established for pollutants of various oxidation reaction rates. While combined AOPs often activate extrinsic oxidants, such as persulfate (PS) and hydrogen peroxide (H_2O_2), the beneficial combination of PCD/H_2O_2 was described only for the in-liquid PCD. The potential activation and synergetic effect of the gas-phase PCD with persulfate addition has not yet been studied.

The experiments were performed in a periodical PCD device consisting of plasma reactor, storage tank of 40 L capacity, water circulation system and pulse generator. The effect of gas-liquid contact surface on oxidation efficiency was studied with model pollutants of oxalate (OXA) and phenol at acidic and alkaline conditions. Oxidation experiments with bisphenol A (BPA) and bisphenol S (BPS) were conducted, following their degradation with and without addition of sodium dodecyl sulfate (SDS) as surfactant $HO^{\bullet}$ scavenger at alkaline pH. The experiments with extrinsic oxidants was conducted with oxalate at various OXA/oxidant ratios. Pulse repetition frequencies of 200 and 880 pulses per second were applied, corresponding to pulse generator output powers of 32 and 123.2 W, respectively. Concentrations of OXA and total organic carbon (TOC) were measured using TOC analyzer; phenol and bisphenol's concentrations were determined with high performance liquid chromatography (HPLC), and the end products of bisphenols' oxidation were quantified with ion chromatography. The potential intermediates of bisphenols were detected with HPLC combined with mass spectrometer (HPLC-MS).

The results showed that the gas-liquid contact surface linearly growing with the spray density exhibited substantial impact on the oxidation rate of slowly reacting OXA within the experimental limits. Rapidly reacting phenol showed an optimum contact surface determined by the discharge power at sufficiently developed interface, above which no oxidation efficiency improvement was observed**.** For example, in acidic

medium, the increase in gas-liquid contact surface for about 4.5 times resulted in the OXA oxidation energy efficiency grown for about 13 times, while the efficiency of phenol oxidation increased for only about 1.3 times.

The results exhibited a beneficial effect at OXA/PS molar ratios from 1:0.1 to 1:1 in acidic medium, indicating the activation of PS by PCD. At optimal OXA/PS molar ratio of 1:0.5, PS addition surpassed unassisted PCD treatment for 1.7 times at lower pulse repetition frequency. In neutral solutions, PS addition resulted in substantially smaller acceleration of OXA oxidation, and in alkaline solutions the effect may be considered as negligible. This could be related to accumulation of radical scavengers, bicarbonate and carbonate anions, at higher pH. Besides, sulfate radical reactions with water molecules produce $HO^{\bullet}$ having shorter lifetime (0.02 μs) compared to the one of $SO_4^{\bullet-}$ (30–40 μs). Contrary to PS, addition of H_2O_2 to PCD-treated solutions exhibited negative or neutral impact in all studied media.

The energy efficiencies of 66.4 and 52.9 g kW^{-1} h^{-1} observed in BPA and BPS oxidation, respectively, surpassed the closest competitors, ozonation and other electric discharge processes, showing PCD as a promising method in removal of bisphenols. The moderate difference between pulse repetition frequencies and the slight effect of contact surface variation on energy efficiency indicate bisphenols reacting rapidly with both long-living O_3 and short-living radicals. This circumstance makes the use of high pulse repetition frequency at shorter treatment time beneficial for the reactor's intensity in action avoiding the trade-off between the energy expense and the time of treatment. The slow TOC removal, however, benefited from higher gas-liquid contact surface: with the gas-liquid contact surface increased from 42 to 115 m^{-1}, the TOC removal increased from 34.7% to 51.1% and from 52.7% to 69.4% for BPA and BPS, respectively. The possible oxidation intermediates detected by HPLC-MS were mainly formed through hydroxylation and cracking of benzene rings, followed by further degradation into short chained aliphatic acids. The oxidation end-products were quantified as acetate, formate and oxalate. The addition of SDS showed a moderately negative impact on energy efficiency in all studied conditions.

The obtained results in this thesis provide necessary theoretical knowledge for optimization of PCD-oxidation of pollutants of various reaction kinetics. The findings contribute to the PCD upscaling and implementation in real-life applications.

Lühikokkuvõte

Impulss koroona elektrilahenduse optimeerimine vesikeskkonna töötlemiseks: hüdrodünaamika ja kineetika lähtuvalt elektrilahenduse parameetritest ning energia efektiivsusest

Tugevatoimeliste raskelt biolagundatavate ravimite, isikliku hügieeni toodete ja plastiühendite tootmine ning kasutamine põhjustab nende akumuleerumist veekogudes ja veeressursside olulist halvenemist, kuna traditsioonilised reoveepuhastusprotsessid pole piisavalt efektiivsed selliseid ühendeid sisaldavate reovete puhastamisel. Seega on selliste reovete puhastamiseks vaja leida alternatiivsed kulutõhusad töötlemismeetodid. Võimalikuks lahenduseks on rakendada täiustatud oksüdatsiooniprotsesse (AOP), mida iseloomustab väga reaktiivse hüdroksüülradikaali ($HO^{\bullet}$) teke. Gaasifaasiline impulss koroona elektrilahendus (PCD), kus töödeldav vesilahus (puhastatav vesi) pihustatakse otse elektroodide vahele plasmatsooni, on üks perspektiivikamaid AOP-sid, millel on võrreldes teiste puhastusprotsessidega kõrgem energiaefektiivsus. Erinevalt laialdaselt kasutatavast osoonimisest, osalevad PCD protsessis saasteainete lagundamisreaktsioonides protsessi käigus genereeritud nii pika- (osoon) kui ka lühikese eluaega (nt $HO^{\bullet}$) reaktiivsed hapnikuosakesed (ROS), muutes seetõttu elektrienergia kasutamise efektiivsemaks. Kuna käesolevas töös uuritud PCD protsess on uudne veepuhastusprotsess, siis on vähe andmeid tööparameetrite kohta, nagu gaas-vedelik kontaktpinna mõju energiaefektiivsusele, mida on uuritud vaid kitsas piirkihi vahemikus. Samuti puuduvad teadmised kontaktpinna mõju kohta reovees sageli esinevate radikaalipüüdurite, pindaktiivsete ainete, juuresolekul. Kuigi kombineeritud AOP-des aktiveeritakse sageli väliseid oksüdante, nagu persulfaati (PS) ja vesinikperoksiidi (H_2O_2), siis PCD ja H_2O_2 kasulikku kombinatsiooni on kirjeldatud ainult vedelfaasilise PCD puhul. Persulfaadi potentsiaalset aktiveerimist ning võimalikku sünergeetilist toimet PCD protsessis pole veel uuritud.

Katsed teostati perioodilises PCD-seadmes, mis koosnes plasmareaktorist, 40-liitrisest veemahutist, vee tsirkulatsioonisüsteemist ning impulssgeneraatorist. Gaas-vedelik kontaktpinna mõju oksüdatsiooni efektiivsusele PCD protsessis uuriti kasutades mudelsaasteainetena oksalaati (OXA) ja fenooli nii happelises kui ka aluselises keskkonnas. Pindaktiivsete radikaalipüüdurite mõju PCD protsessile uuriti Bisfenool A (BPA) ja bisfenool S (BPS) oksüdatsiooni katsetes. Katsed viidi läbi ilma pindaktiivse aineta ja lisades BPA ja BPS algselt aluselistesse vesilahustesse naatriumdodetsüülsulfaati (SDS) kui pindaaktiivset $HO^{\bullet}$-püüdurit. Väliste oksüdeerijate mõju OXA lagundamisele uuriti kasutades väliste oksüdeerijate erinevate OXA/oksüdeerija dooside suhtega happelises keskkonnas. Järgnevad katsed viidi läbi optimaalse OXA/oksüdeerija doosi suhtega neutraalses ja aluselises keskkonnas. Katsetes rakendati impulsse sagedusega 200 ja 880 impulss/s, mis vastavad impulssgeneraatori väljundvõimsustele vastavalt 32 ja 123,2 W. OXA kontsentratsiooni ja orgaanilise süsiniku üldsisaldust (TOC) mõõdeti TOC-analüsaatoriga; fenooli ja bisfenooli kontsentratsioonid määrati kõrgefektiivse vedelikkromatograafiaga (HPLC) ning bisfenoolide oksüdatsiooni lõpp-produktid ioonkromatograafiaga. Bisfenoolide

oksüdatsiooni potentsiaalsed vaheühendid tuvastati kasutades HPLC-d koos mass-spektromeetriga (HPLC-MS).

Katsete tulemused näitasid, et gaas-vedelik kontaktpind kasvas lineaarselt pihustustihedusega ning avaldas olulist mõju aeglaselt reageeriva OXA oksüdatsioonikiirusele. Kiiresti reageeriva fenooli vesilahuse töötlemisel eksisteeris antud elektrilahenduse võimsusel piisavalt väljakujunenud piirpinna korral teatud optimaalne kontaktpinna suurus, millest suurema kontaktpinna korral oksüdatsiooni efektiivsuse paranemist ei täheldatud. Näiteks happelises keskkonnas OXA oksüdatsioonil kasvas 4,5-kordsel gaas-vedelik kontaktpinna suurenemisel energiaefektiivsus umbes 13 korda, samal ajal kui fenooli oksüdatsiooni efektiivsus suurenes vaid umbes 1,3 korda.

PCD protsessi koos väliste oksüdantidega (PS või H_2O_2) uuriti OXA lagundamise katsetes, kusjuures tähelepanu oli suunatud võimalikule sünergeetilisele efektile. Tulemused näitasid positiivset toimet OXA/PS molaarsuhetel 1/0,1 kuni 1/1 happelises keskkonnas, tõestades PS aktiveerimist PCD poolt. Optimaalse OXA/PS molaarsuhte 1/0,5 juures ületas kombinatsiooni - PCD koos PS lisamisega - efektiivsus PCD töötluse efektiivsust ilma PS-ta 1,7 korda madalamal impulsi sagedusel. OXA oksüdatsioonil neutraalsetes lahustes oli PS lisamisel oluliselt väiksem mõju ning leeliselises keskkonnas võib seda mõju pidada tühiseks. See võib olla seotud radikaalipüüdurite, vesinikkarbonaadi ja karbonaadi anioonide suurema kontsentratsiooniga kõrgema pH juures. Lisaks genereeritakse sulfaatradikaalide reaktsioonides veemolekulidega $HO^{\bullet}$-radikaale, mille eluiga on lühem (0,02 µs) kui $SO_4^{\bullet-}$-radikaalidel (30–40 µs). Vastupidiselt PS lisamisele, avaldas H_2O_2 lisamine PCD-protsessile negatiivset või tühist mõju kõigi uuritud parameetrite juures.

Doktoritöös uuriti ka bisfenoolide lagundamist PCD-protsessis erinevatel tööparameetritel nii SDS-i juuresolekul kui ka ilma. BPA ja BPS lagundamisel saavutatud energiaefektiivsused 66,4 ja 52,9 g kW^{-1} h^{-1} ületasid PCD-protsessiga konkureerivate protsesside - osoonimise ja teiste elektrilahendusprotsesside - energiaefektiivsusi. Seega võib PCD-protsessi pidada paljulubavaks protsessiks bisfenoolide lagundamisel. Mõõdukas erinevus impulsi sagedustes ja kontaktpinna muutumise vähene mõju energiaefektiivsusele näitavad, et bisfenoolid reageerivad kiiresti mõlema ROS-ga s.t nii osooni kui ka radikaalidega. Selle asjaolu tõttu on kõrgema sagedusega impulsi kasutamine PCD-protsessis (millega kaasneb lühem töötlemisaeg) kasulik reaktori töö intensiivsuse osas, ühtlasi välditakse sellega energiakulu ja töötlemisaja vahelist kompromissi. Aeglasele TOC vähendamisele aitas aga kaasa suurem gaas-vedeliku kontaktpind: kui gaas-vedeliku kontaktpind suurenes 42 kuni 115 m^{-1}, siis suurenes TOC vähenemine 34,7 kuni 51,1% BPA puhul ning BPS-i puhul 52,7-lt kuni 69,4%-ni. Bisfenoolide oksüdatsioonil HPLC-MS-ga leitud potentsiaalsed vaheühendid, mis moodustusid põhiliselt hüdroksülatsiooni ja benseeni tuuma lõhkumise teel, muundati järgnevalt lühikese ahelaga alifaatseteks hapeteks. Oksüdatsiooni lõpp-produktidena kvantifitseeriti atsetaat, formaat ja oksalaat. SDS-i lisamisega kaasnes kõigis uuritud tingimustes mõõdukalt negatiivne mõju energiaefektiivsusele.

Käesoleva doktoritöö tulemusena on saadud teadmised, mis on vajalikud erineva reaktsioonikineetikaga saasteainete PCD oksüdatsiooni optimeerimiseks ning PCD seadme skaleerimiseks ja reaalsete rakenduste juurutamiseks.

Appendix 1

Publication I

Tikker, P., Kornev, I., Preis, S., 2020. Oxidation energy efficiency in water treatment with gas-phase pulsed corona discharge as a function of spray density. J. lectrostat. 106, 103466. https://doi.org/10.1016/j.elstat.2020.103466

Journal of Electrostatics 106 (2020) 103466

Contents lists available at ScienceDirect

Journal of Electrostatics

journal homepage: http://www.elsevier.com/locate/elstat

Oxidation energy efficiency in water treatment with gas-phase pulsed corona discharge as a function of spray density

P. Tikker [a], I. Kornev [b], S. Preis [a,*]

[a] Department of Materials and Environmental Technology, Tallinn University of Technology, Ehitajate tee 5, 19086, Tallinn, Estonia
[b] R&D Laboratory 'Clean Water', National Research Tomsk Polytechnic University, 30 Lenin Ave., Tomsk, 634050, Russian Federation

ARTICLE INFO

Keywords:
Advanced oxidation processes
AOPs
Gas-liquid contact surface
Hydroxyl radical
Ozone
Plasma

ABSTRACT

Gas-phase pulsed corona discharge (PCD) shows promising energy efficiency in oxidation of aqueous pollutants. Further progress requires knowledge in efficiency dependent on the contact surface of treated water sprinkled to the discharge zone. Experimental studies focused on the dependency used phenol and oxalate solutions at various pH for variable oxidation kinetics. For slow reactions within the experimental limits, oxidation rate was growing substantially with the spray density. Rapid oxidation showed an optimum spray density determined by discharge power at sufficiently developed interface. The oxidation kinetics fits to description of a pseudo-second order process predicting optimum choice of sprinkling rate.

1. Introduction

Traditional wastewater biological treatment is often insufficient towards recalcitrant organic compounds. Accumulation of those in the environment together with scarcity of available drinking water sources thus dictate necessity in cost-effective advanced treatment methods [1,2]. One of the promising ways is the use of advanced oxidation processes (AOPs) pursuing to the market mostly in the form of water ozonation. In AOPs, pollutants are degraded mostly by hydroxyl radical HO· [3], forming in a set of processes including UV/H_2O_2, Fenton and TiO_2/UV [4]. Among AOPs, a growing interest towards electric discharges is observed, where organic substances are oxidised by highly reactive oxidants generated at the gas-liquid interface [5,6]. Malik et al. (2010) in his review described the gas-phase pulsed corona discharge (PCD) reactors with the treated solutions sprayed to the discharge zone as the most efficient [7]. Later, Sugai et al. (2015) described the removal of indigo carmine benefitting from increased flow rate in a sprinkled PCD reactor, although giving data on nozzles without the contact surface numbers [8]. Pokryvailo et al. (2007) considered both, corona-above-water and aerosol reactors in phenol oxidation with a priority of the aerosol one, although the fog formation is an energy-consuming process [9]. Pulsed corona discharge has been reported having high energy efficiency surpassing the closest competitor, conventional ozonation, minimum twofold [10,11].

Previous studies established the relation between gas-liquid contact surface area and oxidation rate only for slowly reacting oxalate within relatively narrow range of spray density [12]. A systematic approach to the task thus requires establishing the relation for organic substances with various oxidation kinetics: establishing the dependence of oxidation efficiency on spray density in PCD reactor with a simple perforated plate sprinkler comprises the research objective.

2. Materials and methods

2.1. Experimental device

The experimental device (Flowrox Oy, Finland) consists of a plasma reactor, a pulse generator and a water circulation system shown in Fig. 1. The plasma reactor contains an electrode system consisting of high voltage electrodes positioned horizontally between two grounded vertical parallel plates. The diameter of the wire electrodes is 0.5 mm, the distance between the grounded plate and the wire electrode is 19 mm and the overall length of the wire electrodes is 20 m. The horizontal cross-section of the plasma zone is 38 mm in width and 500 mm in length. The total volume of the discharge reactor is 110 L. Water circulation system comprises a pump (Iwaki Co. Ltd., Japan) and a frequency regulator (Yaskawa, Japan), which is used to control the pump engine rotation rate. The pump is used to feed water to the top of the reactor, where it is dispersed and showered to the plasma zone by a perforated plate. In the latter sized 30 mm in width and 500 mm in

* Corresponding author.
E-mail address: sergei.preis@taltech.ee (S. Preis).

https://doi.org/10.1016/j.elstat.2020.103466
Received 6 January 2020; Received in revised form 13 March 2020; Accepted 8 April 2020
0304-3886/© 2020 Elsevier B.V. All rights reserved.

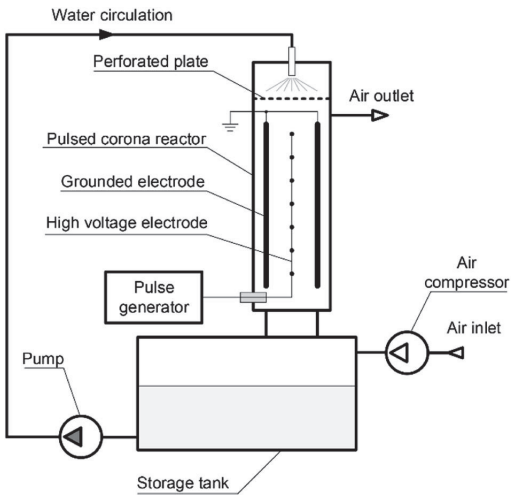

Fig. 1. Schematic diagram of the experimental system.

length, 51 holes were drilled in a bisecting single row with a diameter of 1 mm. The high voltage pulses are generated at frequencies of 50–880 pulses per second (pps), which corresponds to 9–123.2 W of an output power. After passing through the reactor, treated water circulates from the storage tank to the top of the reactor thus executing a batch mode of operation.

2.2. Chemicals and sample preparation

For the oxidation experiments, oxalate ($C_2O_4^{2-}$) and phenol were chosen as target pollutants. Oxalate is a well-known refractory compound with a slow oxidation rate, which is contrary to rapidly reacting phenol. Both substances show different oxidation rates at different pH conditions. Experiments, therefore, were conducted in acidic and alkaline media. Oxalic acid, when dissolved in distilled water at experimental concentrations, set the initial pH at 3.0, and pH of sodium oxalate solution was adjusted to 10.3 ± 0.2. Phenol aqueous solutions were regulated to pH value of 3 and 11.5. The adjustment was done with H_2SO_4 and NaOH 5.0-M solutions.

All oxidation experiments were conducted with 20-L samples of solutions in ambient conditions at the initial concentration of 100 mg L^{-1}. Solution were prepared in 1-L measuring cylinder with bidistilled water, which was then diluted to a total volume of 20 L in the reactor tank. Distilled water was used in experiments to avoid precipitation with water hardness cations.

2.3. Analyses

Content of oxalate having no intermediate oxidation products was determined measuring total organic carbon (TOC) using Multi N/C 3100 analyser (Analytic Jena, Germany). Aqueous phenol concentration was measured by the YL 9300 HPLC (YL Instrument Co., Korea) equipped with XBridge BEH C18 Column (130 Å, 3.5 μm, 3 mm × 150 mm). The analysis was performed using an isocratic method with a mobile phase comprised of a mixture of 60% water (acidified with 0.1% acetic acid) and 40% acetonitrile. Samples were analysed at the wavelength of 270 nm and the flow rate of 0.2 mL min^{-1}. The pH was measured using a digital pH/Ion meter (Mettler Toledo S220, USA).

2.4. Contact surface measurement

The gas-liquid contact surface was measured by classical method of sulphite oxidation by air oxygen in the presence of cobalt sulphate catalyst [13]. After the catalyst addition, 0.1-M sodium sulphite solution was circulated through the system at various spray densities. Oxidation rate of Na_2SO_3 into Na_2SO_4 was determined iodometrically using sodium thiosulfate as titrant. The contact surface was calculated as described previously [12].

2.5. Oxidation experiments

Two PCD input powers were provided at 200 and 880 pps, input power 32 and 123.2 W, respectively. The flow rate of treated water was between 2.3 and 28.2 L min^{-1}, which corresponds to spray density from 0.002 to 0.0243 m s^{-1}. The latter is calculated using Eq. (1):

$$q = \frac{v}{S} \tag{1}$$

where v is the flowrate of water, m^3 s^{-1}, S is the horizontal cross section area of plasma zone, m^2, which in the experimental device is 0.019 m^2. The treatment process was started after the pulse generator was turned on. For 200 pps, samples were collected up to 60 min treatment time, and for 880 pps – 15 min. Prior to sampling, the pulse generator was turned off and treated solutions mixed for at least 3 min to allow uniformity in concentration. The energy efficiency *E*, g kW^{-1} h^{-1}, in oxidation experiments were calculated using Eq. (2):

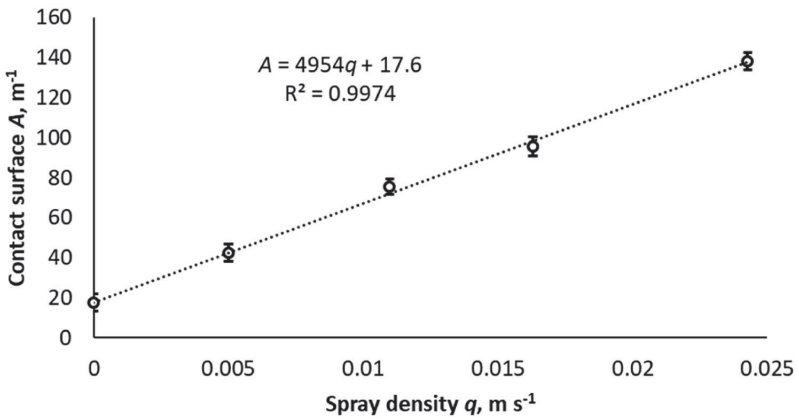

Fig. 2. Dependence of gas-liquid contact surface area A on spray density q in PCD device.

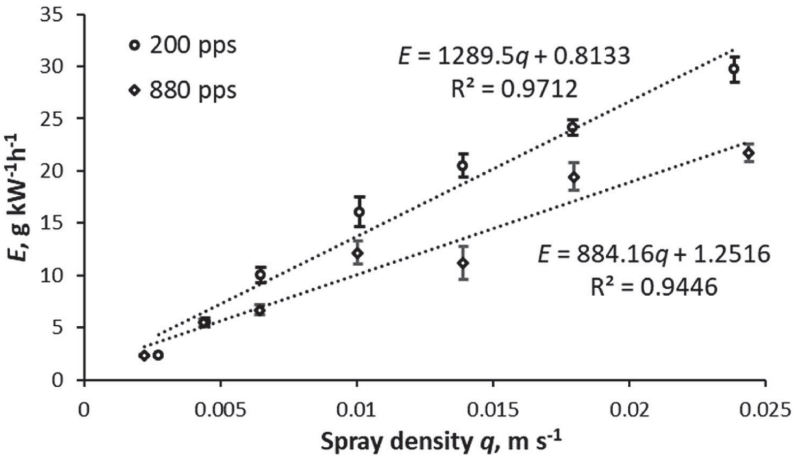

Fig. 3. Dependence of oxidation energy efficiency E on spray density q in PCD treatment at 200 and 880 pps: oxalic acid at pH 3.0.

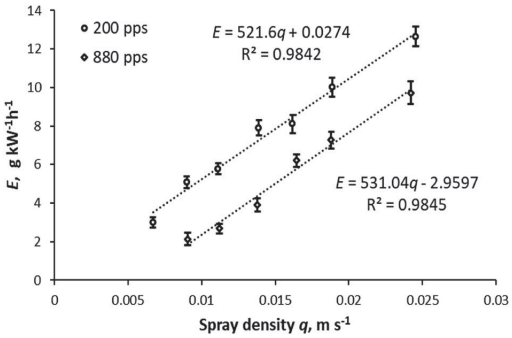

Fig. 4. Dependence of oxidation energy efficiency E on spray density q in PCD treatment at 200 and 880 pps: sodium oxalate at pH 10.3 ± 0.2.

$$E = \frac{\Delta C \cdot V}{W} \tag{2}$$

where ΔC is the decrease of pollutant concentration, g m^{-3}, V is the volume of treated solution sample, m^3, and W is the pulsed energy input to the generator, kWh. The energy efficiency values were found for every sampling point subsequently comprising the average efficiency in all oxidation experiments.

3. Results and discussion

3.1. Contact surface

Contact surface A, m^{-1} (m^2 m^{-3}), was found to have a linear dependence on spray density (Fig. 2). As the latter increased from 0 to 0.0243 m s^{-1}, the contact surface reached from 17.6 to 138 m^{-1}, respectively, as described in Eq. (3) with correlation factor R^2 averaging 0.9974:

$$A = 4954q + 17.6 \tag{3}$$

where q is the spray density, m s^{-1}. At the horizontal cross-section area of plasma zone of 0.019 m^2, the maximum spray density was provided with the aqueous media flow rate of 0.47 L s^{-1} at maximum feeding capacity of the pump used in the experiments adjusted using the frequency controller at 50 Hz. The pressure in the feeding line did not exceed 0.6 bar at the maximum flow rate.

3.2. Energy efficiency in oxidation: impact of gas-liquid contact surface

3.2.1. Slow reactions

Oxidation efficiency of oxalic acid and sodium oxalate within the range of experimental conditions was found to have a linear dependence on spray density (Figs. 3 and 4). One can see higher removal efficiencies in acidic medium: oxalic acid removal reached up to 48% in 60 min at 200 pps and 35% in 15 min at 880 pps treatment time, respectively. In alkaline conditions, only up to 20% at 200 pps and 15% at 880 pps was achieved for sodium oxalate treated for 60 and 15 min, respectively. The energy dose delivered to the reactors comprised 1.60 and 1.54 kWh m^{-3} at the end of treatment at 200 (60 min) and 880 (15 min) pps, respectively. During the experiments, pH of acidic solutions remained practically constant, whereas pH of alkaline solutions decreased from 10.3 ± 0.2 to 8.5 ± 0.2.

In case of oxalic acid, average energy efficiency reached up to 30.0 g kW^{-1} h^{-1} at 200 pps and about 22.0 g kW^{-1} h^{-1} at 880 pps, when the spray density increased up to maximum technically available value of 0.0243 m s^{-1}. One should notice that Ajo et al., 2015 [12] reported maximum oxidation efficiency of oxalic acid reached in solutions containing about 60 mg L^{-1} of the target compound 3.8–5.4 g $kW^{-1}h^{-1}$ dependent on the pulse repetition rate at the contact surface from 48 to 65 m^{-1}. These numbers are well consistent with the ones obtained in the present research operating with 1.5 times higher oxalic acid concentrations, although twofold increased contact surface numbers resulted consistently in higher oxidation efficiencies. For sodium oxalate at pH around 10.3, efficiencies of 12.7 g kW^{-1} h^{-1} at 200 pps and 9.7 g kW^{-1} h^{-1} at 880 pps were achieved at the maximum contact surface of 138 m^{-1}.

Considering the behaviour of rapidly reacting phenol (see below), one can suggest approximation of oxidation efficiency to a constant value for other organic compounds. This makes the curves expectedly resembling exponents. However, for the practical observation needs, the linear equation approach is justified within the experimental limits. Linear equations serve a basis for optimisation of spray density for various kinetics sufficient for practical quantitative assessments of perforated plate performance. The linear dependence of oxalate oxidation efficiency on the contact surface is consistent with the surface character of the reaction proved earlier [14,15]: since oxalate is mostly oxidised with OH-radicals, its oxidation rate is proportional to the

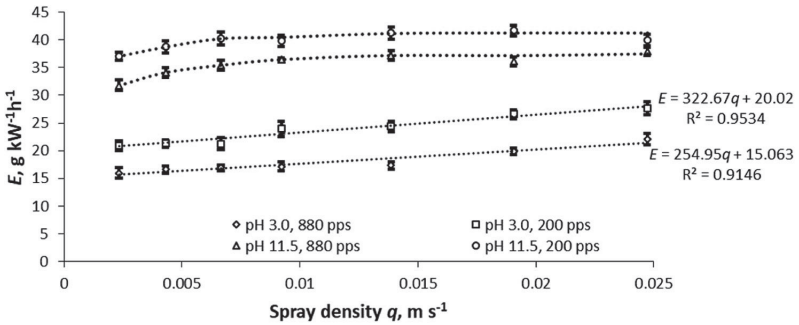

Fig. 5. Dependence of oxidation energy efficiency E on spray density q in PCD treatment of phenolic solutions at 200 and 880 pps and pH 3.0 and 11.5.

surface treated with the discharge. The difference in the slope angles for oxalate at different pH values is explained by a difference in reaction rates being noticeably smaller alkaline pH. Higher pulse repetition frequency also resulted in smaller oxidation energy efficiency, as discussed earlier [11]. The impact of frequency is partly explained by the role of ozone, responsible for about 20–25% of oxalate oxidation as established in Refs. [12,15] and observed in this research at various pulse repetition frequencies. Longer treatment at reduced pulse repetition frequencies provides longer contact of treated solutions with long-living ozone, giving it time for better utilization. Concentration of ozone in PCD reactors was found earlier reaching equilibrium concentration of 5 mg L^{-1} in air regardless the pulse repetition frequency [10].

3.2.2. Fast reactions

Fig. 5 shows similar tendency in degradation of aqueous phenol with initial pH 3.0, where maximum average energy efficiency of 27.7 and 22.0 g kWh^{-1} was achieved at 200 and 880 pps, respectively. Unlike with oxalate, the spray density did not drastically affect the removal efficiency, which may be explained by rapid reaction of phenol not only with hydroxyl radicals, but also with molecular ozone making the oxidants consumed even at low contact surface areas. For alkaline medium at pH about 11.5, where the oxidation rate is even higher, the contact surface exhibited only minimal effect on efficiency at low contact surface range; with the developed surface, the oxidation efficiency oscillated practically within a narrow range staying generally at a constant range determined by the power of pulses delivered to reactor. Thus, oxidation efficiency at 200 pps fits in the range from 37 to 41 g kWh^{-1} and at 880 pps – from 32 to 38 g kWh^{-1} showing slight growth only for the low contact surface numbers. The PCD reactor seems to be working at the efficiencies close to maximum available values with reactive oxygen species consumed thus making the production of those limiting the process rate. These results suggest that for a relatively rapid reaction of phenol oxidation, a gas-liquid interface sufficient for oxidants consumption was developed already at low spray densities, and energy efficiency appeared to depend on the amount of generated reactive oxygen species.

Aqueous phenol degradation was improved about 1.5 times in alkaline medium (Fig. 5), increasing the removal rate at 200 pps from 45% at pH 3.0–70% at pH 11.5, and, at 880 pps, from 35% to 62% with the equivalent change in pH. This acceleration is related to phenol dissociation into phenolates reported to be more reactive towards ozone than molecular phenol [16,17]. A similar degradation characteristic in PCD was observed previously [11].

3.3. Process kinetics dependent on contact surface

Pseudo-second order kinetics was found to be useful in characterization of heterogeneous PCD oxidation process, in which the reaction rate was described using Eq. (4) [11]:

$$\frac{dC}{dt} = k_2 * C * \frac{P}{V} \tag{4}$$

where k_2 is the pseudo-second order reaction rate constant, $m^3\ J^{-1}$; C is the concentration of the pollutant, mol m^{-3}; P is the pulsed power delivered to the reactor, W; V is volume of the discharge zone, m^3, in the experimental device 0.0137 m^3.

The pseudo-second process rates were calculated, and the reaction rate coefficients k_2 are given in Table 1. The coefficients are growing with contact surface analogously to the oxidation energy efficiency thus indicating mass-transfer phenomena involved in chemisorption. One should notice that in oxidation of oxalate, a growth in the reaction rate somewhat surpasses the one of the contact surface area, which is potentially explained with intensified mass transfer at higher flow rates and gaseous turbulence caused by the intensified sprinkling.

Table 1
Dependence of pseudo-second order rate coefficient k_2 on contact surface in PCD treatment for reactants of various oxidation kinetics.

$k_2 \cdot 10^8$, $m^3\ J^{-1}$	Contact surface, m^{-1}								
	31 ± 2	40 ± 1	51 ± 1	63 ± 1	71 ± 3	86 ± 1	98 ± 2	110 ± 3	137 ± 4
200 pps									
Oxalic acid	0.44	1.05	1.93		3.09	4.44		4.68	5.68
Sodium oxalate			0.81	1.48	1.66	2.62	2.19	2.93	3.60
Phenol pH 3.0	4.22	4.27	4.26	4.84		4.94		5.29	5.44
Phenol pH 11.5	7.69	7.96	8.03	8.09		8.33		8.34	7.88
880 pps									
Oxalic acid	0.44	1.04	1.28		2.33	2.08		3.81	4.14
Sodium oxalate				0.63	0.78	0.84	1.80	2.14	2.86
Phenol pH 3.0	3.20	3.29	3.39	3.44		3.52		4.01	4.31
Phenol pH 11.5	6.63	7.06	7.20	7.56		7.76		7.46	7.64

4. Conclusions

The dependency of oxidation efficiency of pulsed corona discharge on gas-liquid contact surface area within its wide span provided by variations in spray density was studied. The results confirmed the surface character of aqueous dissolved organic compounds. Radical-driven slow reactions, such as oxidation of oxalates, unambiguously benefit from developed contact surface. A minor disproportion in 'efficiency – surface area' relation in favour of efficiency was identified for oxalates, likely caused by intensified mass transfer at higher flow rates. Oxidation rate of rapidly reacting phenolate in alkaline media only moderately benefits from intensified contact surface at low spray densities, becoming virtually independent of it with increasing flow rates. This indicates complete consumption of oxidants generated in the reactor even at moderately developed contact surface.

Observations in oxidation kinetics support the pseudo-second order of the process described earlier [11], implying a possibility for PCD reactions being optimized by a proper choice of spray density dependent on the aqueous pollutant reactivity. Pseudo-second order rate coefficients growing with increasing contact surface indicate chemisorption character of oxidation. The results of the study supply practical knowledge for a proper watering regime in PCD reactors with simple perforated plate sprinklers targeting optimizing energy consumption at appropriate oxidation rate.

Declaration of competing interest

I declare no conflicts of interests.

Acknowledgments

This work was supported by the Institutional Development Program of Tallinn University of Technology for 2016–2022, project 2014-2020.4.01.16-0032 from EU Regional Development Fund, and the Research Group Support project PRG776 of Estonian Research Council.

References

[1] N. Vieno, T. Tuhkanen, L. Kronberg, Elimination of pharmaceuticals in sewage treatment plants in Finland, Water Res. 41 (2007) 1001–1012, https://doi.org/10.1016/j.watres.2006.12.017.

[2] P. Ajo, S. Preis, T. Vornamo, M. Mänttäri, M. Kallioinen, M. Louhi-Kultanen, Hospital wastewater treatment with pilot-scale pulsed corona discharge for removal of pharmaceutical residues, J. Environ. Chem. Eng. 6 (2018) 1569–1577, https://doi.org/10.1016/j.jece.2018.02.007.

[3] J. Hoigné, H. Bader, Rate constants of reactions of ozone with organic and inorganic compounds in water-II. Dissociating organic compounds, Water Res. 17 (1983) 185–194, https://doi.org/10.1016/0043-1354(83)90099-4.

[4] S. Gligorovski, R. Strekowski, S. Barbati, D. Vione, Environmental implications of hydroxyl radicals (•OH), Chem. Rev. 115 (2015) 13051–13092, https://doi.org/10.1021/cr500310b.

[5] J. Kornev, N. Yavorovsky, S. Preis, M. Khaskelberg, U. Isaev, B.N. Chen, Generation of active oxidant species by pulsed dielectric barrier discharge in water-air mixtures, Ozone Sci. Eng. 28 (2006) 207–215, https://doi.org/10.1080/01919510600704957.

[6] P.J. Bruggeman, M.J. Kushner, B.R. Locke, J.G.E. Gardeniers, W.G. Graham, D. B. Graves, R.C.H.M. Hofman-Caris, D. Maric, J.P. Reid, E. Ceriani, D. Fernandez Rivas, J.E. Foster, S.C. Garrick, Y. Gorbanev, S. Hamaguchi, F. Iza, H. Jablonowski, E. Klimova, J. Kolb, F. Krcma, P. Lukes, Z. MacHala, I. Marinov, D. Mariotti, S. Mededovic Thagard, D. Minakata, E.C. Neyts, J. Pawlat, Z.L. Petrovic, R. Pflieger, S. Reuter, D.C. Schram, S. Schröter, M. Shiraiwa, B. Tarabová, P.A. Tsai, J.R.R. Verlet, T. Von Woedtke, K.R. Wilson, K. Yasui, G. Zvereva, Plasma-liquid interactions: a review and roadmap, Plasma Sources Sci. Technol. 25 (2016), https://doi.org/10.1088/0963-0252/25/5/053002.

[7] M.A. Malik, Water purification by plasmas: which reactors are most energy efficient? Plasma Chem. Plasma Process. 30 (2010) 21–31, https://doi.org/10.1007/s11090-009-9202-2.

[8] T. Sugai, P.T. Nguyen, A. Tokuchi, W. Jiang, Y. Minamitani, The effect of flow rate and size of water droplets on the water treatment by pulsed discharge in air, IEEE Trans. Plasma Sci. 43 (2015) 3493–3499, https://doi.org/10.1109/TPS.2015.2450741.

[9] A. Pokryvailo, M. Wolf, Y. Yankelevich, E. Abramzon, A. Welleman, A compact high-power pulsed corona source for treatment of pollutants in heterogeneous media, Dig. Tech. Pap. Int. Pulsed Power Conf. 34 (2007) 1188–1191, https://doi.org/10.1109/PPC.2005.300550.

[10] I. Panorel, I. Kornev, H. Hatakka, S. Preis, Pulsed corona discharge for degradation of aqueous humic substances, Water Sci. Technol. Water Supply 11 (2011) 238–245, https://doi.org/10.2166/ws.2011.045.

[11] S. Preis, I.C. Panorel, I. Kornev, H. Hatakka, J. Kallas, Pulsed corona discharge: the role of Ozone and hydroxyl radical in aqueous pollutants oxidation, Water Sci. Technol. 68 (2013) 1536–1542, https://doi.org/10.2166/wst.2013.399.

[12] P. Ajo, I. Kornev, S. Preis, Pulsed corona discharge in water treatment: the effect of hydrodynamic conditions on oxidation energy efficiency, Ind. Eng. Chem. Res. 54 (2015) 7452–7458, https://doi.org/10.1021/acs.iecr.5b01915.

[13] P.V. Danckwerts, Gas-liquid Reactions, McGraw-Hill Book Co., 1970. https://books.google.ee/books?id=upxTAAAAMAAJ.

[14] P. Ajo, I. Kornev, S. Preis, Pulsed corona discharge induced hydroxyl radical transfer through the gas-liquid interface, Sci. Rep. 7 (2017) 1–6, https://doi.org/10.1038/s41598-017-16333-1.

[15] Y.X. Wang, I. Kornev, C.H. Wei, S. Preis, Surfactant and non-surfactant radical scavengers in aqueous reactions induced by pulsed corona discharge treatment, J. Electrost. 98 (2019) 82–86, https://doi.org/10.1016/j.elstat.2019.03.001.

[16] E. Marotta, E. Ceriani, M. Schiorlin, C. Ceretta, C. Paradisi, Comparison of the rates of phenol advanced oxidation in deionized and tap water within a dielectric barrier discharge reactor, Water Res. 46 (2012) 6239–6246, https://doi.org/10.1016/j.watres.2012.08.022.

[17] T. Poznyak, R. Tapia, J. Vivero, I. Chairez, Effect of pH to the decomposition of aqueous phenols mixture by ozone, J. Mex. Chem. Soc. 50 (2006) 28–35.

Appendix 2

Publication II

Tikker, P., Dulova, N., Kornev, I., Preis, S., 2021. Effects of persulfate and hydrogen peroxide on oxidation of oxalate by pulsed corona discharge. Chem. Eng. J. 411, 128586. https://doi.org/10.1016/j.cej.2021.128586

Chemical Engineering Journal 411 (2021) 128586

Contents lists available at ScienceDirect

Chemical Engineering Journal

journal homepage: www.elsevier.com/locate/cej

Effects of persulfate and hydrogen peroxide on oxidation of oxalate by pulsed corona discharge

Priit Tikker [a], Niina Dulova [a,*], Iakov Kornev [b], Sergei Preis [a,*]

[a] Department of Materials and Environmental Technology, Tallinn University of Technology, Ehitajate Tee 5, 19086 Tallinn, Estonia
[b] R&D Laboratory 'Clean Water', National Research Tomsk Polytechnic University, 30 Lenin Ave., Tomsk 634050, Russian Federation

ARTICLE INFO

Keywords:
AOPs
Plasma
Activated persulfate
Hydroxyl radicals
Gas-liquid contact surface
Oxalic acid

ABSTRACT

Application of gas-phase pulsed corona discharge (PCD) to oxidation of aqueous pollutants shows unequalled energy efficiency among advanced oxidation processes (AOPs). Improved AOPs often activate extrinsic oxidants. Experimental research was undertaken into sodium persulfate and hydrogen peroxide activation by PCD in oxidation of 1.11 mM oxalate. Oxidant and target compound concentration ratios, pH, gas-liquid contact surface and pulse repetition frequency were studied as control parameters. Results implicated a beneficial effect at oxalate/persulfate molar ratios from 1:0.1 to 1:1 in acidic medium with the optimum at 1:0.5, moderate contact surface and lower frequency. However, the observed synergism of PCD/PS combination decreased with increasing the initial pH of the treated solution. Hydrogen peroxide exhibited negative or neutral impact in all media. Non-assisted PCD proved the most energy efficient approach towards water treatment at neutral and alkaline conditions.

1. Introduction

Production and usage of highly potent non-biodegradable pharmaceuticals, personal care products and pesticides result in their accumulation in waterbodies [1,2]. Insufficient performance of traditional wastewater treatment processes and accumulation of recalcitrant pollutants in the environment causes a significant deterioration of aquatic resources [1,3]. This makes alternative cost-effective treatment methods necessary to solve the problem.

Advanced oxidation processes (AOPs) successfully used to degrade recalcitrant compounds [3,4] involve generation of hydroxyl radical ($HO^{\bullet}$) in amounts sufficient to affect water purification at ambient pressure and temperature [5]. $HO^{\bullet}$ is highly reactive ($E^0 = 2.80$ V) and less selective than e.g. molecular ozone ($E^0 = 2.07$ V) degrading variety of organic pollutants with higher efficiency [6]. Hydroxyl radicals are formed in a variety of processes such as ozonation combinations, UV/TiO_2, water sonolysis, and water electrolysis [3,6,7]. Hydrogen peroxide combinations with ozone (O_3), UV radiation, iron and other catalysts (Fenton process) has shown to be a source of $HO^{\bullet}$ [3,6–8]. An interest has risen also in respect to sulfate radical ($SO_4^{\bullet-}$) processes (SR-AOPs) [9,10]: sulfate radical is also highly reactive ($E^0 = 2.60 – 3.1$ V) [1,9,10] although more selective due to reacting mainly through the electron transfer, while $HO^{\bullet}$ reacts either through electron transfer, hydrogen abstraction or electrophilic addition [1]. Sulfate radical is more likely to react with target organic compounds due to its longer lifetime (30 – 40 μs) than hydroxyl radicals (0.02 μs) [1]. $SO_4^{\bullet-}$ may be generated either by activation of persulfate ($S_2O_8^{2-}$, PS) (Eq. (1)) or peroxymonosulfate (HSO_5^-, PMS) (Eq. (2)) [1]. Although direct reactions of both PS and PMS with organic substances are possible, these, however, tend to be slow in respect to the majority of substances [10,11]. The latter circumstance is related to lower oxidation potentials of PS ($E^0 = 2.01$ V) and PMS ($E^0 = 1.4$ V) anions [10,11].

$$S_2O_8^{2-} + \text{activator} \rightarrow SO_4^{\bullet-} + (SO_4^{\bullet-} \text{ or } SO_4^{2-}) \quad (1)$$

$$HSO_5^- + \text{activator} \rightarrow SO_4^{\bullet-} + (HO^{\bullet} \text{ or } HO^-) \quad (2)$$

Activation of PS and PMS is classified into two categories, energy- and catalyst-based activations [10]. In energy-based activation, peroxide link (-O=O-) is fissured forming $SO_4^{\bullet-}$ (Eqs. (3) and (4)) [10]. The source of energy is either heat [1], UV [12], short-wave radiation [13] or ultrasound [14].

$$HSO_5^- + \text{energy} \rightarrow SO_4^{\bullet-} + HO^{\bullet} \quad (3)$$

$$S_2O_8^{2-} + \text{energy} \rightarrow 2SO_4^{\bullet-} \quad (4)$$

* Corresponding authors.
E-mail addresses: niina.dulova@taltech.ee (N. Dulova), sergei.preis@taltech.ee (S. Preis).

https://doi.org/10.1016/j.cej.2021.128586
Received 14 September 2020; Received in revised form 11 January 2021; Accepted 14 January 2021
Available online 20 January 2021
1385-8947/© 2021 Elsevier B.V. All rights reserved.

The catalysts may be either transition metals (M^{n+}) (Eqs. (5) and (6)), non-metals, such as activated carbon, bases (alkaline activation) or active particles [10,11,15–17].

$$HSO_5^- + M^{n+} \rightarrow M^{(n+1)+} + SO_4^{\bullet -} + HO^- \quad (5)$$

$$S_2O_8^{2-} + M^{n+} \rightarrow M^{(n+1)+} + SO_4^{\bullet -} + SO_4^{2-} \quad (6)$$

Dependent on solution pH, other radicals formed in sulfate radical reactions participate further in degradation of pollutants. For example, $SO_4^{\bullet -}$ reacts with water producing $HO^{\bullet}$ (Eq. (7)) dominating in alkaline solutions (Eq. (8)); at neutral pH, $SO_4^{\bullet -}$ and $HO^{\bullet}$ participate equally in reactions, whereas in acidic media sulfate radical is a dominant reactive species [10,11].

$$SO_4^{\bullet -} + H_2O \rightarrow SO_4^{2-} + HO^{\bullet} + H^+ \quad (7)$$

$$SO_4^{\bullet -} + HO^- \rightarrow SO_4^{2-} + HO^{\bullet} \quad (8)$$

Activation in SR-AOPs may be achieved in using electric discharges presenting promising methods in environmental applications [18–20]. In gas-phase discharges, long- (O_3) and short-living ($HO^{\bullet}$, atomic oxygen radical $O^{\bullet}$) oxidative species are formed through high-energy electron collisions with surrounding atoms and molecules (Eqs. (9)–(12)).

$$O_2 + e^- \rightarrow 2O^{\bullet} + e^- \quad (9)$$

$$O^{\bullet} + O_2 + (O_2, O_3 \text{ or } N_2) \rightarrow O_3 + (O_2, O_3 \text{ or } N_2) \quad (10)$$

$$H_2O + e^- \rightarrow HO^{\bullet} + H^{\bullet} + e^- \quad (11)$$

$$HO^{\bullet} + HO^{\bullet} \rightarrow H_2O_2 \quad (12)$$

Among various electric discharges [21–24], the highest energy efficiencies were reported for gas-phase pulsed corona discharge (PCD) reactors, where solution is sprayed directly into plasma zone, thus utilizing short-living radicals formed at the gas–liquid interface [25,26]. To achieve higher pollutant removal efficiency, electric discharges were combined with PS and hydrogen peroxide [4,27–30]. Even though potential activators of PS and H_2O_2, such as high energy electrons and short-living species, are formed in PCD, the authors failed to find publications regarding corona-activated PS, although less energy-efficient dielectric barrier discharge (DBD) was studied in combinations with PS [4,30] and PMS [28].

In current study, oxalate ($C_2O_4^{2-}$, OXA) was chosen as a target pollutant in PCD, PCD/PS and PCD/H_2O_2 systems as a refractory intermediate commonly formed during oxidation of organic pollutants [31]. Although OXA was studied for its refractory properties, it is also a pollutant regularly detected in natural waters [32]. High oxalate concentrations cause harmful health effects, such as kidney damage, lithiasis and, according to the latest studies, even breast cancer [33]. Regardless earlier reported synergetic effect of PCD/H_2O_2 combination in degradation of highly reactive 4-chlorophenol [34], the authors failed to find earlier reported studies related to PCD-activated PS and potential synergy of PCD with H_2O_2 in degradation of refractory compounds. In addition, the authors of present research applied the technique of different pulse parameters improving the energy efficiency of treatment for orders of magnitude compared to [34]. Thus, an experimental study was undertaken into effects of PS and H_2O_2 additions to PCD treatment of aqueous OXA solutions together with impacts of process control parameters on the treatment energy efficiency - oxidant and target compound concentration ratios, pH, gas–liquid contact surface and pulse repetition frequency.

2. Materials and methods

2.1. Chemicals

Oxalic acid dihydrate ($C_2H_2O_4{\cdot}2H_20$, ≥99%) was obtained from Lach-Ner, Ltd. (Czech Republic). Sodium oxalate ($Na_2C_2O_4$, ≥99%), sodium persulfate ($Na_2S_2O_8$, ≥99%), sodium hydroxide (NaOH, ≥98%) and sodium sulfite (Na_2SO_3, ≥99%) were purchased from Merck KGaA (Germany). Solution of H_2O_2 (≥30%) was obtained from Thermo Fischer Scientific, Ltd. (USA).

2.2. Experimental device

Experiments were conducted in a periodical PCD reactor constructed from stainless steel by Flowrox Oy, Finland. The device includes plasma reactor, storage tank of 40 L capacity, water circulation system, and pulse generator, presented previously in earlier publication [35]. The plasma reactor of 110 L interior volume consists of electrode system with twenty-four horizontal high voltage electrodes with diameter of 0.5 mm placed between two grounded vertical parallel plates. The distance between wire electrodes and grounded plate is 18 mm making the size of horizontal cross-section of the plasma zone 36 mm in width and 500 mm in length. The solution to be treated is pumped to the top of reactor with a pump (Iwaki Co. Ltd., Japan), which engine rotation rate is controlled with a frequency regulator (Yaskawa, Japan). At the top of reactor, solution is dispersed into plasma zone through a perforated plate with 51 perforations of 1 mm diameter in a single row. Perforated plate is 30 mm in width and 500 mm in length. Pulse generator provides high voltage pulses to the reactor at frequencies within the span from 50 to 880 pulses per second (pps), corresponding to output power 9–123.2 W, respectively. After passing the plasma zone, treated water falls to a storage tank, from where it is circulated back to the top of reactor.

2.3. Experimental procedure

Oxalate degradation in PCD, PCD/PS and PCD/H_2O_2 systems was studied at ambient temperature 20 ± 2 °C. Solutions were prepared in 1-L volumetric flask with subsequent dilution of its content to a total volume of 20 L by distilled water in the reactor tank making the initial OXA concentration 1.11 mM in all experiments. Pre-selected amounts of H_2O_2 and PS were dissolved in a 200 mL volumetric flasks and added to the tank before the start of treatment. The studied OXA/oxidant molar ratios were 1:0.1, 1:0.25, 1:0.5 and 1:1, corresponding to the oxidant concentrations of 0.111, 0.278, 0.555 and 1.11 mM, respectively.

Experiments were conducted in acidic, neutral and alkaline media. At experimental conditions, oxalic acid dissolved in distilled water set the initial pH 3.0. To adjust pH of sodium oxalate solution at 7.4 ± 0.2 and 10.4 ± 0.2, 5-M NaOH solution was used. The flowrate of treated water circulation was between 5.0 and 29.5 L min^{-1}, providing the circulation time of the sample volume from about 4 min to 40 s, respectively, which correspond to the spray densities (q) of 0.005 to 0.027 m s^{-1}, calculated by using equation (Eq. (13)).

$$q = \frac{v}{S} \quad (13)$$

where v – flowrate of solution, $m^3\ s^{-1}$; S – horizontal cross section area of plasma zone, m^2.

Since oxalate degradation efficiency depends linearly on spray density, the maximum flowrate was chosen for PCD experiments, unless stated otherwise. From spray density values, the contact surface area was calculated according to equation (Eq. (14)) [35].

$$A = 4954q + 17.6 \quad (14)$$

where q – spray density, m s^{-1} , i.e. $m^3\ m^{-2}\ s^{-1}$, relative to the PCD reactor cross-sectional area.

Experiments were performed at two generator power output values of 32 W and 123.2 W, corresponding to frequencies of 200 and 880 pps. Plasma treatment time comprised up to 60 min at 200 pps and 15 min at 880 pps with similar energy doses of 1.60 and 1.54 kWh m^{-3}, respectively, delivered to the reactor at the end of treatment. For proper sampling, the treated solutions were circulated in the reactor for four

minutes after the pulse generator was turned off for equalization in concentrations. The energy efficiency E, g kW^{-1} h^{-1}, was calculated using equation (Eq. (15)).

$$E = \frac{\Delta C^{*} V}{W} \quad (15)$$

where ΔC – decrease of OXA concentration, g m^{-3}; V – volume of treated solution, m^3; W – energy consumption derived from the generator power output and the time of treatment, kWh.

Non-plasma reference experiments with OXA/PS and OXA/H_2O_2 at an OXA/oxidant molar ratio of 1:1 were conducted in a 1-L glass beakers containing 800 mL of treated solution. These experiments were conducted at the pH values identical to the ones used in PCD treatment. In all oxidation experiments, oxidation reactions were quenched by adding sodium sulfite crystals to vials at the Na_2SO_3/oxidant molar ratio of 10:1. All experiments (plasma and non-plasma) were duplicated with the results deviations fitting into 5-% confidential interval.

2.4. Analytical methods

Since OXA has no stable organic oxidation intermediates, pollutant content was determined by measuring total organic carbon (TOC) using Multi N/C 3100 analyzer (Analytic Jena, Germany). TOC removal percentage (%) was calculated using Eq. (16).

$$TOC\ \ removal = \left(1 - \frac{TOC_t}{TOC_0}\right) * 100\% \quad (16)$$

where TOC_0 and TOC_t are the TOC values at treatment times 0 and t, mg C L^{-1}

Besides TOC, the content of total inorganic carbon (TIC) was measured. Residual H_2O_2 was measured using spectrophotometer (Genesys 10S, Thermo Scientific) at 410 nm by adding samples to the Ti^{4+} solution to form pertitanic acid [36]. Solution pH was measured using a digital pH/Ion meter (Mettler Toledo S220).

3. Results and discussion

3.1. Effect of pH on OXA oxidation in PCD

During experiments, pH of acidic and neutral solutions remained practically constant, while decreased in alkaline medium from 10.4 ± 0.2 to 9.3 ± 0.3. The pH descent in alkaline solutions is likely related to formation of nitric acid in PCD, having little effect in acidic medium [37]. In neutral solutions, residuals of sodium oxalate and bicarbonate preserved pH at a constant level. The results of OXA PCD oxidation in acidic, neutral and alkaline media are given as TOC removal and oxidation energy efficiency in Fig. 1.

Oxalate degradation decreased significantly with increasing pH. Accordingly, TOC removal declined from 51.5% to 33% and 14% as pH increased from 3.0 to 7.4 and 10.4, making the energy efficiencies 31.2, 19.8 and 8.6 g kW^{-1} h^{-1} in acidic, neutral and alkaline media, respectively. The difference in efficiencies is related to $HO^{\bullet}$ oxidation potential E^0 decreasing with growing pH from 2.8 V in acidic medium to 1.9 V in neutral pH [38]. Supposedly, at lower oxidation potential, reaction rate of hydroxyl radical formed at the gas–liquid interface with oxalate is lower than recombination and other side-reactions resulting in a lesser efficiency as pH rises. In addition, it has been previously determined with pulse radiolysis that hydroxyl radical has higher rate constant with the oxalate form of $C_2O_4H^-$ ($3.2 \cdot 10^7$ M^{-1} s^{-1}) than with the form of $C_2O_4^{2-}$ ($5.3 \cdot 10^6$ M^{-1} s^{-1}) [39]. While at pH 3 oxalic acid exists as $C_2O_4H^-$, starting from pH 6 only $C_2O_4^{2-}$ is present in solution (Eqs. (17) and (18)) [39]. This fact may also be a reason for the lower oxidation efficiency in neutral and alkaline media compared to acidic one.

$$C_2O_4H_2 \leftrightarrow C_2O_4H^- + H^+,\ pK_{a1} = 1.27 \quad (17)$$

$$C_2O_4H^- \leftrightarrow C_2O_4^{2-} + H^+,\ pK_{a2} = 4.28 \quad (18)$$

Concerning PCD-generated ozone, it has been previously proven, that oxalate reacts slowly with molecular ozone being mostly degraded by hydroxyl radicals [40]. Indirect ozonation, i.e. decomposition of O_3 in aqueous solutions with $HO^{\bullet}$ formation through series of reactions accelerated with alkali (Eqs. (19)–(25)) [3,6] did not, nevertheless, promote oxalate degradation.

$$O_3 + HO^- \rightarrow HO_2^- + O_2 \quad (19)$$

$$O_3 + HO_2^- \rightarrow HO_2^{\bullet} + O_3^{\bullet -} \quad (20)$$

$$O_3^{\bullet -} + H_2O \rightarrow HO^{\bullet} + O_2 + HO^- \quad (21)$$

$$HO_2^{\bullet} \rightarrow H^+ + O_2^{\bullet -} \quad (22)$$

$$O_2^{\bullet -} + O_3 \rightarrow O_2 + O_3^{\bullet -} \quad (23)$$

$$O_3^{\bullet -} + H^+ \rightarrow HO_3^{\bullet} \quad (24)$$

$$HO_3^{\bullet} \rightarrow HO^{\bullet} + O_2 \quad (25)$$

Besides lower $HO^{\bullet}$ oxidation potential, the reduced oxalate degradation at higher pH may be related to a reaction between ozone and hydroxyl radical occurring in alkaline medium forming less reactive hydroperoxyl radical ($HO_2^{\bullet}$) ($E^0 = 1.65$ V) (Eq. (26)) [3,41].

$$O_3 + HO^{\bullet} \rightarrow HO_2^{\bullet} + O_2 \quad (26)$$

Thus, the negative effect of increased pH is possibly related to two phenomena, $HO^{\bullet}$ scavenging with ozone and, similarly, with bicarbonates (HCO_3^-)/carbonates (CO_3^{2-}) accumulated from the contact of treated OXA solution with atmospheric CO_2. The first reaction (Eq. (26))

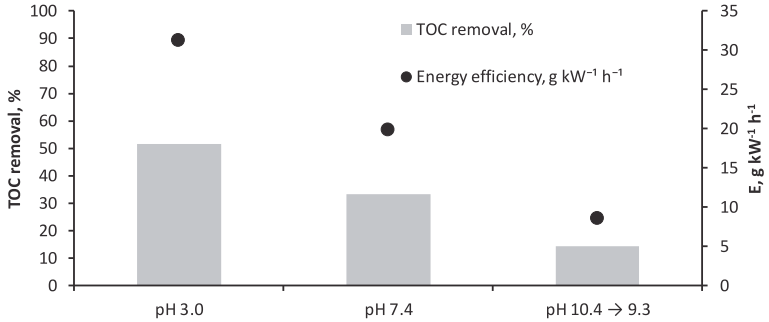

Fig. 1. OXA mineralization as TOC removal and oxidation energy efficiency in PCD system at different initial pH ($[OXA]_0 = 1.11$ mM, pulse repetition frequency 200 pps, treatment time 60 min, delivered energy dose 1.60 kWh m^{-3}).

between ozone and $HO^{\bullet}$ was described as a fast one in alkaline media at pH > 8 [41]. This reaction has a second order reaction rate constant from $1 \cdot 10^8$ M^{-1} s^{-1} to $2 \cdot 10^9$ M^{-1} s^{-1}, which exceeds the $HO^{\bullet}$ scavenging with bicarbonate ($8.5 \cdot 10^6$ M^{-1} s^{-1}) and carbonate ($3.9 \cdot 10^8$ M^{-1} s^{-1}) for at least an order of magnitude (Eqs. (27) and (28)) [15,42,43]. Notably, the concentration of TIC was about 8.6 and 10.2 mg C L^{-1}, i.e. about 43 and 51 mg $L^{-1}$of bicarbonate/carbonate in 1 h of treatment in neutral and alkaline media, respectively. In turn, the TIC content in acidic medium did not exceed 1.9 mg C L^{-1}. This high bicarbonate/carbonate concentration in neutral and alkaline media compensates the difference in reaction rate constants thus making both factors influencing the oxidation rate.

$$HO^{\bullet} + HCO_3^- \rightarrow CO_3^{\bullet -} + H_2O \quad (27)$$

$$HO^{\bullet} + CO_3^{2-} \rightarrow CO_3^{\bullet -} + HO^- \quad (28)$$

Ozone concentration, from the other side, in air in PCD reactor was measured earlier [25] comprising about 5 mg L^{-1}. This concentration is sufficient to provide an equilibrium ozone concentration in water at 20 °C of about 1.0–1.6 mg L^{-1} [44], which makes its role in hydroxyl radicals scavenging comparable to the one of bicarbonate and carbonate at concentrations for an order of magnitude higher than the one of ozone.

However, despite the TOC removal in basic medium with the energy efficiency as low as 8.6 g kW^{-1} h^{-1}, PCD surpasses the traditional ozonation in this parameter, which is 2.2 g kW^{-1} h^{-1} at similar pH values [40], for almost four times.

3.2. OXA oxidation in PCD/PS and PCD/H_2O_2 systems

Oxalate non-plasma degradation in direct reactions with PS and H_2O_2 in acidic, neutral and alkaline medium is shown in Fig. 2. Accordingly, no oxalate degradation occurred at 1:1 oxidant/oxalate molar ratio for 60 min indicating an absent reactivity of PS and H_2O_2 with oxalate at experimental conditions.

The effects of PS or H_2O_2 additions to PCD oxidation were studied at 1:1 oxidant/oxalate molar ratio in acidic environment. The highest removal was achieved in PCD/PS combination, where TOC content was reduced for up to 95% (Fig. 2) surpassing oxidation with PCD plasma by about 1.8 times. This indicates PCD activating PS producing sulfate radicals with further formation of additional $HO^{\bullet}$ (Eq. (7)). Persulfate in PCD/PS combination is presumably activated by reactions with species formed in plasma, such as e_{aq}^-, $HO^{\bullet}$, $HO_2^{\bullet}$, $H^{\bullet}$ and $O_2^{\bullet -}$ (Eqs. (29)–(32)) [3,6,45–47]. The role of $H^{\bullet}$ radical, however, is reasonably negligible due to its scavenging by abundant oxygen [48]. Potentially, UV radiation (Eqs. (33) and (34)) and strong electric field may also activate PS [4,18].

$$e_{aq}^- + S_2O_8^{2-} \rightarrow SO_4^{\bullet -} + SO_4^{2-} \quad (29)$$

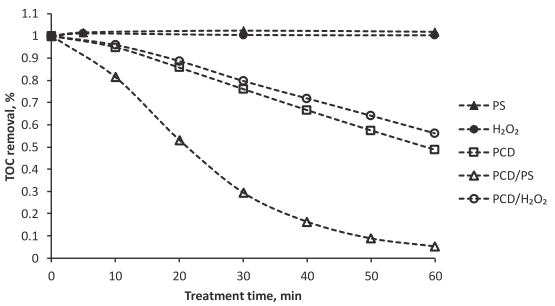

Fig. 2. OXA mineralization as TOC removal in non-plasma (PS and H_2O_2 oxidation), PCD, PCD/PS and PCD/H_2O_2 systems (initial pH 3.0, $[OXA]_0$ = $[PS]_0$ = $[H_2O_2]_0$ = 1.11 mM, pulse repetition frequency 200 pps).

$$HO^{\bullet} + S_2O_8^{2-} \rightarrow SO_4^{\bullet -} + HSO_4^- + 0.5O_2 \quad (30)$$

$$HO_2^{\bullet} + S_2O_8^{2-} \rightarrow SO_4^{\bullet -} + SO_4^{2-} + O_2 + H^+ \quad (31)$$

$$O_2^{\bullet -} + S_2O_8^{2-} \rightarrow SO_4^{\bullet -} + SO_4^{2-} + O_2 \quad (32)$$

$$UV + S_2O_8^{2-} \rightarrow 2SO_4^{\bullet -} \quad (33)$$

$$UV + H_2O_2 \rightarrow 2HO^{\bullet} \quad (34)$$

In PCD/H_2O_2 combination, an opposite trend in OXA degradation was observed as compared to PCD/PS system (Fig. 2). Addition of H_2O_2 to OXA solution at a molar ratio of 1:1 resulted in TOC removal decreased from 51.5% in PCD to 44% in PCD/H_2O_2 combination. The result may be related to an excess amount of H_2O_2 reacting with hydroxyl radical observed earlier (Eq. (35)) [6,27,49]. For example, oxidation of OXA at its initial concentration of 0.08 M in UVC/H_2O_2 combination demonstrated degradation decreased from 100% to 82% with H_2O_2 concentration increased from 0.1 M to 1 M [49].

$$H_2O_2 + HO^{\bullet} \rightarrow HO_2^{\bullet} + H_2O \quad (35)$$

3.3. Effect of oxidant concentration on OXA oxidation in PCD/PS and PCD/H_2O_2 systems

Concentrations of PS and H_2O_2 were reported as factors of oxidation efficiency in combinations with DBD, UV and catalysts; while too low concentrations provide insufficient benefits, excess ones make PS and H_2O_2 acting as radical scavengers reducing oxidation efficiency [12,15,27,30,49]. Since acidic medium provides the most efficient OXA degradation in PCD, the impact of added oxidant concentrations in PCD/PS and PCD/H_2O_2 systems was studied at pH 3, which did not practically change during the experiments. As shown in Fig. 3a for PCD/PS oxidation, OXA oxidation efficiency was growing with increased PS addition being likely related to generation of $SO_4^{\bullet -}$ improving OXA degradation.

Even the application of the lowest PS dose of 0.111 mM resulted in noticeable increase in the TOC removal by PCD/PS system. Accordingly, 51.5% and 56% OXA were mineralized in 1 h of treatment with the PCD and PCD/PS system. The OXA/PS molar ratios of 1:0.25 and 1:0.5 resulted in 68% and 87% TOC removal, respectively. A further increase in PS dose, however, brought only a moderate improvement in OXA oxidation achieving 95% of TOC removal at the OXA/PS molar ratio of 1:1. The oxidation energy efficiencies in PCD/PS combination comprised 34 and 53 g kW^{-1} h^{-1} at OXA/PS molar ratios of 1:0.1 and 1:0.5 thus showing a substantial growth, although further twofold upsurge in PS dosage resulted in modest growth of efficiency to 56 g kW^{-1} h^{-1}. This could be related to a fixed amount of oxidants acting as PS activators produced in PCD at the applied power. Besides, at high concentrations of persulfate, sulfate radicals may recombine (Eq. (36)) or become scavenged by excess $S_2O_8^{2-}$ (Eq. (37)) [45,50]. One can see from Table 1 that in PCD treatment of OXA aqueous solution, H_2O_2 accumulated up to 0.114 mM. Addition of PS, however, resulted in the content of H_2O_2 noticeably reduced with a tendency of decreased H_2O_2 production with increased PS amounts, which may be explained by partial consumption of $HO^{\bullet}$ in reaction with persulfate (Eq. (30)) or $SO_4^{\bullet -}$ (Eq. (38)), and, additionally, leaving less chance for hydroxyl radicals to recombine to H_2O_2 (Eq. (12)) [45,50]. Seemingly, equilibrium between H_2O_2 formation and consumption was achieved at the OXA/PS molar ratio between 1:0.5 and 1:1, when a tradeoff between activation and quenching reactions is reached (Eqs. (36)–(43)).

$$SO_4^{\bullet -} + SO_4^{\bullet -} \rightarrow S_2O_8^{2-} \quad (36)$$

$$SO_4^{\bullet -} + S_2O_8^{2-} \rightarrow SO_4^{2-} + S_2O_8^{\bullet -} \quad (37)$$

$$SO_4^{\bullet -} + HO^{\bullet} \rightarrow HSO_5^- \quad (38)$$

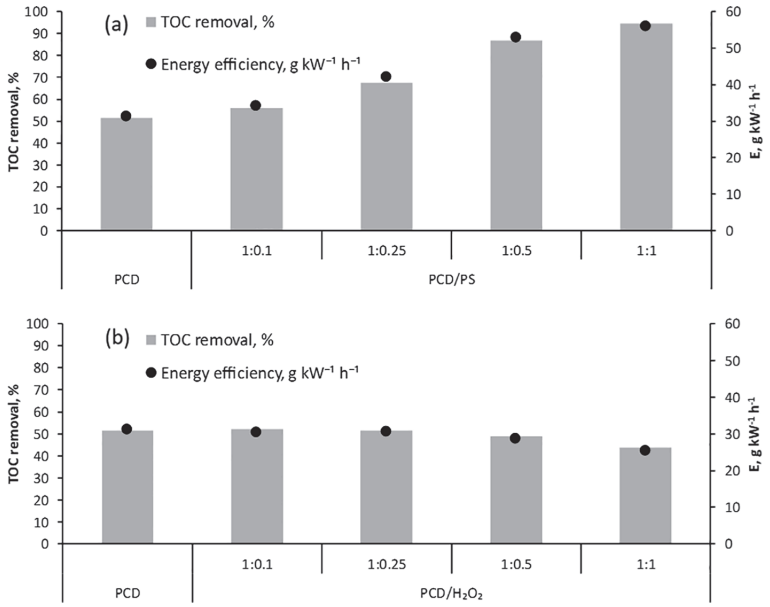

Fig. 3. OXA mineralization as TOC removal and oxidation energy efficiency in PCD, PCD/PS (a) and PCD/H_2O_2 (b) systems at different OXA/oxidant molar ratios (initial pH 3.0, $[OXA]_0$ = 1.11 mM, treatment time 60 min, pulse repetition frequency 200 pps).

Table 1
Concentration of H_2O_2 in OXA solutions treated by PCD, PCD/PS and PCD/H_2O_2 systems (initial pH 3.0, $[OXA]_0$ = 1.11 mM, pulse repetition frequency 200 pps).

Process	OXA/oxidant molar ratio	H_2O_2, mM			
		0 min	10 min	30 min	60 min
PCD	–	–	0.022	0.063	0.114
PCD/PS	1:0.1	–	0.019	0.069	0.108
	1:0.25	–	0.021	0.056	0.103
	1:0.5	–	0.017	0.043	0.058
	1:1	–	0.008	0.025	0.010
PCD/H_2O_2	1:0.1	0.111	0.124	0.157	0.177
	1:0.25	0.278	0.284	0.295	0.292
	1:0.5	0.555	0.561	0.538	0.494
	1:1	1.100	1.082	1.029	0.914

$$HO^{\bullet} + S_2O_8^{2-} \rightarrow S_2O_8^{\bullet-} + HO^- \quad (39)$$

$$S_2O_8^{\bullet-} \rightarrow 2SO_4^{2-} \quad (40)$$

$$SO_4^{\bullet-} + HSO_5^- \rightarrow HSO_4^- + SO_5^{\bullet-} \quad (41)$$

$$HO^{\bullet} + HSO_5^- \rightarrow H_2O + SO_5^{\bullet-} \quad (42)$$

$$2SO_5^{\bullet-} \rightarrow S_2O_8^{2-} + O_2 \quad (43)$$

Recombination of hydroxyl radicals producing hydrogen peroxide was described earlier [51] and confirmed for electric discharges applied to aqueous media [52]. The reaction of $HO^{\bullet}$ with PS also takes place, see Eqs. (39) and (42) [50]. Naturally, increased PS concentration will result in higher probability of reaction between $HO^{\bullet}$ and PS thus reducing the chance for hydroxyl radicals recombination. One can see from Table 1 that hydrogen peroxide was produced in amounts from two to ten times smaller on course of the treatment dependent on the PS content being increased tenfold from 0.1 to 1.0 M ratio with PS, having the effect of added PS increasing in time of treatment.

A quantitative comparison of the selected reaction rates taking place in the PCD/PS system gives the following: i) $HO^{\bullet}$ recombination reaction rate constant is $5.5 \cdot 10^9$ M^{-1} s^{-1} (Eq. (12)) [53]; ii) $HO^{\bullet}$ reacts with PS at $1.2 \cdot 10^7$ M^{-1} s^{-1} (Eq. (39)) [50]; iii) $HO^{\bullet}$ with $SO_4^{\bullet-}$ reacts at $1 \cdot 10^{10}$ M^{-1} s^{-1} (Eq. (38)) [50]; iv) PS accepts electron producing $SO_4^{\bullet-}$ at $1.2 \cdot 10^{10}$ M^{-1} s^{-1} (Eq. (29)) [54], and v) $SO_4^{\bullet-}$ recombines back to PS at the rate constant of $7.6 \cdot 10^8$ M^{-1} s^{-1} (Eq. (36)) [55] . One can presume that although the reaction of $HO^{\bullet}$ with PS is two orders of magnitude slower than the recombination of hydroxyl radicals, the reactions between hydroxyl and sulfate radicals is of the same order of magnitude, as well as the electronic reduction of PS. This makes it possible to assess the ability of PS to use a part of hydroxyl radicals in side reactions as highly probable.

It should be also noted that the formation of superoxide radical ($O_2^{\bullet-}$) may occur in equilibrium with hydroperoxyl radical, which exists in equilibrium at pK_a = 4.8 [8]. $O_2^{\bullet-}$ may be involved in formation of hydrogen peroxide being reduced (Eq. (44)). However, reduction reactions in aqueous solutions containing PS and active oxidants derived from its reactions present a doubtful possibility of additional formation of H_2O_2. Instead, upon protonation of $O_2^{\bullet-}$, $HO_2^{\bullet}$ has an increased redox potential and is an oxidant [56]. Therefore, addition of PS oxidant may also result in reduced production of H_2O_2 in OXA solution treated by PCD as observed (Table 1).

$$O_2^{\bullet-} + e^- + 2H^+ \rightarrow H_2O_2 \quad (44)$$

Considering the expense of persulfate, the treatment at the OXA/PS molar ratio of 1:0.5 was chosen for further experimentation as the more cost-effective one.

Contrary to the PCD/PS system, additions of H_2O_2 to PCD treatment of OXA aqueous solutions at OXA/H_2O_2 molar ratios from 1:0.1 to 1:1 did not promote OXA degradation in acidic medium (Fig. 3b). At initial H_2O_2 concentrations of 0.111 mM and 0.278 mM corresponding to molar ratios of 1:0.1 and 1:0.25, no improvement in OXA degradation was observed; the TOC removals and energy efficiency values were similar with the ones obtained in PCD treatment within the range of 51.5 – 52.0% and 30.5 – 31.2 g kW^{-1} h^{-1}, respectively. Further increase in H_2O_2 dose slightly reduced OXA degradation rate indicating an excess of H_2O_2 starting from its initial concentration of 0.555 mM, which promotes scavenging reactions (Eq. (35)). Surplus effect of H_2O_2 may also

be seen in Table 1: increasing at ratios 1:0.1 and 1:0.25, H_2O_2 concentration decreased on course of treatment at higher OXA/H_2O_2 molar ratios, i.e. hydrogen peroxide consumption prevailed over its formation thus supporting explanation of its negative role in OXA oxidation. Since H_2O_2 is formed and accumulated in PCD treated oxalate solutions indicating equilibrium between its production and consumption, addition of hydrogen peroxide makes little difference in OXA degradation rate even at the lowest doses of added H_2O_2. For the reason of uniformity in comparison with the PCD/PS process, OXA/H_2O_2 molar ratio of 1:0.5 was chosen for further experiments with PCD/H_2O_2 system.

3.4. Effect of pH on OXA oxidation in PCD/PS and PCD/H_2O_2 systems

Besides oxidant dose, pH is also an important factor affecting oxidation of organic pollutants with activated PS and H_2O_2 [2,6,10,11]. Experiments with the PCD/PS and PCD/H_2O_2 system were performed at the OXA/oxidant molar ratio of 1:0.5 in acidic, neutral and alkaline media (Fig. 4). Analogous to PCD treatment, similar pH impacts were observed in experiments with the addition of oxidants. As discussed above, OXA PCD oxidation efficacy decreased with increasing pH (Fig. 1). A similar tendency was observed with PCD/PS and PCD/H_2O_2 treatment. In the PCD/PS system, the OXA removal decreased with increasing pH to a substantially bigger extent than that in PCD treatment. Thus, at pH 3, the TOC removal in PCD/PS treatment proceeded 1.7 times faster than in PCD, at pH 7.4 ± 0.2 the difference between TOC removals comprised only 5% with the energy efficiencies of 22.3 and 19.8 g kW^{-1} h^{-1} in PCD/PS and PCD treatment, respectively. At pH 10.4 ± 0.2, the effect of PS addition comprised about 6% increased energy efficiency at overall low, 8.6 to 9.1 g kW^{-1} h^{-1}, oxidation efficiencies.

In PCD/H_2O_2 treatment, negligible effect of hydrogen peroxide addition was observed in all pH ranges with oxidation efficiencies of about 28.6, 18.8 and 7.7 g kW^{-1} h^{-1} in acidic, neutral and alkaline media, respectively.

For PCD/PS combined system, the lower degradation rate of OXA in neutral and alkaline media may be related to $SO_4^{\bullet-}$ reactions with H_2O and HO^- (Eqs. (7) and (8)) forming $HO^{\bullet}$, the dominant species in pollutant degradation [10,11]. Shorter compared to $SO_4^{\bullet-}$ lifetime and lower oxidation potential of $HO^{\bullet}$ at higher pH offer a reason for lower rates of OXA oxidation [1,38]. In addition, the inhibition could have been caused by the increased bicarbonate/carbonate content that accumulated during treatment. As with the PCD system, the TIC content increased to about 4.7 mg L^{-1} in neutral and 5.6 mg L^{-1} in alkaline medium during a one-hour PCD/PS treatment, indicating the presence of elevated HCO_3^- and CO_3^{2-} concentrations in solution. In turn, bicarbonate and carbonate are well-known sulfate radical scavengers, creating less reactive carbonate radicals (Eqs. (45) and (46)) [11,12,15].

$$SO_4^{\bullet-} + HCO_3^- \rightarrow HCO_3^{\bullet} + SO_4^{2-} \quad (45)$$

$$SO_4^{\bullet-} + CO_3^{2-} \rightarrow CO_3^{\bullet-} + SO_4^{2-} \quad (46)$$

Regarding combined PCD/H_2O_2 system, TOC removal similar with PCD at pH 7.4 ± 0.2 and pH 10.4 ± 0.2 may be related to H_2O_2 instability at higher pH. Unstable at neutral and alkaline pH hydrogen peroxide, however, did not contribute to the OXA oxidation (Table 2). Remaining stable at pH 3.0, H_2O_2 was not obviously contributing to the OXA oxidation as well.

As shown in Table 2, considerably smaller amount of hydrogen peroxide was accumulated in OXA solutions treated with PCD and PCD/PS as pH changed from acidic to neutral. Further pH increase resulted in negligible accumulation of hydrogen peroxide. Similarly, rapid decomposition of added H_2O_2 was observed at higher pH reaching practically zero concentration after 60-min treatment in PCD/H_2O_2 combination at initial pH 10.4 ± 0.2. Since both PCD and PCD/H_2O_2 treatment approaches showed similar OXA oxidation results in neutral and alkaline media, hydrogen peroxide was presumably readily and uselessly reacting with ozone and interface-borne hydroxyl radicals playing little role in OXA oxidation most probably compensating consumed active oxidants with newly produced replacement.

3.5. Effect of gas–liquid contact surface on OXA oxidation

Gas-liquid contact surface affects oxidation efficiency of waterborne pollutants in plasma treatment. Since short-living $HO^{\bullet}$ radicals are formed at the gas–liquid interface, these degrade pollutants at the vicinity of interface [25]. This makes oxidation rate of $HO^{\bullet}$-oxidized oxalate dependent on the interface area [35]. The performance of combined oxidation dependent on the contact surface was studied for both PCD/PS and PCD/H_2O_2 combinations compared to PCD. Experiments were conducted at OXA/oxidant molar ratios of 1:0.5 in acidic medium (Fig. 5). The tendencies seen at all tested contact surfaces show similarity: the most efficient PCD/PS system is followed by PCD and PCD/H_2O_2. In all oxidant combinations, TOC removal and oxidation efficiency grow consistently with increasing contact surface at an even pace.

Table 2
Concentration of H_2O_2 in OXA solutions treated by PCD, PCD/PS and PCD/H_2O_2 systems at different initial pH ($[OXA]_0$ = 1.11 mM, $[PS]_0$ = $[H_2O_2]_0$ = 0.555 mM, pulse repetition frequency 200 pps).

pH	Process	H_2O_2, mM			
		0 min	10 min	30 min	60 min
3.0	PCD	–	0.022	0.063	0.114
	PCD/PS	–	0.017	0.043	0.058
	PCD/H_2O_2	0.555	0.561	0.538	0.494
7.4	PCD	–	0.015	0.013	0.015
	PCD/PS	–	0.002	0.007	0.015
	PCD/H_2O_2	0.555	0.483	0.323	0.169
10.4 → 9.3	PCD	–	0.002	0.001	0.001
	PCD/PS	–	0	0.006	0
	PCD/H_2O_2	0.555	0.337	0.022	0.003

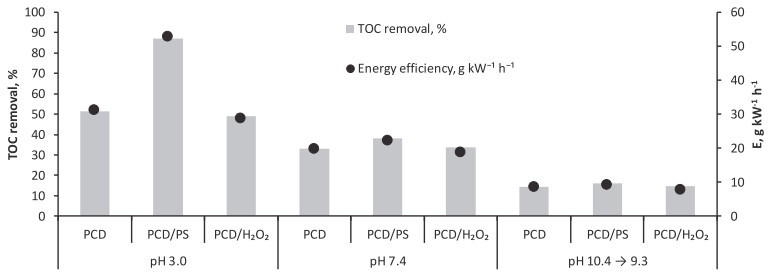

Fig. 4. OXA mineralization as TOC removal and oxidation energy efficiency in PCD, PCD/PS and PCD/H_2O_2 systems at different initial pH ($[OXA]_0$ = 1.11 mM, $[PS]_0$ = $[H_2O_2]_0$ = 0.555 mM, treatment time 60 min, pulse repetition frequency 200 pps).

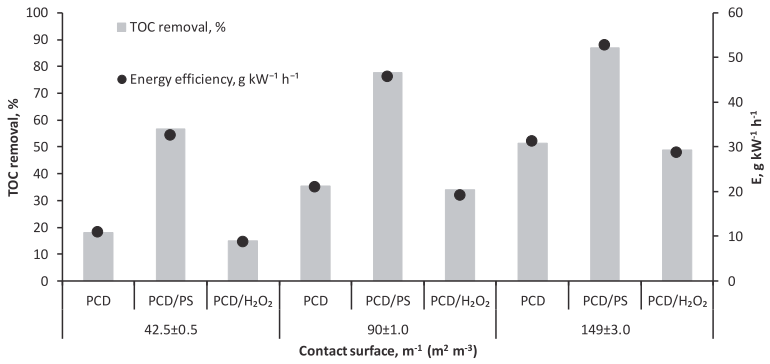

Fig. 5. OXA mineralization as TOC removal and oxidation energy efficiency in PCD, PCD/PS and PCD/H_2O_2 systems at different gas–liquid contact surface values (initial pH 3.0, $[OXA]_0 = 1.11$ mM, $[PS]_0 = [H_2O_2]_0 = 0.555$ mM, treatment time 60 min, pulse repetition frequency 200 pps).

In PCD/PS treatment, the TOC removal and energy efficiency exceeded those of PCD shown even at the highest value of the contact surface, offering, in technical terms, a trade-of between the contact surface development and the addition of PS to the treated solution. One should notice, however, that the effect of PS addition to the PCD treatment of OXA solution is somewhat alleviated with increased contact surface being relatively smaller at higher solution circulation rate thus making the impact of contact surface area smaller for the PCD/PS combination.

Addition of hydrogen peroxide caused slight inhibition of OXA oxidation at all contact surfaces, although the oxidation efficiency consistently increased with increasing interface; compared to PCD oxidation, TOC removal and energy efficiency decreased for only 1.5–3.0% and 1.8–2.6 g kW^{-1} h^{-1}, respectively. From Table 3, one can see formation of hydrogen peroxide being practically indifferent towards the contact surface in PCD of acidic OXA solution: both the rate of H_2O_2 accumulation and its finally achieved concentration are of the same order of magnitude at all tested contact surface numbers. Similar to that, hydrogen peroxide accumulated in the OXA solution treated with PCD/PS combination with the rate indifferent towards the contact surface. However, H_2O_2 in PCD/H_2O_2 system was consumed in scavenging reactions at somewhat higher rate with growing contact surface, which may find logical explanation in overall accelerated oxidation at larger contact surface (Fig. 5).

3.6. Effect of pulse repetition frequency on OXA oxidation

Pulse repetition frequency determines the utilization of short- and long-living oxidative species in reactions [25]. The energy dose determined by the number of pulses delivered to the reactor provides the amount of reactive oxygen species (ROS) spread over the treatment time. The performance of PCD/oxidant combinations in OXA degradation dependent on the pulse repetition frequency was studied at 200 and 880 pps in acidic medium at OXA/oxidant molar ratio of 1:0.5 and gas–liquid contact surface 149 ± 3 m^{-1} (Fig. 6). Irrespective of combination, TOC removal and energy efficiency were moderately higher at 200 pps. For both applied pulse repetition frequencies, OXA oxidation efficiency followed the expectedly descending order of PCD/PS > PCD > PCD/H_2O_2.

Previously, the higher efficiency at lower pulse repetition frequency was attributed to ozone participation in OXA degradation [25]. At higher frequencies, ozone has less time to react between pulses, when every next pulse destroys residues of reactive oxygen species generating a new set of those giving long-living ozone less chance for useful utilization of the previous pulse energy. Since aqueous ozone oxidizes OXA predominantly via $HO^{\bullet}$ formation, moderate effect in TOC removal and energy efficiency was observed with the change in pulse repetition frequency for all oxidant combinations. Neither persulfate nor hydrogen peroxide benefited much from extended ozone lifetime during longer treatment at lower frequency witnessing predominant radical mechanism of their activation in target or scavenging reactions.

However, it should be borne in mind that while increasing pulse repetition frequency results in somewhat reduced oxidation efficiency, it also results in approximately four times reduced treatment time, within which comparable treatment result is achieved.

Table 3
Concentration of H_2O_2 in OXA solutions treated by PCD, PCD/PS and PCD/H_2O_2 systems at different gas–liquid contact surface values (initial pH 3.0, $[OXA]_0 = 1.11$ mM, $[PS]_0 = [H_2O_2]_0 = 0.555$ mM, pulse repetition frequency 200 pps).

A, m^{-1} (m^2 m^{-3})	Process	H_2O_2, mM			
		0 min	10 min	30 min	60 min
42.5 ± 0.5	PCD	–	0.024	0.063	0.115
	PCD/PS	–	0.016	0.041	0.080
	PCD/H_2O_2	0.555	0.558	0.559	0.551
90 ± 1	PCD	–	0.018	0.061	0.127
	PCD/PS	–	0.015	0.041	0.068
	PCD/H_2O_2	0.555	0.548	0.538	0.534
149 ± 3	PCD	–	0.022	0.063	0.114
	PCD/PS	–	0.017	0.043	0.058
	PCD/H_2O_2	0.555	0.561	0.538	0.494

3.7. Operation costs in OXA oxidation

Since no oxidation enhancement was observed with hydrogen peroxide addition to the OXA aqueous solution treated with PCD, no cost estimate of PCD/H_2O_2 combination makes sense. The PS cost of 1.5 EUR kg^{-1} is considered relevant at the moment of reporting based on the average price on market. For the cost comparison, the PS cost was converted to the electric energy expense, which in Europe comprises for non-household consumption 0.115 EUR kW^{-1} h^{-1} [57] making the PS energy expense equivalent to 13 kWh kg^{-1}. At the OXA/PS molar ratio of 1:0.5, the energy efficiency of OXA removal in PCD/PS treatment at pH 3.0, gas–liquid contact surface 149 ± 3 m^{-1} and pulse repetition frequency 200 pps comprised 53 g kW^{-1} h^{-1}, which exceeds the corresponding number for PCD in air at similar experimental conditions for 1.7 times. At neutral and alkaline pH, PS did not exhibit significant acceleration of oxidation reaction thus making its economic effect negligible. For example, at initial pH 10.4 ± 0.2, the energy efficiency of OXA oxidation in non-accompanied PCD comprised 8.6 g kW^{-1} h^{-1}, whereas addition of PS in 1:0.5 ratio resulted in 9.1 g kW^{-1} h^{-1} if calculated together with the PS cost, i.e. the difference does not exceed 6%. Conclusively, additions of PS into the PCD treatment of aqueous

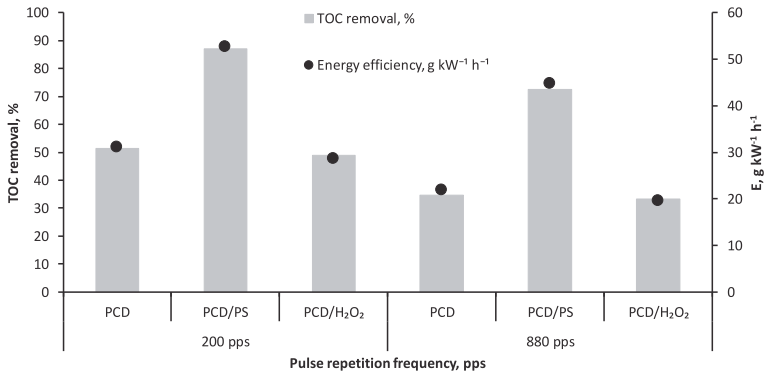

Fig. 6. OXA mineralization as TOC removal and oxidation energy efficiency in PCD, PCD/PS and PCD/H_2O_2 systems at different pulse repetition frequency values (initial pH 3.0, $[OXA]_0 = 1.11$ mM, $[PS]_0 = [H_2O_2]_0 = 0.555$ mM, treatment time 60 min at 200 pps and 15 min at 880 pps).

solutions containing slowly reacting OXA make sense in acidic media only. Under neutral and alkaline media conditions, non-assisted PCD remains preferable treatment option for simpler operation without involving additional chemicals transportation, storage and dosing.

4. Conclusions

Synergism of persulfate addition to aqueous solutions of refractory oxalate treated in pulsed corona discharge reactor was observed with the optimum performance in acidic medium at the OXA/PS molar ratio of 1:0.5. Accordingly, compared to PCD treatment, OXA mineralization improved 1.7 times at a slightly increased combined cost. In addition, the application of PCD/PS system for OXA oxidation in acidic medium showed the strongest synergy at the lowest gas–liquid contact surface tested in experiments. In turn, the increased interface improved PCD performance to a larger extent than the one of PCD/PS combination. In neutral solutions, PS addition resulted in substantially smaller acceleration of oxalate oxidation, and in alkaline solutions the effect may be considered as negligible explained by decreased oxidative potential of $HO^{\bullet}$ radicals activating persulfate. From the energy and chemical expenses, non-assisted PCD treatment of neutral and alkaline aqueous media appears preferable.

A comprehensive study undertaken in this research did not reveal conditions beneficial for hydrogen peroxide application. Thus, hydrogen peroxide additions to PCD treatment of oxalate solutions showed inhibiting or neutral effect towards oxalate oxidation explained by $HO^{\bullet}$ radicals scavenging in reactions with H_2O_2. Further studies in PCD/H_2O_2 application towards other pollutants are necessary for conclusions in respect to potential synergetic effect of hydrogen peroxide.

Declaration of Competing Interest

The authors declare that they have no known competing financial interests or personal relationships that could have appeared to influence the work reported in this paper.

Acknowledgement

This work was supported by the Institutional Development Program of Tallinn University of Technology for 2016-2022, project 2014-2020.4.01.16-0032 from EU Regional Development Fund, and the Research Group Support project PRG776 of Estonian Research Council. The authors thank Mirjam Lätt and Anne Mari Kääp for their assistance in experiments.

References

[1] S. Guerra-Rodríguez, E. Rodríguez, D.N. Singh, J. Rodríguez-Chueca, Assessment of sulfate radical-based advanced oxidation processes for water and wastewater treatment: A review, Water (Switzerland). 10 (2018) 1828, https://doi.org/10.3390/w10121828.

[2] A.R. Ribeiro, O.C. Nunes, M.F.R. Pereira, A.M.T. Silva, An overview on the advanced oxidation processes applied for the treatment of water pollutants defined in the recently launched Directive 2013/39/EU, Environ. Int. 75 (2015) 33–51, https://doi.org/10.1016/j.envint.2014.10.027.

[3] E.M. Cuerda-Correa, M.F. Alexandre-Franco, C. Fernández-González, Advanced oxidation processes for the removal of antibiotics from water. An overview, Water (Switzerland) 12 (2020) 102, https://doi.org/10.3390/w12010102.

[4] S. Tang, D. Yuan, Y. Rao, N. Li, J. Qi, T. Cheng, Z. Sun, J. Gu, H. Huang, Persulfate activation in gas phase surface discharge plasma for synergetic removal of antibiotic in water, Chem. Eng. J. 337 (2018) 446–454, https://doi.org/10.1016/j.cej.2017.12.117.

[5] W.H. Glaze, J.-W. Kang, D.H. Chapin, The chemistry of water treatment processes involving ozone, hydrogen peroxide and ultraviolet radiation, Ozone Sci. Eng. 9 (4) (1987) 335–352, https://doi.org/10.1080/01919518708552148.

[6] V. Homem, L. Santos, Degradation and removal methods of antibiotics from aqueous matrices - A review, J. Environ. Manage. 92 (10) (2011) 2304–2347, https://doi.org/10.1016/j.jenvman.2011.05.023.

[7] A. Sharma, J. Ahmad, S.J.S. Flora, Application of advanced oxidation processes and toxicity assessment of transformation products, Environ. Res. 167 (2018) 223–233, https://doi.org/10.1016/j.envres.2018.07.010.

[8] R.J. Watts, A.L. Teel, Chemistry of modified fenton's reagent (catalyzed H2O2 propagations–CHP) for in situ soil and groundwater remediation, J. Environ. Eng. 131 (4) (2005) 612–622, https://doi.org/10.1061/(ASCE)0733-9372(2005)131:4(612).

[9] Y. Huang, C. Han, Y. Liu, M.N. Nadagouda, L. Machala, K.E. O'Shea, V.K. Sharma, D.D. Dionysiou, Degradation of atrazine by ZnxCu1−xFe2O4 nanomaterial-catalyzed sulfite under UV–vis light irradiation: Green strategy to generate SO4 [rad]−, Appl. Catal. B Environ. 221 (2018) 380–392, https://doi.org/10.1016/j.apcatb.2017.09.001.

[10] L.W. Matzek, K.E. Carter, Activated persulfate for organic chemical degradation: A review, Chemosphere 151 (2016) 178–188, https://doi.org/10.1016/j.chemosphere.2016.02.055.

[11] S. Wacławek, H.V. Lutze, K. Grübel, V.V.T. Padil, M. Černík, D.D. Dionysiou, Chemistry of persulfates in water and wastewater treatment: A review, Chem. Eng. J. 330 (2017) 44–62, https://doi.org/10.1016/j.cej.2017.07.132.

[12] M. Izadifard, G. Achari, C.H. Langford, Degradation of sulfolane using activated persulfate with UV and UV-Ozone, Water Res. 125 (2017) 325–331, https://doi.org/10.1016/j.watres.2017.07.042.

[13] J. Criquet, N. Karpel Vel Leitner, Radiolysis of acetic acid aqueous solutions-effect of pH and persulfate addition, Chem. Eng. J. 174 (2011) 504–509, https://doi.org/10.1016/j.cej.2011.07.079.

[14] S. Chakma, S. Praneeth, V.S. Moholkar, Mechanistic investigations in sono-hybrid (ultrasound/Fe2+/UVC) techniques of persulfate activation for degradation of Azorubine, Ultrason. Sonochem. 38 (2017) 652–663, https://doi.org/10.1016/j.ultsonch.2016.08.015.

[15] E. Kattel, M. Trapido, N. Dulova, Oxidative degradation of emerging micropollutant acesulfame in aqueous matrices by UVA-induced H2O2/Fe2+ and S2O82−/Fe2+ processes, Chemosphere 171 (2017) 528–536, https://doi.org/10.1016/j.chemosphere.2016.12.104.

[16] W.S. Chen, Y.C. Jhou, C.P. Huang, Mineralization of dinitrotoluenes in industrial wastewater by electro-activated persulfate oxidation, Chem. Eng. J. 252 (2014) 166–172, https://doi.org/10.1016/j.cej.2014.05.033.

[17] R. Xiao, Z. Luo, Z. Wei, S. Luo, R. Spinney, W. Yang, D.D. Dionysiou, Activation of peroxymonosulfate/persulfate by nanomaterials for sulfate radical-based advanced

oxidation technologies, Curr. Opin. Chem. Eng. 19 (2018) 51–58, https://doi.org/10.1016/j.coche.2017.12.005.
[18] P. Bruggeman, C. Leys, Non-thermal plasmas in and in contact with liquids, J. Phys. D. Appl. Phys. 42 (5) (2009) 053001, https://doi.org/10.1088/0022-3727/42/5/053001.
[19] M. Magureanu, C. Bradu, V.I. Parvulescu, Plasma processes for the treatment of water contaminated with harmful organic compounds, J. Phys. D. Appl. Phys. 51 (31) (2018) 313002, https://doi.org/10.1088/1361-6463/aacd9c.
[20] U. Kogelschatz, Dielectric-barrier discharges: their history, discharge physics, and industrial applications, Plasma Chem. Plasma Process. 23 (2003) 1–46, https://doi.org/10.1023/A:1022470901385.
[21] K.H. Hama Aziz, H. Miessner, S. Mueller, D. Kalass, D. Moeller, I. Khorshid, M.A. M. Rashid, Degradation of pharmaceutical diclofenac and ibuprofen in aqueous solution, a direct comparison of ozonation, photocatalysis, and non-thermal plasma, Chem. Eng. J. 313 (2017) 1033–1041, https://doi.org/10.1016/j.cej.2016.10.137.
[22] J.-L. Brisset, J. Fanmoe, E. Hnatiuc, Degradation of surfactant by cold plasma treatment, J. Environ. Chem. Eng. 4 (1) (2016) 385–387, https://doi.org/10.1016/j.jece:2015.11.011.
[23] A. Khlyustova, N. Sirotkin, Plasma-assisted oxidation of benzoic acid, Front. Chem. Sci. Eng. 14 (4) (2020) 513–521, https://doi.org/10.1007/s11705-019-1825-0.
[24] M. Magureanu, C. Bradu, D. Piroi, N.B. Mandache, V. Parvulescu, Pulsed corona discharge for degradation of methylene blue in water, Plasma Chem. Plasma Process. 33 (1) (2013) 51–64, https://doi.org/10.1007/s11090-012-9422-8.
[25] S. Preis, I.C. Panorel, I. Kornev, H. Hatakka, J. Kallas, Pulsed corona discharge: the role of ozone and hydroxyl radical in aqueous pollutants oxidation, Water Sci. Technol. 68 (2013) 1536–1542, https://doi.org/10.2166/wst.2013.399.
[26] M.A. Malik, Water purification by plasmas: which reactors are most energy efficient? Plasma Chem. Plasma Process. 30 (1) (2010) 21–31, https://doi.org/10.1007/s11090-009-9202-2.
[27] G. Iervolino, V. Vaiano, V. Palma, Enhanced azo dye removal in aqueous solution by H2O2 assisted non-thermal plasma technology, Environ. Technol. Innov. 19 (2020), 100969, https://doi.org/10.1016/j.eti.2020.100969.
[28] J. Wu, Q. Xiong, J. Liang, Q. He, D. Yang, R. Deng, Y. Chen, Degradation of benzotriazole by DBD plasma and peroxymonosulfate: Mechanism, degradation pathway and potential toxicity, Chem. Eng. J. 384 (2020) 123300, https://doi.org/10.1016/j.cej.2019.123300.
[29] C.A. Aggelopoulos, S. Meropoulis, M. Hatzisymeon, Z.G. Lada, G. Rassias, Degradation of antibiotic enrofloxacin in water by gas-liquid nsp-DBD plasma: Parametric analysis, effect of H2O2 and CaO2 additives and exploration of degradation mechanisms, Chem. Eng. J. 398 (2020) 125622, https://doi.org/10.1016/j.cej.2020.125622.
[30] K. Shang, X. Wang, J. Li, H. Wang, N. Lu, N. Jiang, Y. Wu, Synergetic degradation of Acid Orange 7 (AO7) dye by DBD plasma and persulfate, Chem. Eng. J. 311 (2017) 378–384, https://doi.org/10.1016/j.cej.2016.11.103.
[31] F.J. Beltrán, F.J. Rivas, R. Montero-de-Espinosa, Catalytic ozonation of oxalic acid in an aqueous TiO2 slurry reactor, Appl. Catal. B Environ. 39 (3) (2002) 221–231, https://doi.org/10.1016/S0926-3373(02)00102-9.
[32] C.D. Vecitis, T. Lesko, A.J. Colussi, M.R. Hoffmann, Sonolytic decomposition of aqueous bioxalate in the presence of ozone, J. Phys. Chem. A. 114 (14) (2010) 4968–4980, https://doi.org/10.1021/jp9115386.
[33] A.M. Castellaro, A. Tonda, H.H. Cejas, H. Ferreyra, B.L. Caputto, O.A. Pucci, G. A. Gil, Oxalate induces breast cancer, BMC Cancer. 15 (2015) 1, https://doi.org/10.1186/s12885-015-1747-2.
[34] Y.Z. Wen, H.J. Liu, W.P. Liu, X.Z. Jiang, Degradation of organic contaminants in water by pulsed corona discharge, Plasma Chem. Plasma Process. 25 (2) (2005) 137–146, https://doi.org/10.1007/s11090-004-8839-0.
[35] P. Tikker, I. Kornev, S. Preis, Oxidation energy efficiency in water treatment with gas-phase pulsed corona discharge as a function of spray density, J. Electrostat. 106 (2020) 103466, https://doi.org/10.1016/j.elstat.2020.103466.
[36] G. Eisenberg, Colorimetric determination of hydrogen peroxide, Ind. Eng. Chem. - Anal. Ed. 15 (5) (1943) 327–328, https://doi.org/10.1021/i560117a011.
[37] S. Preis, I. Panorel, S. Llauger Coll, I. Kornev, Formation of nitrates in aqueous solutions treated with pulsed corona discharge: the impact of organic pollutants, Ozone Sci. Eng. 36 (1) (2014) 94–99, https://doi.org/10.1080/01919512.2013.836955.
[38] P. Wardman, Reduction potentials of one electron couples involving free radicals in aqueous solution, J. Phys. Chem. Ref. Data. 18 (4) (1989) 1637–1755, https://doi.org/10.1063/1.555843.
[39] K. Sehested, N. Getoff, F. Schwoerer, V.M. Markovic, S.O. Nielsen, Pulse radiolysis of oxalic acid and oxalates, J. Phys. Chem. 75 (6) (1971) 749–755, https://doi.org/10.1021/j100676a004.
[40] P. Ajo, I. Kornev, S. Preis, Pulsed corona discharge in water treatment: the effect of hydrodynamic conditions on oxidation energy efficiency, Ind. Eng. Chem. Res. 54 (30) (2015) 7452–7458, https://doi.org/10.1021/acs.iecr.5b01915.
[41] U. von Gunten, Ozonation of drinking water: Part I. Oxidation kinetics and product formation, Water Res. 37 (7) (2003) 1443–1467, https://doi.org/10.1016/S0043-1354(02)00457-8.
[42] J.C. Crittenden, S. Hu, D.W. Hand, S.A. Green, A kinetic model for H2O2/UV process in a completely mixed batch reactor, Water Res. 33 (10) (1999) 2315–2328, https://doi.org/10.1016/S0043-1354(98)00448-5.
[43] Y.-P. Chiang, Y.-Y. Liang, C.-N. Chang, A.C. Chao, Differentiating ozone direct and indirect reactions on decomposition of humic substances, Chemosphere 65 (11) (2006) 2395–2400, https://doi.org/10.1016/j.chemosphere.2006.04.080.
[44] S. Preis, R. Munter, E. Siirde, Kinetic description of industrial wastewater ozonation processes, Ozone Sci. Eng. 10 (4) (1988) 379–392, https://doi.org/10.1080/01919518808552392.
[45] Y. Yang, H. Guo, Y. Zhang, Q. Deng, J. Zhang, Degradation of bisphenol A using ozone/persulfate process: kinetics and mechanism, Water. Air. Soil Pollut. 227 (2016) 53, https://doi.org/10.1007/s11270-016-2746-x.
[46] K. Shang, W. Li, X. Wang, N. Lu, N. Jiang, J. Li, Y. Wu, Degradation of p-nitrophenol by DBD plasma/Fe2+/persulfate oxidation process, Sep. Purif. Technol. 218 (2019) 106–112, https://doi.org/10.1016/j.seppur.2019.02.046.
[47] Z. Liu, W. Guo, X. Han, X. Li, K. Zhang, Z. Qiao, In situ remediation of ortho-nitrochlorobenzene in soil by dual oxidants (hydrogen peroxide/persulfate), Environ. Sci. Pollut. Res. 23 (19) (2016) 19707–19712, https://doi.org/10.1007/s11356-016-7188-x.
[48] R. Ono, X. Zhang, A. Komuro, Effect of oxygen concentration on the postdischarge decay of hydroxyl density in humid nitrogen-oxygen pulsed streamer discharge, J. Phys. D. Appl. Phys. 53 (42) (2020) 425201, https://doi.org/10.1088/1361-6463/ab98c3.
[49] H.-J. Lee, D.-W. Kang, J. Chi, D.H. Lee, Degradation kinetics of recalcitrant organic compounds in a decontamination process with UV/H2O2 and UV/H2O2/TiO2 processes, Korean J. Chem. Eng. 20 (3) (2003) 503–508, https://doi.org/10.1007/BF02705556.
[50] S. Wang, N. Zhou, Removal of carbamazepine from aqueous solution using sono-activated persulfate process, Ultrason. Sonochem. 29 (2016) 156–162, https://doi.org/10.1016/j.ultsonch.2015.09.008.
[51] E. Codorniu-Hernández, K.W. Hall, D. Ziemianowicz, S. Carpendale, P.G. Kusalik, Aqueous production of oxygen atoms from hydroxyl radicals, Phys. Chem. Chem. Phys. 16 (47) (2014) 26094–26102, https://doi.org/10.1039/C4CP02959C.
[52] H. Uchiyama, Q.L. Zhao, M.A. Hassan, G. Andocs, N. Nojima, K. Takeda, K. Ishikawa, M. Hori, T. Kondo, EPR-spin trapping and flow cytometric studies of free radicals generated using cold atmospheric argon plasma and X-ray irradiation in aqueous solutions and intracellular milieu, PLoS One. 10 (2015) 1–19. https://doi.org/10.1371/journal.pone.0136956.
[53] G.V. Buxton, C.L. Greenstock, W.P. Helman, A.B. Ross, Critical review of rate constants for reactions of hydrated electrons, hydrogen atoms and hydroxyl radicals (•OH/•O−in aqueous aolution, J. Phys. Chem. Ref. Data. 17 (1988) 513–886, https://doi.org/10.1063/1.555805.
[54] L. Wojnárovits, E. Takács, Rate constants of sulfate radical anion reactions with organic molecules: A review, Chemosphere 220 (2019) 1014–1032, https://doi.org/10.1016/j.chemosphere.2018.12.156.
[55] G. Merga, C.T. Aravindakumar, B.S.M. Rao, H. Mohan, Pulse radiolysis study of the reactions of of SO4•- with some substitued benzenes in aqueous solution, J. Chem. Soc. Faraday Trans. 90 (1994) 597–604.
[56] K. Krumova, G. Cosa, Chapter 1 Overview of reactive oxygen species, in: Singlet Oxyg. Appl. Biosci. Nanosci. Vol. 1, The Royal Society of Chemistry, 2016: pp. 1–21. https://doi.org/10.1039/9781782622208-00001.
[57] EU non-household electricity and gas prices, (2019). https://ec.europa.eu/eurostat/web/products-eurostat-news/-/DDN-20190521-1 (accessed August 28, 2020).

Appendix 3

Publication III

Tikker, P., Nikitin, D., Preis, S., 2022. Oxidation of aqueous bisphenols A and S by pulsed corona discharge: impacts of process control parameters and oxidation products identification. Chem. Eng. J. 438, 135602. ttps://doi.org/10.1016/j.cej.2022.135602

Chemical Engineering Journal 438 (2022) 135602

Contents lists available at ScienceDirect

Chemical Engineering Journal

journal homepage: www.elsevier.com/locate/cej

Oxidation of aqueous bisphenols A and S by pulsed corona discharge: Impacts of process control parameters and oxidation products identification

Priit Tikker, Dmitri Nikitin, Sergei Preis *

Department of Materials and Environmental Technology, Tallinn University of Technology, Ehitajate Tee 5, 19086 Tallinn, Estonia

ARTICLE INFO

Keywords:
Pulsed corona discharge
Surfactant radical scavenger
AOPs
Bisphenol A
Bisphenol S
Gas–liquid interface

ABSTRACT

Widespread usage of bisphenol A (BPA) and its potential replacement bisphenol S (BPS) has led to their presence in natural waterbodies. The experimental research into degradation of both aqueous pollutants by application of gas-phase pulsed corona discharge (PCD) was undertaken with variation of process control parameters, pulse repetition frequency, gas–liquid contact surface and addition of surfactant OH-radical scavenger sodium dodecyl sulphate (SDS). Although the contact surface variation had only a moderate impact on bisphenols degradation, its effect was stronger in total organic carbon removal. The addition of SDS showed a moderately negative impact on energy efficiency at all studied conditions. The obtained results showed energy efficiency surpassing the closest competitors, ozonation and other electric discharge processes. The detected major oxidation intermediates were mainly formed through hydroxylation and cracking of benzene rings, followed by further degradation into short chained aliphatic acids. The oxidation end-products were quantified as acetate, formate and oxalate.

1. Introduction

Over the last decades, anthropogenic activities resulted in rising concentrations of micro-pollutants in the aquatic environment becoming a worldwide issue of increasing environmental concern. Micro-pollutants are emerging highly potent compounds in the environment in concentrations at μg L^{-1} to ng L^{-1} levels. Being biorefractory, these substances accumulate in surface- and groundwater, and soils causing cumulative negative effects on aquatic life along its multi-generational exposure [1–3]. The impact of micro-pollutants on human health and the environment is not yet completely clear, although the main negative effects, such as short-term and long-term toxicity, endocrine disrupting and antibiotic resistance of microorganisms, are well-known. Natural or manmade micro-pollutants include pharmaceuticals, personal care products, steroid hormones, pesticides, and industrially emitted compounds (surfactant alkylphenol polyethoxylates, phenolic compounds, phthalates and other plasticizers) originated from industrial wastewaters, landfill leachates, runoff from livestock and aquaculture, domestic and hospital effluents. Since wastewater treatment plants are less effective in micro-pollutants elimination, these are passing through intact to surface waters threatening the aquatic life and spelling trouble for drinking water supplies [1,4].

To date, the European Union have environmental quality standards only for 45 priority substances stated by the Directive 2013/39/EU [5]. Since additions to the list require information about the risks micro-pollutants pose to the aquatic environment, there is a watch list of potential water pollutants monitored by the EU Member States. Established by the Decision (EU) 2018/840 from June 5, 2018, an updated watch list in the field of water policy [6] consists of eight compounds, including endocrine disrupting compounds (EDCs) interfering with human reproduction and development systems, - phthalates, bisphenols and pharmaceuticals [7]. One of these chemicals, bisphenol A (BPA), is widespread due to its massive and consistently increasing production as the main component of polycarbonate plastics of outstanding chemical and physical properties used in production of plastic bottles, toys, sportswear, CDs etc. [8]. Also, BPA is widely used as a bulk chemical for epoxy resins, stabilizer and antioxidant for plastics [8,9]. Bisphenol A was found in wastewater treatment plant effluents at concentrations up to 370 μg L^{-1} and in surface waters - up to 56 μg L^{-1} [10]. In Japan, the highest BPA concentration of 17.2 mg L^{-1} was detected in leachate from a landfill containing plastic wastes [9].

The EU banned the BPA usage in baby feeding bottles with its Directive 2011/8/EU [11,12]. Additionally, the EU Directive 2020/

* Corresponding author.
E-mail address: sergei.preis@taltech.ee (S. Preis).

https://doi.org/10.1016/j.cej.2022.135602
Received 21 December 2021; Received in revised form 18 February 2022; Accepted 1 March 2022
Available online 3 March 2022
1385-8947/© 2022 Elsevier B.V. All rights reserved.

2184 requires a guarantee for drinking water containing no>2.5 μg L^{-1} of BPA by 2026 [13]. Since limits were also set for food plastic containers, BPA substitution with bisphenol S (BPS) has been started in production [14,15]. Although considerably less studies have been conducted with BPS, this, nevertheless, has been also found to be a potential endocrine disruptor [11,16] already detected in surface water: up to 7.2 μg L^{-1} were registered in Adyar River, India. Emissions of BPS and its presence in the environment will probably grow since its production is progressively increasing [14,17].

Since conventional wastewater treatment does not provide sufficient removal of micro-pollutants [4,18,19], emerging technologies such as advanced oxidation processes (AOPs) are under consideration as pre- or post-treatment part [20,21]. These processes exploit reactive oxygen species (ROS), mostly hydroxyl radicals (OH-radicals) degrading organic pollutants, and differ by the way the ROS are generated. They include ozonation at pH > 8.5, Fenton reaction, electrochemical oxidation, photocatalysis, non-thermal plasma (NTP) and combinations of those.

Among NTPs, there has been a growing interest towards gas-phase electric discharges. In gas–liquid environment, these plasmas generate short-living (e.g. HO-radicals) and long-living ROS (ozone) through impacts of high-energy electrons with surrounding atoms and molecules in water vapour and air, respectively. Formation of HO-radicals at the treated aqueous solution surface comprises the principal feature of this approach resulting in useful energy utilization in reactions at the gas–liquid interface. While generated ozone participates in pollutant degradation being dissolved in the bulk of solution, the HO-radicals may only react directly with pollutant at the proximity to the gas–liquid interface due to their short lifetime. Since the mass transfer between the gas and liquid phases becomes important for the radical reactions, the study into its optimization requires establishing the dependence of oxidation efficiency on the contact surface [22–24]. The advancement in NTP application to water purification consists of the gas-phase pulsed corona discharge (PCD), in which the mass transfer is improved by dispersing the treated solution in the form of droplets, jets and films directly to the plasma zone. By using PCD, promising energy efficiencies have been reported in degradation of humic substances [25], pharmaceuticals [26] and azo-dyes [27]. Impacts of the surfactant scavengers to the oxidation rate and the energy efficiency of PCD oxidation confirmed the interface character of HO-radical reactions [28]. However, the effect of surfactant scavenger on surface-borne reactions at various gas–liquid contact surfaces still needs to be clarified. Therefore, the experimental study was undertaken into BPA and BPS PCD-oxidation with special attention towards effects of the plasma-liquid contact surface and an impact of surfactant radical scavenger on the energy efficiency. The comparison of the results obtained in the research with the data on other AOPs applied to bisphenols' oxidation was also conducted, including the study in the oxidation reaction pathways.

2. Materials and methods

2.1. Chemicals

Bisphenol A ($C_{15}H_{16}O_2$, ≥97%) and sodium hydroxide (NaOH, ≥98%) was purchased from Merck KGaA (Germany). Bisphenol S ($C_{12}H_{10}O_4S$, ≥99%) was obtained from Thermo Fischer Scientific, Ltd. (USA). Sodium dodecyl sulphate (SDS, $NaC_{12}H_{25}SO_4$) of analytical grade was purchased from Lach-Ner, Ltd. (Czech Republic).

2.2. Experimental device

The experiments were performed using the equipment made by Flowrox Oy (Finland). The plasma stainless steel reactor in total volume of 110 L consists of an electrode system with 24 high voltage wire electrodes with the diameter of 0.5 mm and total length of 20 m, positioned horizontally between two grounded vertical parallel plate electrodes. The distance between wire electrodes and the grounded plate is 18 mm. The distance between wire electrodes is 30 mm. Treated solutions were dispersed through the perforated plate (30 × 500 mm) with 51 perforations of 1 mm diameter positioned above the wire electrodes as shown earlier [29]. The device consists of PCD reactor with the 40-L storage tank, pulse generator and circulation pump (Iwaki Co. Ltd., Japan) with the frequency regulator (Yaskawa, Japan) used to control the rotation rate of the pump's electric motor with the water flow rate controlled from 2.0 to 28.5 L min^{-1}, making the spray densities worth of 0.002 to 0.26 m s^{-1}. The spray densities were calculated by using Eq. (1):.

$$q = \frac{v}{S} \tag{1}$$

where v – flowrate of solution, m^3 s^{-1};

S – horizontal cross section area of plasma zone, m^2.

The horizontal cross section of plasma zone S was found by multiplying the distance between two grounded electrodes (36 mm) by the width of a grounded electrode (500 mm), giving a value of 0.018 m^2.

The gas–liquid contact surface area in the reactor previously measured using sulphite oxidation method [29] follows Eq.2:.

$$A = 4954q + 17.6 \tag{2}$$

where A – gas–liquid contact surface, m^{-1} (m^2 m^{-3}),

q – spray density, m s^{-1}.

High voltage pulses generated at repetition frequencies from 50 to 880 pulses per second (pps) provide from 9 to 123.2 W of output power. The pulse amplitude voltage, current and duration were 18 kV, 380 A and 100 ns, respectively. The pulse characteristics were quantified with a Rigol DS1102E Mixed Signal Oscilloscope, a Tektronix P6015 high voltage probe (Tektronix Inc., USA) and a current monitor PT-7802 (PinTek, China).

2.3. Experimental procedure

In order to determine and obtain reliable bisphenol degradation data even at their residual, i.e., less than 5% of initial concentrations, higher initial concentrations of bisphenols were chosen than reported in polluted natural and wastewaters. All experiments were conducted at ambient conditions with 10-L samples of solutions containing BPA or BPS in the initial concentrations of about 50 mg L^{-1}. 0.5 g of BPA were dissolved in 1-L flask with bi-distilled water containing 10 mL of 1-M NaOH to accelerate dissolution in the ultrasonic bath within 20–30 min at 50 °C. The solution was cooled to a room temperature and diluted by distilled water to the total volume of 10 L in the reactor tank. The BPS solution was prepared similarly to BPA having the ultrasonic bath replaced with warm water bath for higher BPS solubility. In the experiments with surfactant scavenger, 1.0 g of SDS was dissolved in 1-L measuring flask with bi-distilled water and then added together with BPA solution to the reactor tank and diluted to a total volume of 10 L making the resultant concentration 100 mg L^{-1} of SDS.

The oxidation experiments were carried out at pulse repetition frequencies of 200 and 880 pps, i.e. input power 32 and 123.2 W, respectively. Plasma treatment time comprised up to 20 min at 200 pps and up to 320 s at 880 pps to provide similar energy doses of 1.07 and 1.10 kWh m^{-3}, respectively. The treated solution flow rates were in the range from 5.5 to 28.5 L min^{-1}, making the spray density (q) ranging from 0.005 to 0.026 m s^{-1}.

Extended plasma treatment experiments, for 95 min at 200 pps (energy dose 5.06 kWh m^{-3}) and 24 min and 40 s at 880 pps (5.07 kWh m^{-3}), were conducted with flowrates of 5.5 L min^{-1} and 22.0 L min^{-1}. Before the treatment, solutions were mixed for 5–10 min at 0.015 m s^{-1} spray density (flow rate at about 16 L min^{-1}) for concentration uniformity. The flow rate was measured using water meter and the stop-watch. Due to BPA and BPS poor solubility in acidic and neutral media, experiments were conducted in alkaline media at pH 9.5 ± 0.5 adjusted

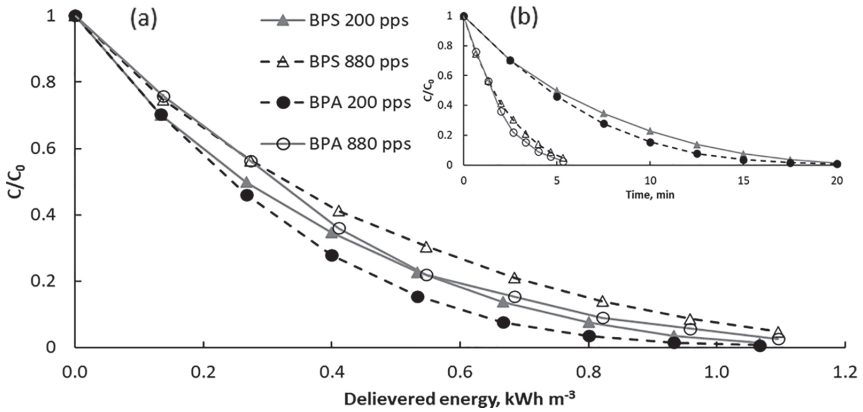

Fig. 1. Relative bisphenols' concentrations as a function of PCD delivered energy dose (a) and treatment time (b): pulse repetition frequencies of 200 and 880 pps, BPA and BPS initial concentration 50 mg L^{-1}, spray density 0.02 m s^{-1}, initial pH 9.5 ± 0.5.

with 5-M NaOH. The experimental run started when the pulse generator was turned on. Samples were collected from the storage tank at pre-set treatment time intervals in correspondence with the planned delivered energy doses. Before sampling, the pulse generator was turned off and the treated solution was mixed by circulating at least six volumes of solution at the set flow rate to obtain uniformity in concentration. The energy efficiency of oxidation measured at 90% of bisphenols removal was calculated using Eq. (3):.

$$E = \frac{\Delta C^{*} V}{W} \tag{3}$$

where E – energy efficiency, g $kW^{-1}h^{-1}$,

ΔC – the decrease in pollutant concentration, g m^{-3},

V – volume of treated solution sample, m^3,.

W – energy consumption as a product of power delivered to the reactor and the time of treatment, kWh.

All experiments were duplicated with the results deviations fitting into 5-% confidence interval.

2.4. Analyses

The contents of bisphenols were measured using YL 9300 high performance liquid chromatograph (HPLC) (YL Instrument Co., South Korea) equipped with XBridge BEH C18 Column (130 Å, 3.5 μm, 3 mm × 150 mm) at a detection wavelength of 275 or 258 nm for BPA and BPS, respectively. The sample injection volume was 20 μL at the eluent flow rate of 0.2 mL min^{-1}. Solutions of BPA were analysed using isocratic method with a mobile phase composed of water acidified with 0.1% acetic acid (40%) and acetonitrile (60%). Samples containing BPS were analysed analogously using the water-acetonitrile ratio of 60:40. Calibrations of BPA and BPS contents were derived in the range from 0.5 to 100 mg L^{-1} with and without SDS additions. The presence of SDS had no effect on calibration results. However, pH affects the area of peaks in chromatograms requiring its thorough adjustment in samples to the range of 10.9 – 11.0 prior to analysis. Samples were filtered through a Millipore Millex-FH cartridge filter (hydrophilic PTFE, pore size 0.45 μm). pH was measured using a digital pH/Ion meter (Mettler Toledo S220, USA). Conductivity measurements were carried out using Multiparameter meter HQ430d (Hach Company, USA).

Identification of oxidation by-products was carried out by HPLC equipped with Phenomenex Gemini NX-C18 column (110 Å, 5 μm, 2 mm x150 mm) combined with mass spectrometer (HPLC-MS, LC-MS 2020, Shimadzu) using diode array detector (HPLC-PDA, SPD-M20A, Shimadzu). Samples containing BPA were analysed using an isocratic method with a mobile phase mixture composed of 55% of aqueous solution of 0.3-% formic acid and 45% of acetonitrile also containing 0.3% of formic acid. Solutions of BPS were analysed analogously using the water-acetonitrile ratio of 70:30. Mass-spectra were acquired by quadrupole mass separation in full-scan mode (scanning range 50–500 m/z). The nebulizing and drying gas flow rates were set to 1.5 and 10.0 L min^{-1}, respectively. The temperatures of the heat block and the desolvation line were set to 250 °C and the interface voltage comprised 4.5 kV. The device was operated in positive ESI mode and the results obtained with MS detector were handled using Shimadzu Lab Solutions software.

Total organic carbon (TOC) was measured using Multi N/C 3100 analyser (Analytic Jena, Germany). TOC removal percentage (%) was calculated using Eq. (4):.

$$TOCremoval = \left(1 - \frac{TOC_t}{TOC_0}\right) * 100\% \tag{4}$$

where TOC_0 and TOC_t are the TOC values at treatment times 0 and t, mg C L^{-1}.

Concentrations of anions in samples were measured using the 761 Compact IC ion chromatograph with chemical suppression of eluent conductivity (Metrohm Ltd). The device was equipped with METROSEP A Supp 5 column (150 mm × 4.0 mm). The sample injection volume was 20 μL. Separation of ions was attained using an eluent mixture of 3.2 mM Na_2CO_3 + 1.0 mM $NaHCO_3$ with flowrate of 0.7 mL min^{-1}.

3. Results and discussion

3.1. Bisphenols degradation efficiency

3.1.1. Oxidation efficiency

One can see PCD rapidly degrading BPA and BPS almost entirely from their starting concentrations of 50 mg L^{-1} at the pulsed energy of 1.07–1.10 kWh m^{-3} delivered within 20 min and 5 min 20 s at 200 and 880 pps, respectively (Fig. 1). The treatment performance expressed as the energy efficiency at 200 pps slightly exceeds the one at 880 pps indicating bisphenols as compounds rapidly reacting with ROS, including long-living ozone. The equality of oxidation results at different pulse repetition frequencies stands either for negligible role of ozone on oxidation, or rapid consumption of ozone. Both bisphenols showed rapid oxidation resulting in their oxidation energy efficiency from 41.7 to 63.7 and 43.4 to 53.3 g $kW^{-1}h^{-1}$ for BPA and BPS, respectively, comparable with rapidly reacting phenol in air atmosphere [29]. This circumstance makes the use of high pulse repetition frequency at shorter treatment

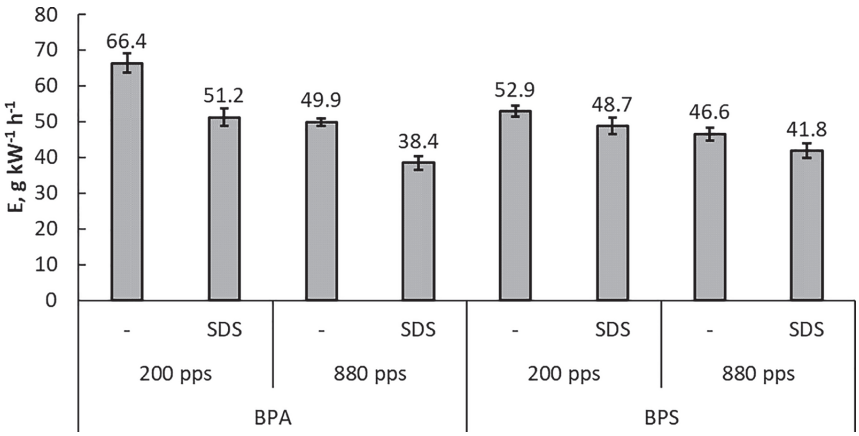

Fig. 2. Energy efficiencies of BPA and BPS oxidation in PCD experiments at different pulse repetition frequencies in absence and presence of SDS surfactant OH-radical scavenger: BPA and BPS initial concentrations 50 mg L^{-1}, bisphenols' removal 90%, initial pH 9.5 ± 0.5, spray density 0.02 m s^{-1}, SDS concentration 100 mg $L^{-1.}$

time beneficial in the reactor's intensity in action avoiding the trade-off between the energy expense and the time of treatment. Oxidation of BPA and BPS by PCD resulted in pH descending during experiments from 9.5 ± 0.5 to about 7.0 explained by accumulation of nitric acid and formation of carboxylic acids as oxidation products [30,31]. Under the experimental conditions, however, oxidation of bisphenols did not change the medium from alkaline-neutral to acidic preventing problems with bisphenols' aqueous solubility.

The better energy efficiencies for both pollutants were observed at 200 pps, although the difference with the energy efficiency at 880 pps was moderate (Fig. 2): the average energy efficiencies of 66.4 and 49.9 g $kW^{-1}h^{-1}$ at 90% removal points were calculated for 200 and 880 pps, respectively, showing the BPA oxidation efficiency decreased for 25% at increased frequency. For BPS, the difference in analogous comparison comprised only 12%, i.e. twofold smaller. Previously, the authors have shown the similar, of about 12% difference in efficiencies of phenol oxidation at starting pH 11 [29]. The difference between BPA and BPS in their sensitivity towards the pulse repetition frequency may be explained by a difference in stoichiometry of oxidation reactions of different molecules if the composition of ROS is expected to be indifferent towards the treated target pollutant. The authors also explained the difference in oxidation rates of various substances by the difference in their hydrophobicity [26], which was also observed between BPA and BPS: BPA is less soluble in water than BPS.

Similar effect of pulse repetition frequency on energy efficiency was observed with BPA solutions containing SDS surfactant: the efficiency of BPA oxidation decreased at increased frequency for about 25%, from 51.2 to 38.4 g $kW^{-1}h^{-1}$ at 200 and 880 pps, respectively. Comparable results were also obtained for BPS, where the increased frequency caused a decrease in energy efficiency from 48.7 g $kW^{-1}h^{-1}$ to 41.8 g $kW^{-1}h^{-1}$, i.e. the difference in BPS oxidation ranged at about 14%. Even though the contact surface was sufficiently developed at higher flow rates, the difference in oxidation rates between frequencies indicate certain, although moderate amount of residual ozone contributing to BPA and BPS oxidation at longer treatment times. The addition of SDS somewhat reduced oxidation efficiency, although one should notice the difference between frequencies: the removal efficiency decreased with SDS addition to a greater extent at 880 than at 200 pps consistently indicating relatively bigger contribution of short-living ROS to BPS oxidation at gas–liquid interface. One can see the difference made by SDS in respect to BPA being bigger than BPS explained below (Fig. 2).

3.1.2. Surfactant impact

In previous works, the authors used addition of surfactant SDS as a scavenger of surface-borne OH-radicals to clarify the importance of surface oxidation of target pollutants [27,28]. The effect of SDS addition, however, appeared to be dependent on the target compound molecular structure: SDS sulphate groups may either interact with the hydrophilic moieties of target pollutants submerging those below the gas–liquid interface thus screening them from the OH-radical attack, or SDS-radical, once formed under the OH-radical attack, may raise the target molecule to the surface for more effective radical oxidation [32]. For rapidly reacting bisphenols, addition of SDS, together with the impacts of contact surface area and pulse repetition frequency, helps clarifying the character of their oxidation. The effect of SDS in oxidation of bisphenols appeared to be to a certain extent negative: only minor decrease in BPS removal rate was noticed with SDS addition, whereas BPA showed a stronger negative effect (Fig. 2). This indicates the screening effect of SDS surfactant attached with its sulphate group to hydrophilic phenolic moieties compensated partly by the affinity between the surfactant radical and a radicalized bisphenol molecule brought closer to the interface. In comparison with phenol [28], PCD oxidation of which was dramatically hindered with SDS addition, bigger and less polar BPA and BPS radicalized molecules show higher affinity with the SDS radical formed at the end of hydrophobic tail. Poorer aqueous solubility of bisphenols also points to their less hydrophilic character than phenol thus being faster oxidized in surface-borne reactions as described earlier [26]. The role of hydrophobicity in the rate of oxidation is also indirectly supported by the fact of poorer BPA aqueous solubility than the one of BPS. This observation confirms complex character of surfactant effect to various pollutants deserving attention also for the practical reason – disclosing the surfactant effect, often characteristic to industrial and municipal wastewaters, to PCD oxidation.

For the completeness of the picture covering the factors potentially influencing the oxidation efficiency, the authors have to repudiate possible technical reasons for the observed neutrality of SDS additions. For example, foaming of SDS solutions never short-circuited the electrodes in the discharge zone. Similarly, addition of SDS did not noticeably change the treated solution conductivity, remaining between 200 and 250 μS cm^{-1}. The latter value only slightly exceeds the solely bisphenol solutions with conductivity values between 150 and 200 μS cm^{-1}. Previous studies showed that the surface resistance of the PCD reactor insulators and, thus, their design becomes practically important

Table 1
Energy efficiencies of BPA and BPS oxidation in AOPs.

Compound	Initial concentration, mg L^{-1}	Process	Treated sample volume, L	Pollutant removal, %	Energy efficiency, g $kW^{-1}h^{-1}$	Reference
BPA	7.98	O_3	2.5	90	27.86 (55.72*)	[43]
	22.8	O_3	5.2	90	35.62 (71.24*)	[39]
	50	O_3	0.4	90	6.39 (12.79*)	[36]
	50	O_3	2.2	90	56.18 (112.37*)	[40]
	100	O_3	1	90	31.22 (62.44*)	[41]
	116	O_3	0.5	90	12.42 (24.83*)	[42]
	91.2	O_3/UVC	0.25	90	1.50 (1.58*)	[38]
	50	O_3/UVA	0.4	90	7.57 (15.12*)	[36]
	50	H_2O_2/UVC	0.02	90	5.37	[36]
	28	Gliding arc	0.3	90	0.02	[45]
	20	Glow discharge	0.15	90	1.25	[46]
	50	DBD	0.5	90	0.31	[44]
	50	DBD	0.003	90	0.01	[47]
	1	O_3/DBD	1.2	90	0.18	[48]
	50	PCD	10	90	66.4	This study
BPS	50	O_3	0.4	90	3.54 (7.08*)	[36]
	50	O_3	1	90	1.48 (2.96*)	[37]
	50	O_3/UVA	0.4	90	5.43 (10.85*)	[36]
	15	UVC	0.034	69	0.007	[15]
	50	H_2O_2/UVC	0.02	90	5.68	[36]
	50	H_2O_2/UVC	1	90	24.90	[37]
	2.28	Sonolysis	0.5	29	0.005	[49]
	50	PCD	10	90	52.9	This study

* - Values obtained with oxygen gas used in the ozone synthesis.

at the treated aqueous solution conductivity exceeding 4–5 mS cm^{-1}, i.e. the treated solution conductivity must be an order of magnitude higher than the one used in the experiments [33]. For example, with the reactor's construction used in the study, previous experiments showed that noticeably negative effect of conductivity on oxidation of Reactive Blue 4 and 19 textile dyes was observed at conductivities above 10 mS cm^{-1} [27]. This makes the conductivity used in this study negligibly low to have an effect on bisphenols' oxidation.

3.1.3. *Bisphenols oxidation compared to other AOPs*

Using available literature, a comparative analysis of energy expense in AOPs applied to BPA and BPS removal was conducted with the results shown in Table 1. The energy expense for ozone synthesis was considered as 15 kWh kg^{-1} O_3 when using oxygen and 30 kWh kg^{-1} O_3 in air [34]. The two-fold difference in energy efficiency was observed also in PCD, when air and oxygen were used [24,25]. The H_2O_2 cost of 1 EUR kg^{-1} is considered relevant at the moment of reporting based on the average market price. For the expense comparison, the H_2O_2 cost was converted to the electric energy expense, which in Europe comprises for non-household consumption 0.115 EUR $kW^{-1}h^{-1}$ [35]. The energy consumed by UVA and UVC photolysis, solely and in combination with other methods, was calculated, where possible, from the photon per

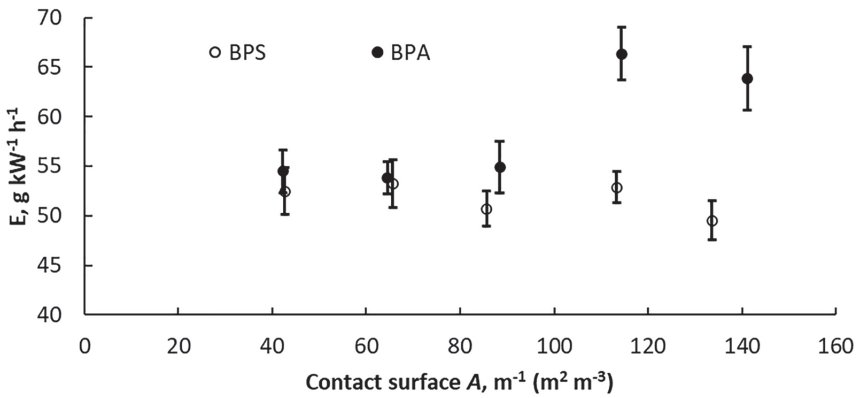

Fig. 3. Bisphenols' oxidation efficiency dependent on the contact surface: pulse repetition frequency 200 pps, pH 9.5 ± 0.5, BPA and BPS starting concentrations 50 mg L^{-1}, bisphenols' removal 90%.

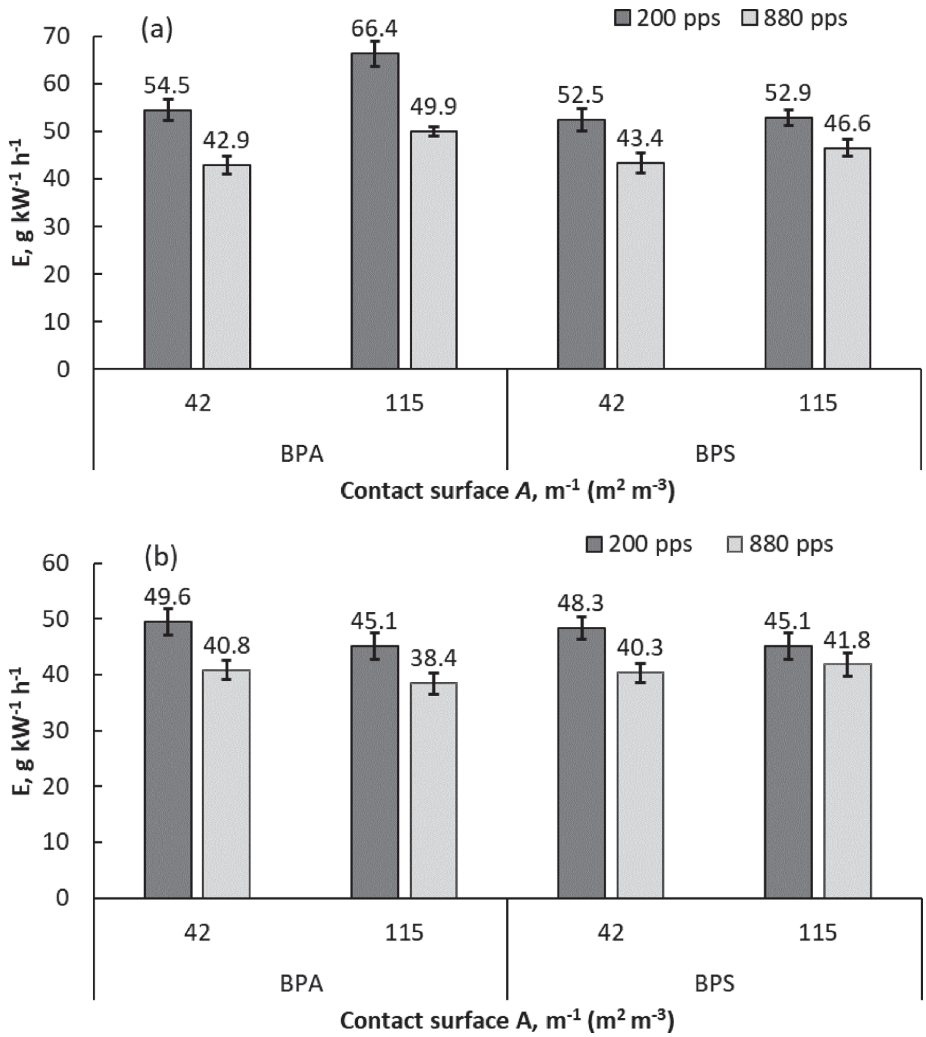

Fig. 4. Impact of contact surface on BPA and BPS oxidation efficiency without SDS (a) and with SDS (b): pulse repetition frequency 200 and 880 pps, initial pH 9.5 ± 0.5, BPA and BPS starting concentrations 50 mg L^{-1}, SDS concentration 100 mg L^{-1}, bisphenols' removal 90%.

second entering the reaction solution [36,37] or, otherwise, from the energy consumed by the UV-lamps [15,38].

One can see that the variety of AOPs was used to successfully degrade BPA and BPS in various concentrations (Table 1). In case of BPA, the highest energy efficiencies were achieved when ozonation was applied, indicating BPA readily reacting with ozone. For example, BPA with its initial concentration of 22.8 mg L^{-1} was degraded for 90% in about 900 s of treatment [39], thus resulting in the energy efficiency of 71.24 g $kW^{-1}h^{-1}$ when oxygen was used. If air would be used for ozone synthesis, this result should comprise 35.62 g $kW^{-1}h^{-1}$, which is about two-fold lower than the efficiency obtained in this study using air as the discharge atmosphere. The BPA ozonation result standing out of the row of studies was reported in [40] showing the energy efficiency as high as 112.37 g $kW^{-1}h^{-1}$ in oxygen (56.18 g $kW^{-1}h^{-1}$ in air) comparable with the result obtained in this research. More recent studies, which reported their results in BPA ozonation, show considerably smaller oxidation yields [36,41–43].

The O_3/UVC and H_2O_2/UVC combinations as well as the other plasma treatment systems appeared to be substantially less energy efficient than PCD in degradation of BPA (Table 1). For example, when dielectric barrier discharge (DBD) with discharge power of 412.5 W was applied to degrade BPA with initial concentration of 50 mg L^{-1}, about 10 min of treatment time was needed to degrade 90% of target compound, giving energy efficiency as low as 0.31 g $kW^{-1}h^{-1}$ [44].

Unlike BPA, BPS oxidation has been studied to a significantly lesser extent giving less data for the comparative analysis. Nevertheless, one can see that BPS treatment with ozone proved to be less energy efficient than the degradation of BPA, having the highest efficiency achieved at 7.08 g $kW^{-1}h^{-1}$ in oxygen [36,40] (Table 1). Although O_3/UVC and H_2O_2/UVC combinations proved to be better options for BPS degradation with maximum efficiencies of 10.85 in oxygen [36] and 24.90 g $kW^{-1}h^{-1}$ [37], respectively, showing BPS being more susceptible towards oxidation with OH-radicals than ozone, the obtained energy efficiency values are at least three times smaller than the one observed in PCD. Among other plasma methods, authors failed to find publications related to BPS degradation by using electric discharge.

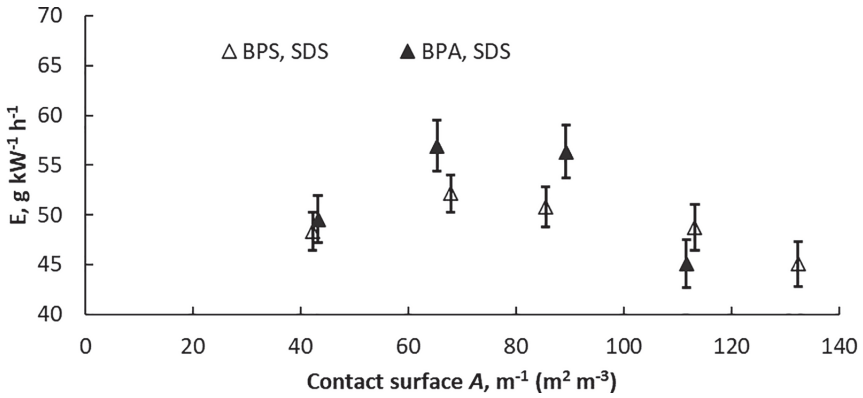

Fig. 5. Dependence of BPA and BPS oxidation efficiency on contact surface in presence of SDS: pulse repetition frequency 200 pps, initial pH 9.5 ± 0.5, BPA and BPS starting concentrations 50 mg L^{-1}, bisphenols' removal 90%, SDS concentration 100 mg L^{-1}.

3.2. Impact of the gas–liquid contact surface on the energy efficiency of oxidation

The effect of gas–liquid contact surface at 200 pps is shown in Fig. 3. The energy efficiency of BPA oxidation increased from about 54.5 to 63.9 g $kW^{-1}h^{-1}$, i.e., for about 17% with the gas–liquid contact surface increased 3.5 times from about 40 to 140 m^{-1} (at the corresponding flow rates 5.5 and 28.5 L min^{-1}, respectively). For BPS, oxidation efficiency appeared to be almost invariant towards spray density values. The difference between dependence characters of BPA and BPS is consistent with their hydrophobicity [26]: less water-soluble BPA demonstrated noticeable growth of oxidation efficiency with increased interface surface, whereas better soluble BPS behaved similarly to phenol being invariant of the contact surface area [29]. The results show, in general, weak dependence of rapid oxidation towards the contact surface within the studied limits explained by ROS reacting fast enough even at experimental minimum contact surface at a gas–liquid interface. Thus, with the rapidly reacting BPA and BPS, the energy efficiency depends mainly on the amount of generated reactive species in the unit of time, which is determined by the pulse generation power. Certain increase in oxidation rate of BPA may also be explained by its faster oxidation with ozone when compared with BPS, which is confirmed by the impact of pulse repetition frequency (Fig. 2) and the data of other studies (Table 1). The indifference of BPS PCD-oxidation towards the interface area indicates, besides lower hydrophobicity, the pollutant's superior susceptibility to OH-radical oxidation.

The effect of gas–liquid contact surface observed for the bisphenols at various pulse repetition frequencies is shown in Fig. 4a. At 880 pps, the contact surface increased from 42 to 115 m^{-1} showed a moderate impact on the average energy efficiency increased only from 42.9 to 49.9 g $kW^{-1}h^{-1}$ and from 43.4 to 46.6 for BPA and BPS, respectively. For clarity of Figure, energy efficiency values of 45.6 and 48.6 g $kW^{-1}h^{-1}$ for BPA, and 44.9 and 45.8 g $kW^{-1}h^{-1}$ for BPS at contact surface of 65 m^{-1} and 87 m^{-1}, were excluded, respectively. Such tendency, i.e. the effect of the contact surface small in BPS oxidation and slightly more pronounced with BPA, is analogous to the one at 200 pps.

Fig. 5 shows the results of PCD treatment of bisphenols solutions at various spray densities, i.e. contact surface areas in presence of SDS. The contact surface value growth from about 40 to 65 m^{-1}has slightly positive effect on BPA degradation: the energy efficiency increased from 49.6 to 57.0 g $kW^{-1}h^{-1}$. Further increase in contact surface has a negative effect resulting in the energy efficiency of 45.1 g $kW^{-1}h^{-1}$ at 115 m^{-1}. The possible reason for the decrease may be an intense foaming occurring at higher flow rates complicating the mass transfer of oxidants and diffusion of BPA to the surface. Another possible explanation of the efficiency decreased at larger contact surfaces in presence of SDS may lay in the balancing between opposing SDS effects on BPA molecules - transfer to the interface for faster oxidation and the interface screening with SDS surfactant molecules slowing down the oxidation [32]. The authors presume the balance under discussion being controlled by the surface concentration of SDS dependent on the contact surface area: at larger contact surface, the decreasing surface concentration of SDS may apparently result in the balance shifting towards screening effect at less effective transportation of BPA molecules towards the interface. Further studies in wider SDS concentration span might bring more clarity in the question, if not a technical difficulty appeared at high flow rates of treated solution containing SDS: at higher SDS concentrations, the foam was developed reaching the inter-electrode gap in the PCD reactor thus obstructing further treatment by partial short-circuiting of the discharge. Also, at SDS concentration used in the study, foaming at the contact surface of 140 m^{-1} (flow rate 28.5 L min^{-1}) was also strong enough to obstruct treatment, making the experiments limited with the contact surface of 115 m^{-1} without the foam reaching the inter-electrode gap.

Similar to BPA, the contact surface growth from 40 to 65 m^{-1}had a positive, although minor effect on BPS energy efficiency from 48.3 to 52.1 g $kW^{-1}h^{-1}$ (Fig. 5). Since considerably less foam was observed during BPS treatment likely related to the difference, with which SDS interacts with more hydrophobic BPA and less hydrophobic BPS, no technical complications were observed at higher flowrates. This allowed the contact surface value increasing up to 140 m^{-1} (flow rate 28.5 L min^{-1}), at which the energy efficiency decreased further to 45.1 g kW^{-1}h likely confirming the balance shift towards SDS screening effect.

In Fig. 4b, the increase of contact surface from 42 to 115 m^{-1} demonstrated minor negative effect on BPA energy efficiency at both tested frequencies. The energy efficiency of BPS oxidation was less sensitive towards the contact surface remaining virtually the same at 880 pps at the considered contact surfaces of 42, 65, 87 and 115 m^{-1}. Similarly, to Fig. 4a, energy efficiencies of 40.5 and 39.8 g $kW^{-1}h^{-1}$ for BPA, and 40.7 and 41.4 g $kW^{-1}h^{-1}$ for BPS at contact surface of 65 m^{-1} and 87 m^{-1}, were excluded in the name for the transparency of Fig. 4b. For both bisphenols, minor effects in energy efficiency at the dramatically increased flow rates discredited the efforts in mass transfer intensifying consistently with rapid oxidation [29].

3.3. Products of bisphenols oxidation

3.3.1. Mineralization

In the study of bisphenols mineralization, the spray density increased from 0.005 to 0.02 m s^{-1} providing gas–liquid contact surface from 42 to

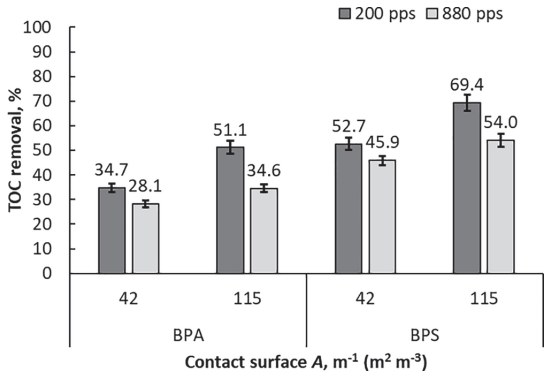

Fig. 6. Impact of contact surface on BPA and BPS TOC removal efficiency: initial pH 9.5 ± 0.5, BPA and BPS starting concentration 50 mg L^{-1}, delivered energy dose 5.06–5.07 kWh m^{-3}.

115 m^{-1} showed no significant difference in TOC removal at the delivered energy doses of about 1.1 kWh m^{-3}, when the parent compound was still present (Fig. 1). For BPA, at this energy dose, TOC removal varied between 9% and 11% regardless of pulse repetition frequency. Similar results were obtained for BPS varying between 9% and 14%. Insignificant differences are likely related to refractory character of products derived from bisphenols oxidation. For the study of in-depth mineralization of bisphenols oxidation products, the experiments at the delivered energy dose of about 5 kWh m^{-3} were carried out. High energy doses resulted in a notable difference in TOC removal dependent on pulse repetition frequencies and contact surface as shown in Fig. 6. The mineralization of BPS may be noticed to be faster than the one of BPA having no simple explanation since the quantified carboxylic anions demonstrate similar composition for both bisphenols (Table 2). The difference in BPA and BPS oxidation intermediates needs to be established in a more detailed study.

One can see that TOC removal benefitted from larger contact surface area and lower pulse repetition frequency. For example, at 200 pps, when contact surface increased from 42 to 115 m^{-1}, TOC removal increased from 34.7% to 51.1% and from 52.7% to 69.4% for BPA and BPS, respectively. Similar tendency was observed previously in degradation of oxalate [29] usually formed together with formate and acetate in oxidation of aromatic compounds [50]. This observation is in agreement with slow oxidation of ultimate oxidation products with surface-borne ROS dependent on the area of contact surface [24]. The difference in TOC removal rates at various pulse repetition frequencies is explained by participation of aqueous ozone decomposing to OH-radicals.

3.3.2. *Anionic products*

To quantify potential oxidation anionic products, treated samples of BPA and BPS were analysed with IC (Table 2). The IC-chromatograms obtained for oxidation products at the delivered energy dose of about 0.5 kWh m^{-3} are presented in Figure S1. Identifiable oxidation by-products were found to be acetate, formate and oxalate earlier reported for BPA ozonation [51,52] and ultrasonic cavitation [53]; electro-Fenton of BPS gave the same products [54]. The major difficulty in analysis of the BPS samples consists of formation of sulphate interfering with quantification of oxalate: having similar retention times, sulphate anion captivates oxalate signal. The sulphate concentration meets the theoretically expected one in samples containing initially 50 mg L^{-1} of BPS treated at the applied energy dose of 5 kWh m^{-3}, i.e. about 19 mg L^{-1}, i.e. the sulphonyl moiety in BPS molecule was completely mineralized. The precise measurement of sulphate and oxalate in intermediate samples was mutually compromised by each other having the sulphate signal more pronounced. For the reason, in the end of oxidation at the highest energy dose no TOC balance could be derived in experiments with BPS. Oxalate in BPA samples was distinctively present without obstacles in quantification, showing the concentrations of acetate, formate and oxalate in the range from 2 to 4 (acetate and formate) to 5–7 (oxalate) mg L^{-1}.The concentrations of oxalate exceeding the ones of acetate and formate were also reported for BPA catalytic ozonation [52]. The TOC sum of carboxylic anions quantified in the end of

Table 2
Concentration of by-products formed in BPA and BPS solutions treated by PCD detected by IC analysis.

Contact surface, m^{-1}	Initial compound	Frequency, pps	Delivered energy, kWh m^{-3}						
			0	0.55	1.1	2.0	3.0	4.0	5.1
			Acetate, mg L^{-1}						
42	BPA	200	0	0.4	1.0	2.1	2.5	1.7	2.5
		880	0	0.4	1.2	2.2	2.7	2.9	3.1
	BPS	200	0	0.7	2.0	3.4	3.4	–	2.4
		880	0	0.3	0.4	0.9	1.2	–	0.9
115	BPA	200	0	0.6	1.1	2.7	3.3	2.9	4.0
		880	0	0.3	0.8	1.5	1.6	2.1	3.2
	BPS	200	0	0.6	1.5	3.8	3.2	–	1.2
		880	0	0.8	1.8	–	–	–	2.5
			Formate, mg L^{-1}						
42	BPA	200	0	0.6	1.6	2.9	2.6	2.7	2.7
		880	0	0.8	1.7	2.4	2.1	1.9	2.4
	BPS	200	0	1.4	2.8	3.9	4.4	–	3.2
		880	0	1,4	2.6	3.5	3.6	–	3.7
115	BPA	200	0	0.8	1.7	2.4	1.6	1.6	1.2
		880	0	0.7	1.7	2.5	2.7	2.7	2.4
	BPS	200	0	1.5	3.2	5.2	3.8	–	0.9
		880	0	1.2	2.6	–	–	–	2.8
			Oxalate*, mg L^{-1}						
42	BPA	200	0	2.9	4.9	5.7	4.4	4.1	4.7
		880	0	1.5	3.4	6.0	6.5	6.2	6.5
115	BPA	200	0	1.4	3.8	6.5	5.3	3.8	4.6
		880	0	1.1	2.8	3.7	3.5	4.8	5.7

* Oxalate and sulphate in BPS PCD-treated samples were not quantified for their mutual interference in IC analysis.

Table 3
Bisphenol A transformation products determined by LC-MS analysis in PCD treatment.

Compound	M/z (g/mol)	Formula	Proposed structure	Proposed pathway
BPA	228	$C_{15}H_{16}O_2$	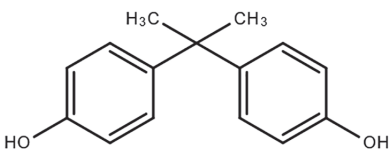	Initial compound
TP1	258	$C_{15}H_{14}O_4$	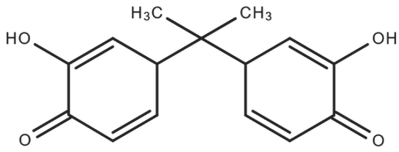	Aromatic ring hydroxylation and oxidation
TP2	276	$C_{15}H_{16}O_5$	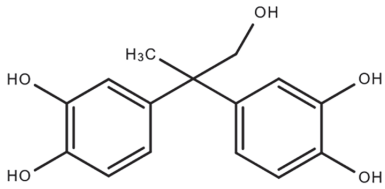	Side chain hydroxylation
TP3	276	$C_{15}H_{16}O_5$	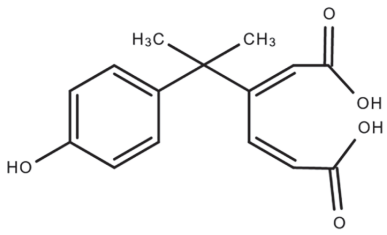	Aromatic ring cleavage
TP4	134	$C_9H_{10}O$	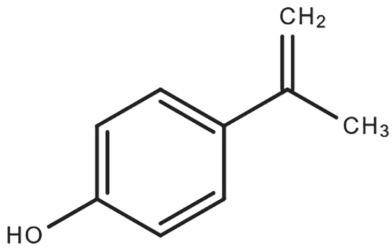	Scission of the bond between phenyl group and isopropylidene carbon

experiments with BPA at the energy dose of 5 kWh m^{-3} did not exceed 17% of the residual TOC.

One can see from Table 2 the contents of acetate, formate and oxalate increasing from the beginning of treatment to the delivered energy dose of 2–4 kWh m^{-3} even after complete removal of bisphenols at about 1.1 kWh m^{-3} indicating further degradation of intermediates formed during oxidation. With the delivered energy dose increased to 5 kWh m^{-3}, some carboxylic anions moderately degraded in their turn, which is consistent with the decreasing TOC (Fig. 6).

Besides carboxylic compounds, nitrate responsible for the pH decreased from 9.5 ± 0.5 to 3.5 ± 0.3 was also detected in the IC analysis. Nitrate formation in PCD was studied earlier showing the efficiency up to 16 g $kW^{-1}h^{-1}$ [30]. It must be noted that the lower frequency of pulse repetition was beneficial for nitrate formation: the amounts of nitrate produced in PCD independently of the bisphenol structure comprised 14.76 and 12.32 g $kW^{-1}h^{-1}$ at 200 and 880 pps, respectively.

3.3.3. *Primary oxidation products*

To assume a potential degradation pathway in PCD, transformation products (TPs) of BPA and BPS were determined with LC-MS analysis (Tables 3 and 4). The obtained oxidation product mass spectra at the delivered energy dose of about 0.5 kWh m^{-3} are presented in Figure S2 and S3. In BPA degradation, five transformation TPs were identified. Hydroxylation of BPA is likely initiated by OH-radical attack to benzene rings [55,56]. After the primary hydroxylation, subsequent hydroxylation follows forming di-hydroxylated BPA [53,55]. Although none of the hydroxylated derivatives was identified in this study, quinone of

Table 4
Bisphenol S transformation products determined by LC-MS analysis in PCD treatment.

Compound	M/z (g/mol)	Formula	Proposed structure	Proposed pathway
BPS	250	$C_{12}H_{10}O_4S$	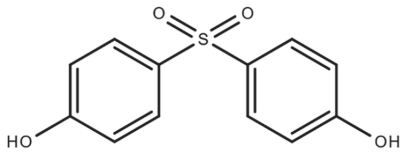	Initial compound
TP5	266	$C_{12}H_{10}O_5S$	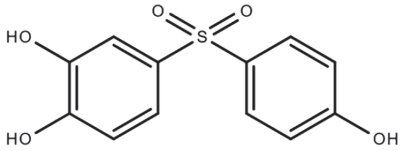	Aromatic ring hydroxylation
TP6	283	$C_{12}H_{10}O_6S$	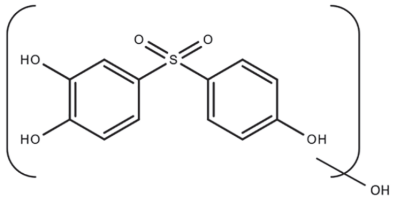	Aromatic ring hydroxylation
TP7	158	$C_6H_6O_3S$	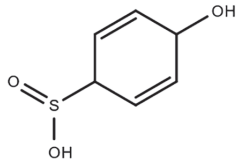	Sulphonyl S-C bond cleavage

dihydroxylated BPA (TP1 in Table 3) was observed as a product of further radical oxidation [53,57]. While further addition of HO-group would cause cleavage of benzene ring, OH-radical may also react with the aliphatic side-chain [36,56], thus hydroxylating the methyl group (TP2) [56]. Ozone also present in the discharge plasma has been reported to readily react with unsaturated bonds, cracking the benzene ring directly of BPA or through mono-hydroxylated BPA to form (2e,4z)-3-(2-(4-hydroxyphenyl)propan-2-yl)*hexa*-2,4-dienedioic acid (TP3) [42,57,58]. Additionally, oxidation by both OH-radical and ozone may result in scission of the bond between phenyl group and isopropylidene carbon, causing a series of reactions to form p-isopropenylphenol (TP4) [44,52,55,56,58]. By further oxidation, the latter TPs presumably followed the benzene ring cleavage into short chain aliphatic acids, such as oxalic-, acetic and formic one, that were detected in IC and further mineralized to CO_2 and H_2O [42,59].

Three BPS transformation products were identified (Table 4). Similar structures of bisphenols allow assuming similarity of reactions with OH-radicals. Mono-hydroxylated BPS (TP5 in Table 4) observed in BPS oxidation was likely formed through the primary hydroxylation [49,60], followed by subsequent OH-radical attack forming di-hydroxylated BPS (TP6). Observation of the primary BPS hydroxylation products in LC-MS, unlike those non-detectable in BPA oxidation, says for the higher stability of the formers due to the inductive effect of sulphonyl moiety. The TP7 was possibly formed through sulfonyl cleavage caused by OH-radicals [61]. Further oxidation expectably triggered opening of benzene ring, causing the formation of sulphate and aliphatic acids similar to those of BPA. It must be noted that none of the described TPs were observed in the samples at the delivered energy dose above 1.35 kWh m^{-3}, likely indicating the formation of simpler structure compounds.

4. Conclusions

Oxidation of bisphenols appeared to be favourable in energy efficiency compared to the closest competitors, ozonation and other electric discharge processes, thus confirming high energy efficiency of PCD in respect of both substances reaching in air 66.4 and 52.9 g $kW^{-1}h^{-1}$ for BPA and BPS, respectively. More effective BPA oxidation is explained by its hydrophobicity exceeding the one of BPS. A moderate effect of pulse repetition frequency on the bisphenols' degradation indicates rapid oxidation with both OH-radicals and ozone.

The dominant character of rapid surface reaction of both bisphenols was confirmed by minor effect of gas–liquid contact surface on the oxidation efficiency, whereas slower mineralization of intermediate oxidation products was more sensitive towards the interface area. The presence of surfactant radical scavenger showed insignificantly negative effect due to the radical screening opposing the surface reaction advancement. Admixtures of surfactants thus showed their minor effect in bisphenols oxidative removal.

The identified oxidation intermediates of bisphenols exhibit major oxidants, OH-radical and ozone forming hydroxyl moieties and cracking the benzene rings. Acetate, formate and oxalate were quantified as oxidation end-products, although sulphate formed in BPS oxidation interfered with oxalate measurement.

Declaration of Competing Interest

The authors declare that they have no known competing financial interests or personal relationships that could have appeared to influence the work reported in this paper.

Acknowledgement

This work was supported by the Institutional Development Program of Tallinn University of Technology for 2016-2022, project 2014-2020.4.01.16-0032 from EU Regional Development Fund.

Appendix A. Supplementary data

Supplementary data to this article can be found online at https://doi.org/10.1016/j.cej.2022.135602.

References

[1] M.O. Barbosa, N.F.F. Moreira, A.R. Ribeiro, M.F.R. Pereira, A.M.T. Silva, Occurrence and removal of organic micropollutants: An overview of the watch list of EU Decision 2015/495, Water Res. 94 (2016) 257–279, https://doi.org/10.1016/j.watres.2016.02.047.

[2] Y. Luo, W. Guo, H.H. Ngo, L.D. Nghiem, F.I. Hai, J. Zhang, S. Liang, X.C. Wang, A review on the occurrence of micropollutants in the aquatic environment and their fate and removal during wastewater treatment, Sci. Total Environ. 473–474 (2014) 619–641, https://doi.org/10.1016/j.scitotenv.2013.12.065.

[3] I. Michael, L. Rizzo, C.S. McArdell, C.M. Manaia, C. Merlin, T. Schwartz, C. Dagot, D. Fatta-Kassinos, Urban wastewater treatment plants as hotspots for the release of antibiotics in the environment: A review, Water Res. 47 (2013) 957–995, https://doi.org/10.1016/j.watres.2012.11.027.

[4] E.M.M. Wanda, H. Nyoni, B.B. Mamba, T.A.M. Msagati, Occurrence of emerging micropollutants in water systems in Gauteng, Mpumalanga, and North West provinces, South Africa, Int. J. Environ. Res. Public Health 14 (2017) 8–20, https://doi.org/10.3390/ijerph14010079.

[5] Off. J. Eur Communities. (2013 (2020)) 1–17, https://doi.org/10.5040/9781782258674.0032.

[6] The European Parliament and the Council of the European Union, COMMISSION IMPLEMENTING DECISION (EU) 2018/840 of 5 June 2018 establishing a watch list of substances for Union-wide monitoring in the field of water policy pursuant to Directive 2008/105/EC of the European Parliament and of the Council and repealing Comm, Off. J. Eur. Union. L 141 (2018) 9–12. https://eur-lex.europa.eu/eli/dec_impl/2018/840/oj.

[7] A.L. Lister, G.J. Van Der Kraak, Endocrine disruption: Why is it so complicated? Water Qual. Res. J. Canada. 36 (2001) 175–190, https://doi.org/10.2166/wqrj.2001.011.

[8] Y. Ma, H. Liu, J. Wu, L. Yuan, Y. Wang, X. Du, R. Wang, P.W. Marwa, P. Petlulu, X. Chen, H. Zhang, The adverse health effects of bisphenol A and related toxicity mechanisms, Environ. Res. 176 (2019), https://doi.org/10.1016/j.envres.2019.108575.

[9] T. Yamamoto, A. Yasuhara, H. Shiraishi, O. Nakasugi, Bisphenol A in hazardous waste landfill leachates, Chemosphere 42 (2001) 415–418, https://doi.org/10.1016/S0045-6535(00)00079-5.

[10] J. Corrales, L.A. Kristofco, W. Baylor Steele, B.S. Yates, C.S. Breed, E. Spencer Williams, B.W. Brooks, Global assessment of bisphenol a in the environment: Review and analysis of its occurrence and bioaccumulation, Dose-Response. 13 (2015) 1–29, https://doi.org/10.1177/1559325815598308.

[11] E. Grignard, S. Lapenna, S. Bremer, Weak estrogenic transcriptional activities of Bisphenol A and Bisphenol S, Toxicol. Vitr. 26 (2012) 727–731, https://doi.org/10.1016/j.tiv.2012.03.013.

[12] The European Parliament and the Council of the European Union, Commission Directive 2011/8/EU, Off. J. Eur. Communities. (2011) 29–32.

[13] The European Parliament and the Council of the European Union, Directive (EU) 2020/2184, EU (revised) Drinking Water Directive. Annex 1. Part B., Off. J. Eur. Communities. 2019 (2020) 35. https://eur-lex.europa.eu/eli/dir/2020/2184/oj.

[14] C. Liao, F. Liu, K. Kannan, Bisphenol S, a new bisphenol analogue, in paper products and currency bills and its association with bisphenol a residues, Environ. Sci. Technol. 46 (2012) 6515–6522, https://doi.org/10.1021/es300876n.

[15] G. Cao, R. He, Z. Cai, J. Liu, Photolysis of bisphenol S in aqueous solutions and the effects of different surfactants, React. Kinet. Mech. Catal. 109 (2013) 259–271, https://doi.org/10.1007/s11144-013-0553-6.

[16] N. Ahsan, H. Ullah, W. Ullah, S. Jahan, Comparative effects of Bisphenol S and Bisphenol A on the development of female reproductive system in rats; a neonatal exposure study, Chemosphere 197 (2018) 336–343, https://doi.org/10.1016/j.chemosphere.2017.12.118.

[17] E. Yamazaki, N. Yamashita, S. Taniyasu, J. Lam, P.K.S. Lam, H.B. Moon, Y. Jeong, P. Kannan, H. Achyuthan, N. Munuswamy, K. Kannan, Bisphenol A and other bisphenol analogues including BPS and BPF in surface water samples from Japan, China, Korea and India, Ecotoxicol. Environ. Saf. 122 (2015) 565–572, https://doi.org/10.1016/j.ecoenv.2015.09.029.

[18] K. Barel-Cohen, L.S. Shore, M. Shemesh, A. Wenzel, J. Mueller, N. Kronfeld-Schor, Monitoring of natural and synthetic hormones in a polluted river, J. Environ. Manage. 78 (2006) 16–23, https://doi.org/10.1016/j.jenvman.2005.04.006.

[19] A.Z. Aris, A.S. Shamsuddin, S.M. Praveena, Occurrence of 17α-ethynylestradiol (EE2) in the environment and effect on exposed biota: A review, Environ. Int. 69 (2014) 104–119, https://doi.org/10.1016/j.envint.2014.04.011.

[20] M. Sillannpää, Advanced water treatment advanced oxidation processes, Elsevier, Amsterdam, 2020 http://lib.ugent.be/catalog/ebk01:4100000010076013.

[21] R. Munter, S. Preis, J. Kallas, M. Trapido, Y. Veressinina, Advanced oxidation processes (AOPs): Water treatment technology for the twenty-first century, Kem. Chem. J. 28 (2001) 354–362.

[22] M. Magureanu, C. Bradu, V.I. Parvulescu, Plasma processes for the treatment of water contaminated with harmful organic compounds, J. Phys. D, Appl. Phys. 51 (2018) aacd9c, https://doi.org/10.1088/1361-6463/aacd9c.

[23] M.A. Malik, D.Á. Vocs, Water purification by plasmas: Which reactors are most energy efficient? Plasma Chem. Plasma Process. 30 (2010) 21–31, https://doi.org/10.1007/s11090-009-9202-2.

[24] S. Preis, I.C. Panorel, I. Kornev, H. Hatakka, J. Kallas, Pulsed corona discharge: the role of ozone and hydroxyl radical in aqueous pollutants oxidation, Water Sci. Technol. 68 (2013) 1536–1542, https://doi.org/10.2166/wst.2013.399.

[25] I. Panorel, I. Kornev, H. Hatakka, S. Preis, Pulsed corona discharge for degradation of aqueous humic substances, Water Sci. Technol, Water Supply. 11 (2011) 238–245, https://doi.org/10.2166/ws.2011.045.

[26] V. Derevshchikov, N. Dulova, S. Preis, Oxidation of ubiquitous aqueous pharmaceuticals with pulsed corona discharge, J. Electrostat. 110 (2021), 103567, https://doi.org/10.1016/j.elstat.2021.103567.

[27] L. Onga, I. Kornev, S. Preis, Oxidation of reactive azo-dyes with pulsed corona discharge: Surface reaction enhancement, J. Electrostat. 103 (2020), 103420, https://doi.org/10.1016/j.elstat.2020.103420.

[28] Y.X. Wang, I. Kornev, C.H. Wei, S. Preis, Surfactant and non-surfactant radical scavengers in aqueous reactions induced by pulsed corona discharge treatment, J. Electrostat. 98 (2019) 82–86, https://doi.org/10.1016/j.elstat.2019.03.001.

[29] P. Tikker, I. Kornev, S. Preis, Oxidation energy efficiency in water treatment with gas-phase pulsed corona discharge as a function of spray density, J. Electrostat. 106 (2020), 103466, https://doi.org/10.1016/j.elstat.2020.103466.

[30] S. Preis, I. Panorel, S. Llauger Coll, I. Kornev, Formation of nitrates in aqueous solutions treated with pulsed corona discharge: the impact of organic pollutants, Ozone Sci. Eng. 36 (2014) 94–99, https://doi.org/10.1080/01919512.2013.836955.

[31] I. Kornev, G. Osokin, A. Galanov, N. Yavorovskiy, S. Preis, Formation of Nitrite- and Nitrate-Ions in Aqueous Solutions Treated with Pulsed Electric Discharges, Ozone Sci. Eng. 35 (2013) 22–30, https://doi.org/10.1080/01919512.2013.720898.

[32] L. Onga, R. Boroznjak, I. Kornev, S. Preis, Oxidation of aqueous organic molecules in gas-phase pulsed corona discharge affected by sodium dodecyl sulphate: Explanation of variability, J. Electrostat. 111 (2021), 103581, https://doi.org/10.1016/j.elstat.2021.103581.

[33] I. Kornev, F. Saprykin, S. Preis, Stability and energy efficiency of pulsed corona discharge in treatment of dispersed high-conductivity aqueous solutions, J. Electrostat. 89 (2017) 42–50, https://doi.org/10.1016/j.elstat.2017.07.001.

[34] I.A. Katsoyiannis, S. Canonica, U. von Gunten, Efficiency and energy requirements for the transformation of organic micropollutants by ozone, O3/H2O2 and UV/H2O2, Water Res. 45 (2011) 3811–3822, https://doi.org/10.1016/j.watres.2011.04.038.

[35] EU non-household electricity and gas prices, (2019). https://ec.europa.eu/eurostat/web/products-eurostat-news/-/DDN-20190521-1 (accessed August 28, 2020).

[36] M. Mehrabani-Zeinabad, C.H. Langford, G. Achari, Advanced oxidative degradation of bisphenol A and bisphenol S, J. Environ. Eng. Sci. 10 (2016) 92–102, https://doi.org/10.1680/jenes.15.00015.

[37] M. Mehrabani-Zeinabad, G. Achari, C.H. Langford, Degradation of Bisphenol S Using O3 and/or H2O2 with UV in a Flow-Through Reactor, J. Environ. Eng. 142 (2016) 06016004, https://doi.org/10.1061/(asce)ee.1943-7870.0001117.

[38] S. Irmak, O. Erbatur, A. Akgerman, Degradation of 17β-estradiol and bisphenol A in aqueous medium by using ozone and ozone/UV techniques, J. Hazard. Mater. 126 (2005) 54–62, https://doi.org/10.1016/j.jhazmat.2005.05.045.

[39] S.E. Kim, N.S. Park, H. Yamada, H. Tsuno, Modeling of decomposition characterisitics of estrogenic chemicals during ozonation, Environ. Technol. 29 (2008) 287–296, https://doi.org/10.1080/09593330802099643.

[40] J. Lee, H. Park, J. Yoon, Ozonation characteristics of bisphenol a in water, Environ. Technol. (United Kingdom) 24 (2003) 241–248, https://doi.org/10.1080/09593330309385555.

[41] K.S. Tay, N.A. Rahman, M.R. Bin Abas, Degradation of bisphenol A by ozonation: Rate constants, influence of inorganic anions, and by-products, Maejo Int. J. Sci. Technol. 6 (2012) 77–94. 10.14456/mijst.2012.7.

[42] E. Kusvuran, D. Yildirim, Degradation of bisphenol A by ozonation and determination of degradation intermediates by gas chromatography-mass spectrometry and liquid chromatography-mass spectrometry, Chem. Eng. J. 220 (2013) 6–14, https://doi.org/10.1016/j.cej.2013.01.064.

[43] T. Garoma, S. Matsumoto, Ozonation of aqueous solution containing bisphenol A: Effect of operational parameters, J. Hazard. Mater. 167 (2009) 1185–1191, https://doi.org/10.1016/j.jhazmat.2009.01.133.

[44] J. Yang, D. Zeng, M. Hassan, Z. Ma, L. Dong, Y. Xie, Y. He, Efficient degradation of Bisphenol A by dielectric barrier discharge non-thermal plasma: Performance, degradation pathways and mechanistic consideration, Chemosphere 286 (2022), 131627, https://doi.org/10.1016/j.chemosphere.2021.131627.

[45] F. Abdelmalek, R.A. Torres, E. Combet, C. Petrier, C. Pulgarin, A. Addou, Gliding Arc Discharge (GAD) assisted catalytic degradation of bisphenol A in solution with ferrous ions, Sep. Purif. Technol. 63 (2008) 30–37, https://doi.org/10.1016/j.seppur.2008.03.036.
[46] L. Wang, X. Jiang, Y. Liu, Degradation of bisphenol A and formation of hydrogen peroxide induced by glow discharge plasma in aqueous solutions, J. Hazard. Mater. 154 (2008) 1106–1114, https://doi.org/10.1016/j.jhazmat.2007.11.016.
[47] H. Zhang, Q. Huang, L. Li, Z. Ke, Q. Wang, Distinguish the Role of DBD-Accompanying UV-Radiation in the Degradation of Bisphenol A, Plasma Chem. Plasma Process. 36 (2016) 585–598, https://doi.org/10.1007/s11090-015-9678-x.
[48] N. Wardenier, Z. Liu, A. Nikiforov, S.W.H. Van Hulle, C. Leys, Micropollutant elimination by O3, UV and plasma-based AOPs: An evaluation of treatment and energy costs, Chemosphere 234 (2019) 715–724, https://doi.org/10.1016/j.chemosphere.2019.06.033.
[49] X. Lu, J. Zhao, Q. Wang, D. Wang, H. Xu, J. Ma, W. Qiu, T. Hu, Sonolytic degradation of bisphenol S: Effect of dissolved oxygen and peroxydisulfate, oxidation products and acute toxicity, Water Res. 165 (2019), 114969, https://doi.org/10.1016/j.watres.2019.114969.
[50] I. Panorel, S. Preis, I. Kornev, H. Hatakka, M. Louhi-Kultanen, Oxidation of aqueous pharmaceuticals by pulsed corona discharge, Environ. Technol. (United Kingdom) 34 (2013) 923–930, https://doi.org/10.1080/09593330.2012.722691.
[51] T. Garoma, S.A. Matsumoto, Y. Wu, R. Klinger, Removal of bisphenol a and its reaction-intermediates from aqueous solution by ozonation, Ozone Sci. Eng. 32 (2010) 338–343, https://doi.org/10.1080/01919512.2010.508484.
[52] J. Mu, S. Li, J. Wang, X. Li, W. Chen, X. Tong, Y. Tang, L. Li, Efficient catalytic ozonation of bisphenol A by three-dimensional mesoporous CeOx-loaded SBA-16, Chemosphere 278 (2021) 130412.
[53] R.A. Torres, C. Pétrier, E. Combet, M. Carrier, C. Pulgarin, Ultrasonic cavitation applied to the treatment of bisphenol A. Effect of sonochemical parameters and analysis of BPA by-products, Ultrason. Sonochem. 15 (4) (2008) 605–611.
[54] N. Imen, L.M. Radhouan, B. Rayana, M. Chiheb, B. Nizar, Electrochemical Advanced Oxidation of 4, 4 ′ -Sulfonyldiphenol on BDD and Pt Anodes in Aqueous Medium, 3 (2014) 436–442.
[55] N. Jiang, X. Li, H.e. Guo, J. Li, K. Shang, N.a. Lu, Y. Wu, Plasma-assisted catalysis decomposition of BPA over graphene-CdS nanocomposites in pulsed gas-liquid hybrid discharge: Photocorrosion inhibition and synergistic mechanism analysis, Chem. Eng. J. 412 (2021) 128627.
[56] B. Darsinou, Z. Frontistis, M. Antonopoulou, I. Konstantinou, D. Mantzavinos, Sono-activated persulfate oxidation of bisphenol A: Kinetics, pathways and the controversial role of temperature, Chem. Eng. J. 280 (2015) 623–633, https://doi.org/10.1016/j.cej.2015.06.061.
[57] M. Deborde, S. Rabouan, P. Mazellier, J.P. Duguet, B. Legube, Oxidation of bisphenol A by ozone in aqueous solution, Water Res. 42 (2008) 4299–4308, https://doi.org/10.1016/j.watres.2008.07.015.
[58] H. Wang, Z. Shen, X. Yan, H. Guo, D. Mao, C. Yi, Dielectric barrier discharge plasma coupled with WO3 for bisphenol A degradation, Chemosphere 274 (2021), 129722, https://doi.org/10.1016/j.chemosphere.2021.129722.
[59] T. Olmez-hanci, D. Dursun, E. Aydin, I. Arslan-alaton, B. Girit, L. Mita, N. Diano, D. G. Mita, M. Guida, Chemosphere 8 / UV-C and H 2 O 2 / UV-C treatment of Bisphenol A : Assessment of toxicity , estrogenic activity , degradation products and results in real water, 119 (2015). 10.1016/j.chemosphere.2014.06.020.
[60] C. Luo, R. Hou, G. Chen, C. Liu, L. Zhou, Y. Yuan, UVC-assisted electrochemical degradation of novel bisphenol analogues with boron-doped diamond electrodes: kinetics, pathways and eco-toxicity removal, Sci. Total Environ. 711 (2020), 134539, https://doi.org/10.1016/j.scitotenv.2019.134539.
[61] A. Kovačič, C. Gys, T. Kosjek, A. Covaci, E. Heath, Photochemical degradation of BPF, BPS and BPZ in aqueous solution: Identification of transformation products and degradation kinetics, Sci. Total Environ. 664 (2019) 595–604, https://doi.org/10.1016/j.scitotenv.2019.02.064.

Oxidation of aqueous bisphenols A and S by pulsed corona discharge: impacts of process control parameters and oxidation products identification

Priit Tikker, Dmitri Nikitin, Sergei Preis*

[1]Department of Materials and Environmental Technology, Tallinn University of Technology, Ehitajate Tee 5, 19086 Tallinn, Estonia

*Corresponding authors: sergei.preis@taltech.ee

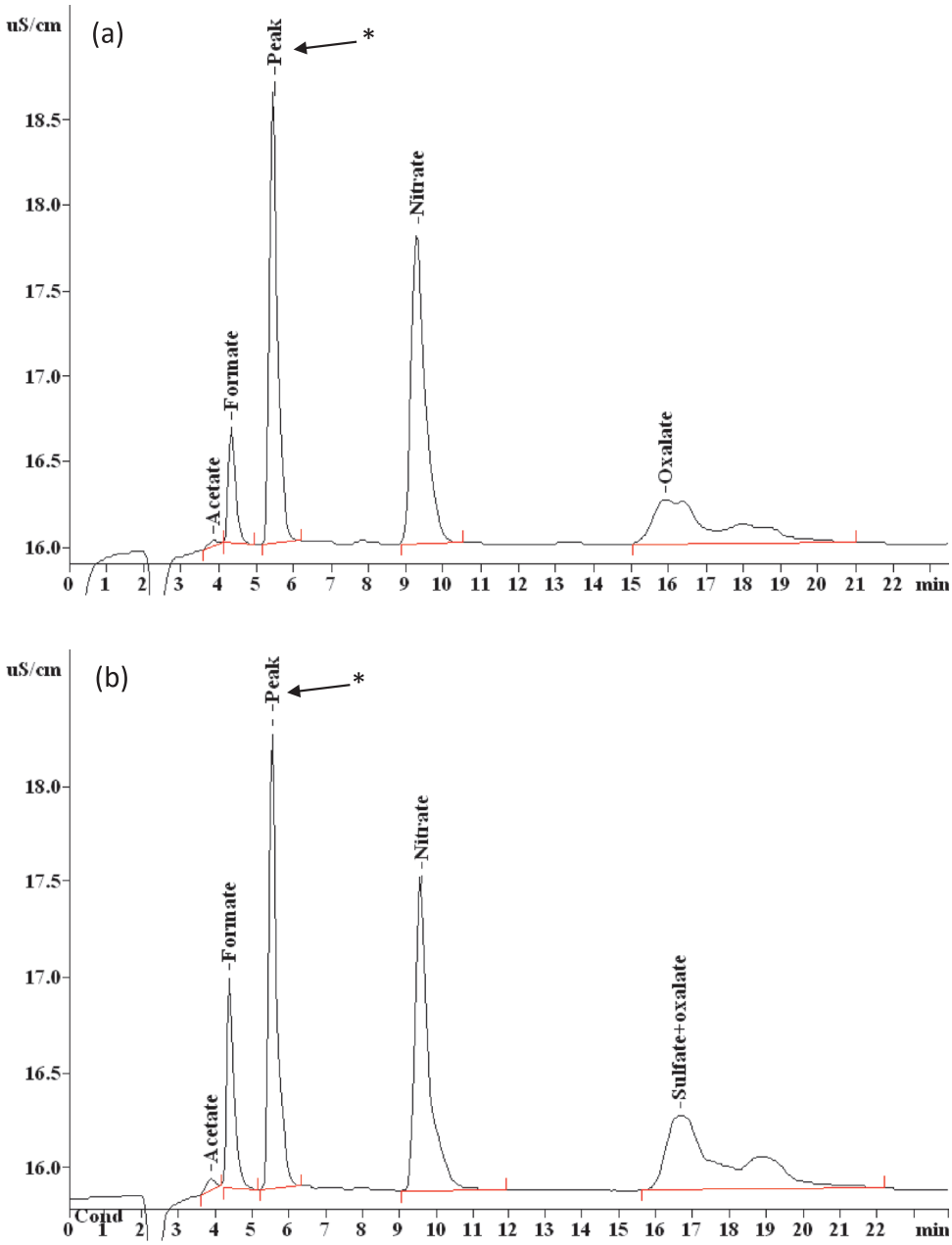

Figure S1. IC chromatographs of oxidation products for (a) BPA and (b) BPS at delivered energy dose of about 0.5 kWh m^{-3}

*Unidentified peak (Peak) is present at chromatograms of initial and treated samples without change in its area, i.e. was unaffected by PCD treatment

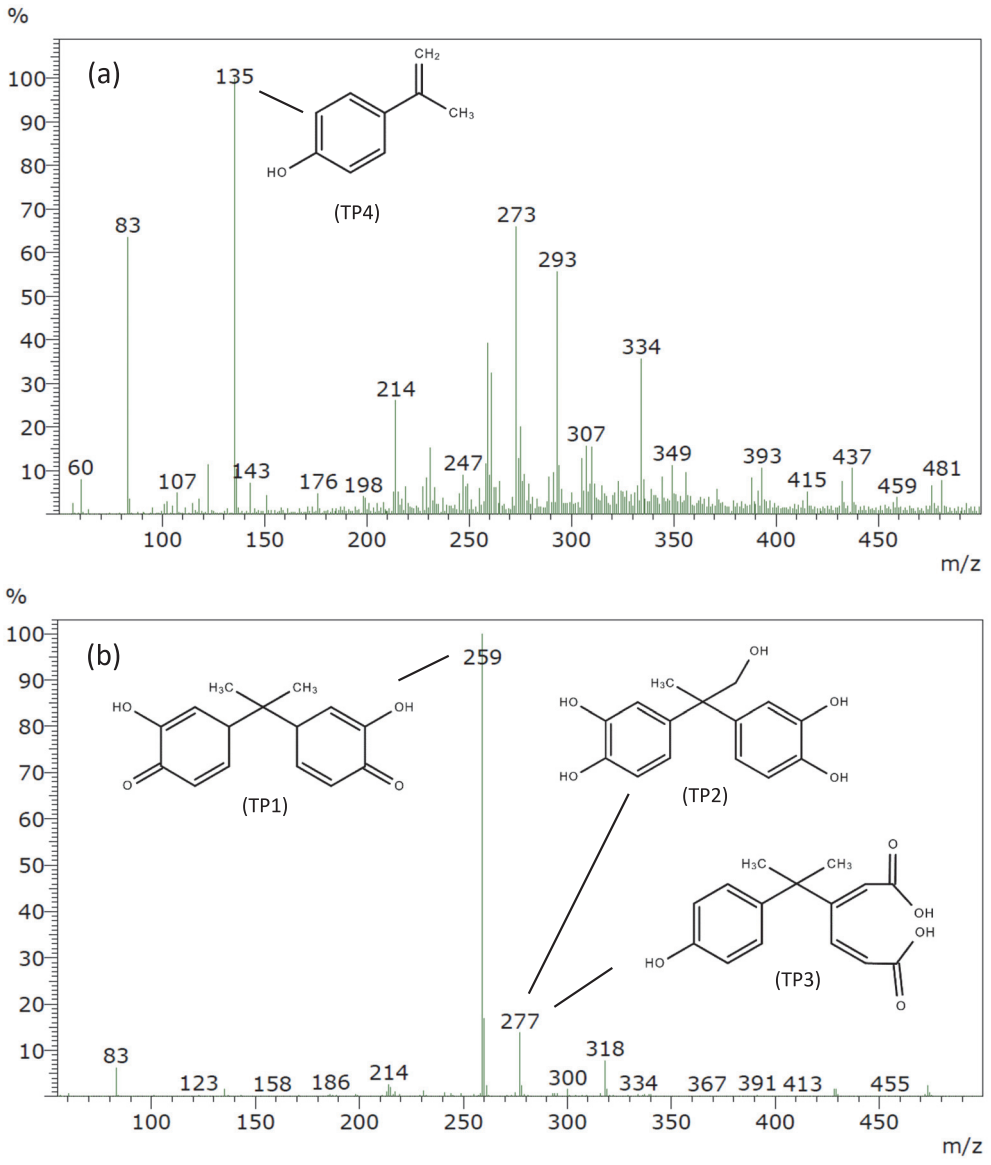

Figure S2. LC-MS spectra of BPA at delivered energy dose of about 0.5 kWh m^{-3}: retention times (a) 3.2 min and (b) 3.5 min

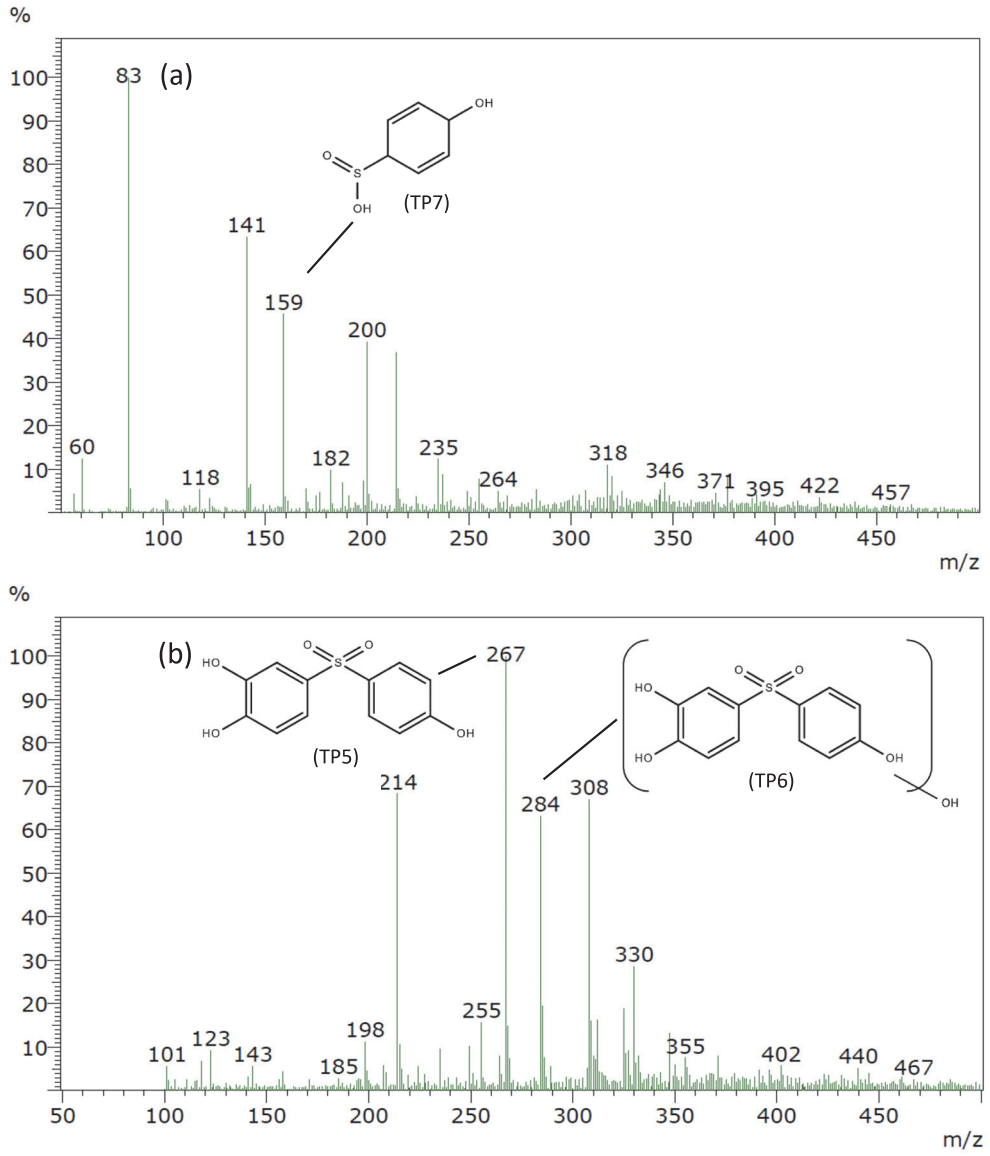

Figure S3. LC-MS spectra of BPS at delivered energy dose of about 0.5 kWh m^{-3}: retention times (a) 3.5 min and (b) 4.3 min

Curriculum vitae

Personal data

Name:	Priit Tikker
Date of birth:	09.12.1992
Place of birth:	Tallinn, Estonia
Citizenship:	Estonian

Contact data

E-mail:	priit.tikker@taltech.ee

Education

2018–2022	Tallinn University of Technology, Chemical and Materials Technology, PhD
2016–2018	Tallinn University of Technology, Chemical and Environmental Technology, Master of Science in Engineering (*Cum laude*)
2012–2015	Tallinn University of Technology, Chemical and Environmental Technology, Bachelor of Science in Engineering (*Cum laude*)
2009–2012	Tallinn ARTE Gymnasium, high school education

Language competence

Estonian	Native speaker
English	Fluent
Russian	Beginner
German	Beginner

Professional employment

2018–2022	Tallinn University of Technology, School of Engineering, Department of Materials and Environmental Technology, Junior Researcher

Defended dissertations:

Master's degree, 2018, (sup) Niina Dulova, Eneliis Kattel-Salusoo, Photochemical oxidation of ceftriaxone by magnetite-activated persulfate, Tallinn University of Technology, School of Engineering, Department of Materials and Environmental Technology

Field of research:

1. Biosciences and Environment; 1.8. Research relating to the State of the Environment and to Environmental Protection; CERCS CLASSIFICATION: T270 Environmental technology, pollution control

4. Natural Sciences and Engineering; 4.11. Chemistry and Chemical Technology; CERCS CLASSIFICATION: T350 Chemical technology and engineering

Participation in research projects:

PRG776 Innovative energy-efficient abatement of aqueous and airborne hazardous pollutants combining pulsed corona discharge plasma with catalysis/photocatalysis LEEAE20017 Expertise of leakage current on water pipes and water parameters of the KUMU Art Museum building

IUT1-7 Chemical engineering approach to removal of priority pollutants and emerging micropollutants from water/wastewater and soil: implementation and optimization of advanced oxidation technologies

Awards:

2022	The City Council Scholarship
2022	Best scientific publication in the field of Engineering and Technology of the year 2021 at Tallinn University of Technology (first author)
2019	The PROM Programme - International scholarship exchange of PhD candidates and academic staff, Visit to Cracow's University of Technology; Cracow, Poland, September 20–29, 2019.
2019	Dora Plus program (activity 1) scholarship for the participation with a poster presentation at 6th European Conference on Environmental Applications of Advanced Oxidation Processes (EAAOP-6); Portoroz-Portorose, Slovenia, June 26–30, 2019.
2019	FMDTK activities scholarship for the participation with a poster presentation at 3rd European Summer School of Environmental Applications on Advanced Oxidation Processes; Alcoy, Spain, June 3–7, 2019.

Supervised dissertations:

Anne Mari Kääp, Master's degree, 2021, (sup) Priit Tikker; Niina Dulova, Degradation of oxalate in water by pulsed corona discharge and hydrogen peroxide combination, Tallinn University of Technology, School of Engineering, Department of Materials and Environmental Technology

Dmitri Nikitin, Master's degree, 2020, (sup) Sergei Preis; Priit Tikker Oxidation of bisphenol A by pulsed corona discharge: impacts of plasma-liquid contact surface and a surfactant radical scavenger, Tallinn University of Technology, School of Engineering, Department of Materials and Environmental Technology

Mirjam Lätt, Master's degree, 2020, (sup) Niina Dulova; Priit Tikker, Degradation of oxalic acid in water by pulsed corona discharge in combination with persulfate, Tallinn University of Technology, School of Engineering, Department of Materials and Environmental Technology

Elulookirjeldus

Isikuandmed

Nimi:	Priit Tikker
Sünniaeg:	09.12.1992
Sünnikoht:	Tallinn, Eesti
Kodakondsus:	Eesti

Kontaktandmed

E-post:	priit.tikker@taltech.ee

Hariduskäik

2018–2022	Tallinna Tehnikaülikool, Keemia- ja materjalitehnoloogia, doktoriõpe
2016–2018	Tallinna Tehnikaülikool, Keemia- ja keskkonnakaitse tehnoloogia, tehnikateaduste magistrikraad (*Cum laude*)
2012–2015	Tallinna Tehnikaülikool, Keemia- ja keskkonnakaitse tehnoloogia, tehnikateaduste bakalaureusekraad (*Cum laude*)
2009–2012	Tallinna ARTE Gümnaasium, keskharidus

Keelteoskus

Eesti keel	Emakeel
Inglise keel	Kõrgtase
Vene keel	Algtase
Saksa keel	Algtase

Teenistuskäik

2018–2022	Tallinna Tehnikaülikool, Inseneriteaduskond, Materjali- ja keskkonnatehnoloogia instituut, doktorant-nooremteadur

Kaitstud lõputööd:

Magistrikraad, 2018, Tseftriaksooni fotokeemiline oksüdatsioon magnetiidiga aktiveeritud persulfaadiga, Tallinna Tehnikaülikool, Inseneriteaduskond, Materjali- ja keskkonnatehnoloogia instituut. Juhendajad Niina Dulova, Eneliis Kattel-Salusoo

Uurimustöö põhisuunad:

1. Bio- ja keskkonnateadused; 1.8. Keskkonnaseisundit ja keskkonnakaitset hõlmavad uuringud; CERCS KLASSIFIKAATOR: T270 Keskkonnatehnoloogia, reostuskontroll

4.Loodusteadused ja tehnika; 4.11. Keemia ja keemiatehnika; CERCS KLASSIFIKAATOR: T350 Keemiatehnoloogia ja -masinaehitus

Osalemine uurimisprojektides:

PRG776 Ohtlike vee ja õhu saasteainete lagundamine innovatiivse energiatõhusa kombineeritud impulss-koroona elektrilahenduse ja katalüüsi/fotokatalüüsiga

LEEAE2001 KUMU kunstimuuseumi hoone veetorustiku uitvoolude ja veeparameetrite ekspertiis

IUT1-7 Keemiatehnikapõhine lähenemisviis prioriteetsete saasteainete ja uute esilekerkivate mikrosaasteainete kõrvaldamisele veest/reoveest ja pinnasest: täiustatud oksüdatsioonitehnoloogiate kasutamine ja optimeerimine

Tunnustused:

2022	Raestipendium
2022	Tallinna Tehnikaülikooli 2021. aasta parim teadusartikkel tehnika ja tehnoloogia valdkonnas (esimene autor)
2019	The PROM Programme - International scholarship exchange of PhD candidates and academic staff stipendium osalemiseks õppevisiidil Kraków'i Tehnikaülikooli, 20.–29. september 2019, Kraków, Poola
2019	Dora Pluss programm (tegevus 1) stipendium osalemiseks posterettekandega konverentsil "The 6th European Conference on Environmental Applications of Advanced Oxidation Processes (EAAOP-6)", 26.–30. juuni 2019, Portorož-Portorose, Sloveenia
2019	TTÜ ASTRA programmi "TTÜ arenguprogramm aastateks 2016-2022" Funktsionaalsete materjalide ja tehnoloogiate doktorikool (2014-2020.4.01.16-0032) stipendium osalemiseks posterettekandega 3rd European Summer School of Environmental Applications on Advanced Oxidation Processes, 3.–7. juuni 2019, Alcoi, Hispaania

Juhendatud magistritööd:

Anne Mari Kääp, magistrikraad, 2021, (juh) Priit Tikker; Niina Dulova, Oksalaadi lagundamine vees impulss koroona elektrilahenduse ja vesinikperoksiidi kombinatsiooniga, Tallinna Tehnikaülikool, Inseneriteaduskond, Materjali- ja keskkonnatehnoloogia instituut

Dmitri Nikitin, magistrikraad, 2020, (juh) Sergei Preis; Priit Tikker, Oxidation of bisphenol A by pulsed corona discharge: impacts of plasma-liquid contact surface and a surfactant radical scavenger (Bisfenool A oksüdeerumine impulss-koroona elektrilahenduse toimel: plasma-vedelik kontaktpinna ja pindaktiivse radikaalpüüdja mõju), Tallinna Tehnikaülikool, Inseneriteaduskond, Materjali- ja keskkonnatehnoloogia instituut

Mirjam Lätt, magistrikraad, 2020, (juh) Niina Dulova; Priit Tikker, Oksaalhappe lagundamine vees impulss-koroona elektrilahenduse ja persulfaadi kombinatsiooniga, Tallinna Tehnikaülikool, Inseneriteaduskond, Materjali- ja keskkonnatehnoloogia instituut

ISSN 2585-6901 (PDF)
ISBN 978-9949-83-872-1 (PDF)